

# Upper-rim Schiff-base calix[4]arenes

*Martin Maria Matthias Stindl*

This thesis is for a  
MASTER OF SCIENCE  
and was submitted to  
Heriot-Watt University

School of Engineering and Physical  
Sciences - Chemistry

September 2009

The copyright in this thesis is owned by the author. Any question from the thesis or use of any of the information contained in it must acknowledge this thesis as the source of the quotation or information.

## ***Abstract***

This study focuses on the synthesis of various Schiff-base calix[4]arenes that may be used as supramolecular building blocks. Two different routes to Schiff-base calix[4]arenes have been examined. One explores the reaction of different amino-pyridines and *p*-formylcalix[4]arenes, while the other utilises the reaction between different *p*-amino-calix[4]arenes with various 2-hydroxybenzaldehydes. In addition, the amino-pyridines employed in the first route have also been used in a reductive amination procedure with *p*-formylcalix[4]arene as an alternative synthetic route due to Schiff-base product instability.

With respect to the 2-hydroxybenzaldehydes chosen for the second route, different functionality was introduced around the benzene ring in order to obtain a range of ligands that may influence the formation of supramolecular assemblies. This influence could be by hydrogen bonding, ionic interactions, halogen-halogen or  $\pi$ -stacking interactions for example. Furthermore, this reaction was carried out on two different *p*-aminocalix[4]arenes. One was flexible (with respect to the movement around the annulus of the calixarene) while the other was locked in the cone conformation by the introduction of lower-rim crown-ether linkages.

Several series of pro-ligands have been synthesised and fully characterised where possible. No supramolecular assemblies have been synthesised as yet due to time restrictions.

### ***Acknowledgement:***

The author would like to thank Dr. Scott Dalgarno for his help, guidance, hints and tips for any problems and assistance with single crystal X-ray diffraction data. Stuart Kennedy, Peter Cowin and Steven Fuhrmann for their help and everyone in Labs WP 120 and 210, Dr. Magnus Bebbington and Dr Richard Wightman for helping with organic synthesis questions. The analytical staff at Heriot-Watt University for their work and the MS serves at Swansea and Edinburgh Universities for the MS-spectra and data, and the EPSRC for funding.

# ACADEMIC REGISTRY

## Research Thesis Submission



Name:	Martin Martia Matthias Stindl		
School/PGL:	EPS - Chem		
Version: <i>(i.e. First, Resubmission, Final)</i>	Final	Degree Sought (Award <b>and</b> Subject area)	MSc Research Supramolecular Chemistry

### Declaration

In accordance with the appropriate regulations I hereby submit my thesis and I declare that:

- 1) the thesis embodies the results of my own work and has been composed by myself
- 2) where appropriate, I have made acknowledgement of the work of others and have made reference to work carried out in collaboration with other persons
- 3) the thesis is the correct version of the thesis for submission and is the same version as any electronic versions submitted\*.
- 4) my thesis for the award referred to, deposited in the Heriot-Watt University Library, should be made available for loan or photocopying and be available via the Institutional Repository, subject to such conditions as the Librarian may require
- 5) I understand that as a student of the University I am required to abide by the Regulations of the University and to conform to its discipline.

\* *Please note that it is the responsibility of the candidate to ensure that the correct version of the thesis is submitted.*

Signature of Candidate:			
-------------------------	--	--	--

### Submission

Submitted By <i>(name in capitals)</i> :	
Signature of Individual Submitting:	
Date Submitted:	

### For Completion in Academic Registry

Received in the Academic Registry by <i>(name in capitals)</i> :			
<b>Method of Submission</b> <i>(Handed in to Academic Registry; posted through internal/external mail):</i>			
<b>E-thesis Submitted (mandatory for final theses from January 2009)</b>			
Signature:			

## ***Content***

<i>1</i>	<i>Introduction to supramolecular chemistry</i>	<i>2</i>
<i>1.1</i>	<i>Common interactions observed in Supramolecular Chemistry</i>	<i>4</i>
<i>1.2</i>	<i>Calixarenes</i>	<i>7</i>
<i>1.3</i>	<i>Synthesis of calixarenes</i>	<i>9</i>
<i>1.4</i>	<i>Hydrogen- bonded calixarene structures</i>	<i>15</i>
<i>1.5</i>	<i>Metal templated calixarene structures</i>	<i>18</i>
<i>1.6</i>	<i>Formation of Schiff bases and common metal coordination modes</i>	<i>20</i>
<i>1.7</i>	<i>Project aims</i>	<i>26</i>
<i>2</i>	<i>Results and Discussion</i>	<i>30</i>
<i>2.1</i>	<i>Amino-pyridine Schiff-base and reductive amination reactions with p-formylcalix[4]arenes</i>	<i>30</i>
<i>2.1.1</i>	<i>Schiff-base imino products</i>	<i>31</i>
<i>2.1.2</i>	<i>Reductive amination products with p-formylcalix[4]arene</i>	<i>33</i>
<i>2.2</i>	<i>Schiff-base reactions between lower-rim protected p-aminocalix[4]-arenes and selected benzaldehydes</i>	<i>34</i>
<i>2.2.1</i>	<i>Tetra-propoxycalix[4]arene Schiff-bases</i>	<i>35</i>
<i>2.2.2</i>	<i>Bis-crown-ether calix[4]arene Schiff-bases</i>	<i>39</i>
<i>2.3</i>	<i>Crystallographic studies</i>	<i>44</i>
<i>3</i>	<i>Experimental</i>	<i>47</i>
	<i>Conclusion</i>	<i>66</i>
	<i>Future Work</i>	<i>67</i>
	<i>References</i>	<i>69</i>
	<i>Appendix</i>	<i>75</i>
	<i>Index of Compounds Synthesised</i>	<i>86</i>

## List of Figures

<b>Figure 1</b>	<i>Schematic representation of <b>a)</b> the lock and key principle, and <b>b)</b> the induced fit model of an enzyme binding a substrate.</i>	2
<b>Figure 2</b>	<i>Self-assembly of monomer <b>1</b> through complementary hydrogen-bonding interactions to form the “tennis ball” assembly <b>2</b>. Hydrogen atoms and peripheral functional groups are omitted for clarity.</i>	3
<b>Figure 3</b>	<i>Metal-directed assembly of triangular ligand <b>4</b> with directing metal centres <b>5</b> to form assembly <b>3</b>. Hydrogen atoms are omitted for clarity.</i>	4
<b>Figure 4</b>	<i><b>a)</b> Schematic representation of an ion-ion interaction in supramolecular chemistry. <b>b)</b> sodium 18-crown-6 complex representing an ion-dipole interaction.</i>	5
<b>Figure 5</b>	<i>Schematic representation of a pair of <b>a)</b> orthogonal dipoles, and <b>b)</b> opposing aligned dipoles.</i>	5
<b>Figure 6</b>	<i>Schematic showing <b>a)</b> hydrogen bonding interactions found between guanine and cytosine in DNA, and <b>b)</b> repulsive and attractive secondary interactions found in hydrogen bonded arrangements.</i>	6
<b>Figure 7</b>	<i>Schematic showing <b>a)</b> representation of <math>\pi</math>-stacking using benzene in the face-to-face and edge-to-face arrangements, and <b>b)</b> a top down view of the electron cloud found in a benzene ring indicating slightly negative and positively charged area.</i>	6
<b>Figure 8</b>	<i><b>a)</b> A vase illustrating a calix[4]arene shape. <b>b)</b> General nomenclature associated with calix[4]arenes.</i>	7
<b>Figure 9</b>	<i>The four main conformations found for calix[4]arenes where <b>R</b> and/or <b>R'</b> can be H, aromatic, aliphatic or combinations thereof.</i>	8
<b>Figure 10</b>	<i>Resorcinol[n]arene and pyrogallol[n]arene.</i>	9
<b>Figure 11</b>	<i>Single crystal X-ray structures of tetrakis(p-cyclohexyl)-biscrown-3-calix[4]arene (<b>12</b>) and tetra-nitro-tetrapropoxycalix[4]arene (<b>13</b>).</i>	11
<b>Figure 12</b>	<i>Calix[4]arene building blocks based used in the assembly of homo- and hetero-dimeric hydrogen-bonded capsules. Hydrogen atoms, lower-rim functionality and the tolyl groups of the urea units are omitted for clarity.</i>	15

<b>Figure 13</b>	<i>The assembly of <b>a)</b> CMRC into a hexameric hydrogen-bonded nano-capsule with structural water molecules, and <b>b)</b> C-alkylpyrogallol[4]arenes into related self-assembled capsules in the absence of structural water molecules. Water molecules are shown as red spheres, and hydrogen atoms and lower rim alkyl chains have been removed for clarity.</i>	16
<b>Figure 14</b>	<i>Schematic of upper-rim Schiff-base calix[4]arene <b>28</b> showing 4-pyridyl functionality.</i>	17
<b>Figure 15</b>	<i>Schematic of calix-tetraporphyrin <b>29</b>.</i>	18
<b>Figure 16</b>	<i>p-Sulfonatocalix[4]arene <b>30</b> and the encapsulation of a sodium 18-crown-6 complex by two molecules of <b>30</b>, resulting in the formation of the “Russian doll” assembly <b>31</b>. Hydrogen atoms are omitted for clarity.</i>	19
<b>Figure 17</b>	<i>Extended pyridyl functionalised resorcinol[4]arene <b>32</b> that assembles in a directed fashion with either palladium or platinum ions to form into the metal-organic capsule <b>33</b>. Hydrogen atoms, lower-rim R groups and additional ligands on metal centres are omitted for clarity.</i>	20
<b>Figure 18</b>	<i>Schiff base formed by the condensation of aniline with salicaldehyde to afford compound <b>34</b>.</i>	21
<b>Figure 19</b>	<i>Ligand <b>35</b> and the tetrahedral supramolecular assembly <b>36</b> resulting from metal-directed assembly. Hydrogen atoms are omitted for clarity.</i>	22
<b>Figure 20</b>	<i>Ligand (<b>37</b>, L) used to synthesise complex <b>38</b>, <b>39</b> and <b>40</b>. Hydrogen atoms are omitted for clarity.</i>	23
<b>Figure 21</b>	<i>Supramolecular building block <b>41</b> which self-assembles into <b>42</b> via the pyridine-nitrogen – zinc interaction. Hydrogen atoms are omitted for clarity.</i>	24
<b>Figure 22</b>	<i>Building block <b>43</b> used to form box shaped supramolecular assemblies.</i>	24
<b>Figure 23</b>	<i>Schematic of the mono-Schiff-base calixarene <b>44</b>, and the assembly mode formed with cupric ions.</i>	25
<b>Figure 24</b>	<i>Schematic of the Schiff-base calix[6]arene <b>46</b> used to form supramolecular complexes (<b>47</b>) with copper or nickel metal ions.</i>	26
<b>Figure 25</b>	<i>Protected and un-protected p-formylcalix[4]arenes to be used as starting materials in this study.</i>	26
<b>Figure 26</b>	<i>Other p-amino and p-formylcalix[4]arenes to be used as rigid or flexible starting materials in this study.</i>	27

<b>Figure 27</b>	<i>Amines and aldehydes selected for Schiff-base formation with p-formyl and p-aminocalix[4]arenes in this study.</i>	27
<b>Figure 28</b>	<i>Compounds <b>50</b> and <b>49</b> obtained via templated bis-crown-ether formation and formylation according to literature procedures.</i>	31
<b>Figure 29</b>	<i>Compounds <b>51-53</b> and <b>54</b> obtained from reaction of tetra-formyl bis-crown-ether calix[4]arene with the three isomers of amino-pyridine or aniline.</i>	32
<b>Figure 30</b>	<i>Compound <b>16a</b> synthesised by bromo-methylation of calix[4]arene and subsequent reaction with HMTA in TFA.</i>	33
<b>Figure 31</b>	<i>Compounds <b>56 - 59</b> synthesised by reductive amination of compound <b>16a</b> with aniline and the three isomers of amino-pyridine.</i>	34
<b>Figure 32</b>	<i>Compounds <b>18a</b> and <b>18b</b> to be used in Schiff-base formation with the selection of benzaldehydes shown.</i>	35
<b>Figure 33</b>	<i>Compounds <b>17a</b>, <b>18a</b> used in the synthesis of <b>60</b>.</i>	36
<b>Figure 34</b>	<i>Compounds <b>61</b> and <b>62</b> synthesised by the reaction of compound <b>18a</b> with benzaldehyde and salicaldehyde respectively.</i>	36
<b>Figure 35</b>	<i>Compounds <b>63</b>, <b>64</b> and <b>65</b> synthesised by the reaction of compound <b>18a</b> with the three isomers of methyl salicaldehyde.</i>	37
<b>Figure 36</b>	<i>Compounds <b>66</b>, <b>67</b> and <b>68</b> synthesised from the reaction of <b>18a</b> with 2-hydroxy-5-nitrobenzaldehyde, 2-hydroxy-5-chlorobenzaldehyde and 2-hydroxy-5-bromobenzaldehyde respectively.</i>	38
<b>Figure 37</b>	<i>Compounds <b>69</b> and <b>70</b> synthesised from the reaction of <b>18a</b> with two isomers of hydroxy-salicaldehyde.</i>	39
<b>Figure 38</b>	<i>Compounds <b>50</b>, <b>17b</b> and <b>18b</b>.</i>	40
<b>Figure 39</b>	<i>Compounds <b>71</b> and <b>72</b> synthesised from the reaction of <b>18b</b> with benzaldehyde and salicaldehyde respectively.</i>	41
<b>Figure 40</b>	<i>Compounds <b>73</b>, <b>74</b> and <b>75</b> synthesised from the reaction of <b>18a</b> with the three isomers of methyl-salicaldehyde.</i>	41
<b>Figure 41</b>	<i>Compounds <b>76</b>, <b>77</b> and <b>78</b> synthesised from the reaction of <b>18b</b> with 2-hydroxy-5-nitrobenzaldehyde, 2-hydroxy-5-chlorobenzaldehyde and 2-hydroxy-5-bromobenzaldehyde respectively.</i>	42
<b>Figure 42</b>	<i>Compounds <b>79</b> and <b>80</b> synthesised from the reaction of <b>18b</b> with 2,4-dihydroxybenzaldehyde and 2,5-dihydroxybenzaldehyde respectively.</i>	43



<b>Figure 43</b>	<i>Stick representation of the single crystal X-ray structure of compound <b>49</b> with a molecule of ethyl-acetate occupying the cavity of the bis-crown-ether calix[4]arene. Hydrogen atoms, except those associated with upper-rim formyl groups and the ethyl acetate guest are omitted for clarity. The two disordered formyl groups are shown in only one of two positions.</i>	44
<b>Figure 44</b>	<i>Packing diagram for compound <b>49</b> showing anti-parallel packing. Hydrogen atoms and ethyl acetate molecules are omitted for clarity.</i>	45
<b>Figure 45</b>	<i>Example of the systematic numbering of calix[4]arenes.</i>	47
<b>Figure 46</b>	<i>Intermolecular interaction of an iodo-group with the oxygen atoms of a nitro-group.</i>	67

## List of Schemes

<b>Scheme 1</b>	<i>Base and acid induced syntheses of p-tert-butylcalix[n]arenes where <math>n = 4-8</math> (<b>7a – e</b>) and 4–20 (<b>7a – q</b>) respectively.</i>	9
<b>Scheme 2</b>	<i>Reaction conditions employed in the selective alkylation of calix[4]arene. The use of a weak base and different reaction times affords the di- or tetra-ester in cone and 1,3-alternate conformations respectively. The use of a stronger base readily affords the tetra-ester in the cone-conformation.</i>	10
<b>Scheme 3</b>	<i>Synthesis of biscrown-ether calix[4]arene.</i>	11
<b>Scheme 4</b>	<i>De-tert-butylation of <b>7</b> to produce <b>14</b>.</i>	12
<b>Scheme 5</b>	<i>Bromination and formylation of calix[4]arene to afford p-bromo and p-formyl calix[4]arene derivatives <b>15</b>(<b>a</b> <math>R = H</math>, <b>b</b> <math>R = \text{alkyl}</math>) and <b>16</b>(<b>a</b> <math>R = H</math>, <b>b</b> <math>R = \text{alkyl}</math>) respectively.</i>	13
<b>Scheme 6</b>	<i>Synthesis of tetra-aminocalix[4]arenes <b>18</b>(<b>a</b> <math>R = n\text{-Pr}</math>, <b>b</b> <math>R = \text{CH}_2\text{CH}_2\text{OCH}_2\text{CH}_2</math>) via the tetra-nitrocalix[4]arene intermediates <b>17</b>(<b>a</b> <math>R = n\text{-Pr}</math>, <b>b</b> <math>R = \text{CH}_2\text{CH}_2\text{OCH}_2\text{CH}_2</math>).</i>	13
<b>Scheme 7</b>	<i>Synthesis of Schiff base calix[4]arenes. <b>19</b> is an example of an unprotected <b>16</b> and <b>20</b> for the protected calixarene.</i>	14
<b>Scheme 8</b>	<i>Reaction to be used to generate Schiff-base calix[4]arenes in this study.</i>	14
<b>Scheme 9</b>	<i>General Schiff-base reaction mechanism.</i>	21

## *List of Glossary*

Å <sup>3</sup>	Armstrong (10 <sup>-10</sup> m)
°C	Degrees centigrade
<sup>1</sup> H	Proton
bs	Broad singlet
cm <sup>-1</sup>	Wavenumber
CMRC	C-methylresorcinol[4]arene
DABCO	1,4-diazabicyclo[2.2.2]octane
DCM	Dichloromethane
dec.	Decomposes
DMF	Dimethylformamide
DMSO	Dimethyl sulfoxide
DNA	Deoxyribonucleic acid
ESI	Electrospray ionisation
Et <sub>2</sub> O	diethyl ether
EtOAc	Ethyl acetate
EtOH	Ethanol
g	Gram
h or hrs	Hour or Hours
HMTA	Hexamine
IR	Infrared
<i>J</i>	Coupling constants in Hertz
m	Mass
<i>m/z</i>	Mass-to-charge ratio
MALDI	Matrix-assisted laser desorption/ionization
mg	Milligram
[M+H] <sup>+</sup>	Molecular ion + hydrogen
MHz	Megahertz
min	Minutes
mL	Millilitre
mmol	Millimoles
[M+Na] <sup>+</sup>	Molecular ion + sodium
[M+Na-H] <sup>+</sup>	Molecular ion + sodium – hydrogen
mol	Moles

mol eq	Molar equivalents
MP	Melting point
MS	Mass spectrometry
MS (4 Å)	Molecular Sieves 4 Armstrong
NBS	<i>N</i> -Bromosuccinimide
Ni(AcO) <sub>2</sub>	Nickel(II) acetate
NMR	Nuclear magnetic resonance
-NO <sub>2</sub>	Nitro functional group
<i>p</i>	para
PhOH	Phenol
ppm	parts per million
RT	Room temperature
sat.	Saturated
<sup>t</sup> Bu	tertiary-butyl
<i>tert</i>	tertiary
TFA	Trifluoroacetic acid
THF	Tetrahydrofuran
UV/vis	Ultraviolet-visible
v/v	Volume/Volume ratio
δ	Chemical shifts

## ***List of Tables***

<b>Table 1</b>	<i>Atomic co-ordinates (<math>\times 10^4</math>) and equivalent isotropic displacement parameters (<math>\text{\AA}^2 \times 10^4</math>) with standard uncertainties (s.u.s) in parentheses. <math>U_{eq}</math> is defined as 1/3 of the trace of the orthogonalized <math>U_{ij}</math> tensor.</i>	76
<b>Table 2</b>	<i>Anisotropic displacement parameters (<math>\text{\AA}^2 \times 10^3</math>). The anisotropic displacement factor exponent takes the form:</i> $-2\pi^2[h^2 a^{*2} U_{11} + \dots + 2 h k a^* b^* U_{12}]$	79
<b>Table 3</b>	<i>Hydrogen atom co-ordinates (<math>\times 10^3</math>) and isotropic displacement parameters (<math>\text{\AA}^2 \times 10^2</math>) with s.u.s in parentheses.</i>	81
<b>Table 4</b>	<i>Interatomic distances (<math>\text{\AA}</math>) with s.u.s in parentheses.</i>	83
<b>Table 5</b>	<i>Angles between interatomic vectors (<math>^\circ</math>) with s.u.s in parentheses.</i>	84
<b>Table 6</b>	<i>Synthesised compounds.</i>	87

# *CHAPTER I*

## *Introduction*

# 1 Introduction to supramolecular chemistry

This area of chemistry, known as ‘supramolecular chemistry’, has been defined by Lehn, who was awarded the Noble Prize in chemistry in 1987 with Pedersen and Cram, as the ‘chemistry of molecular assemblies and of the intermolecular bond’, or as ‘chemistry beyond the molecule’.<sup>1</sup> Supramolecular chemistry is a relatively young discipline dating back to the 1960’s and early 1970’s, but some basic principles go back as far as the 19<sup>th</sup> century. One of the concepts dating back this far is the enzymatic mechanism known as the ‘lock and key’ principle, which was proposed by Emile Fischer (Figure 1a).<sup>1</sup> Enzymes use this principle to bind specific molecules in their binding sites without changing the overall conformation of the enzyme. Another principle related to the enzyme binding a substrate is the ‘induced fit’. This is where the enzyme has to change its conformation to fit a substrate as shown in Figure 1b.

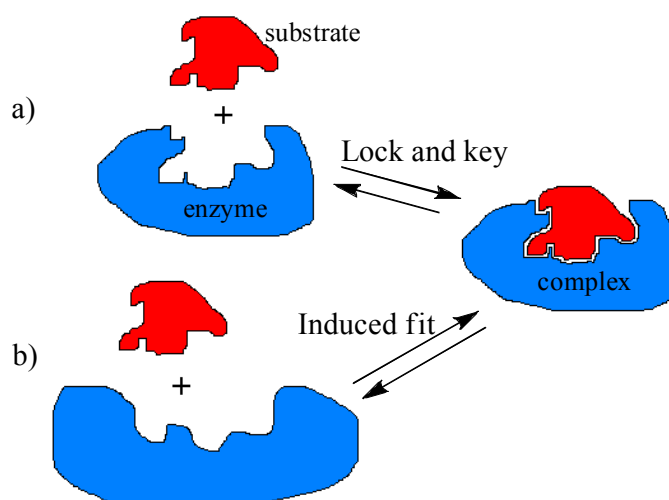


**Figure 1.** Schematic representation of **a)** the lock and key principle, and **b)** the induced fit model of an enzyme binding a substrate.

These concepts are involved in the self-assembly of supramolecular assemblies, where the host molecule relates to the enzyme and the guest to the substrate. Another fundamental discovery widely utilised in supramolecular chemistry is non-covalent interactions such as hydrogen bonding (section 1.1). Most supramolecular assemblies reported to date in this field are held together by such interactions or are specifically assembled by directing metal centres through metal-ligand interactions, as can be seen in later sections.<sup>1</sup>

One of the first molecular building blocks that was shown to self-assemble into a supramolecular assembly is shown in Figure 2.<sup>2,3</sup> Two molecules of monomer **1** assemble to afford the dimeric capsule **2**, also known as the ‘tennis ball’. This is a very apt example where a molecule was specifically designed to utilise hydrogen-bonding interactions to assemble into a supramolecular capsule. The internal cavity of **2** has an estimated volume of  $\sim 50 \text{ \AA}^3$ , which is big enough to encapsulate small molecules such as methane, ethane and the noble gases.<sup>2,3</sup> By changing the size of the aromatic backbone, different sized capsules can subsequently be synthesised. One such structure, related to **2**, is the ‘softball’.<sup>2,3</sup> This has a bigger internal cavity with a volume of approximately  $240 - 320 \text{ \AA}^3$ . Both capsule-types can capture and release smaller molecules (relative to cavity size), while bigger capsules can bind multiple guests.

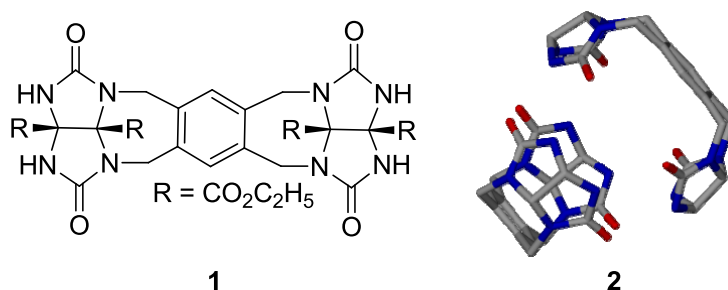


**Figure 2.** Self-assembly of monomer **1** through complementary hydrogen-bonding interactions to form the “tennis ball” assembly **2**. Hydrogen atoms and peripheral functional groups are omitted for clarity.<sup>2,3</sup>

The ‘host-guest’ chemistry concept is vital in supramolecular chemistry. This area of chemistry involves the binding of a guest molecule such as a solvent molecule, metal ion, or small complex within a host such as a calix[4]arene. This can be facilitated by various non-covalent interactions. One definition of a host is ‘a molecular entity that possesses a *convergent* binding site’,<sup>1</sup> while a guest can be defined as ‘possessing a *divergent* binding site’.<sup>1</sup> Examples of hosts, other than enzymes, are synthetic cyclic compounds possessing a sizeable central hole or cavity, *e.g.* crown-ethers, calix[*n*]arenes and cyclodextrins.<sup>1</sup>

An alternative type of host assembly is **3**.<sup>4</sup> This metal-organic polyhedron is constructed from four triangular ligands, **4**, and six directing palladium-metal complexes **5**. The triangular ligands occupy the sides of a trigonal bipyramid, while the directing metal centres occupy the vertices of the assembly, acting as hinges. Ligands such as **4** have been widely studied in the literature for assembly purposes.<sup>3-6</sup> The use



of these assembly principles is described in the context of calixarene building units later in this chapter.

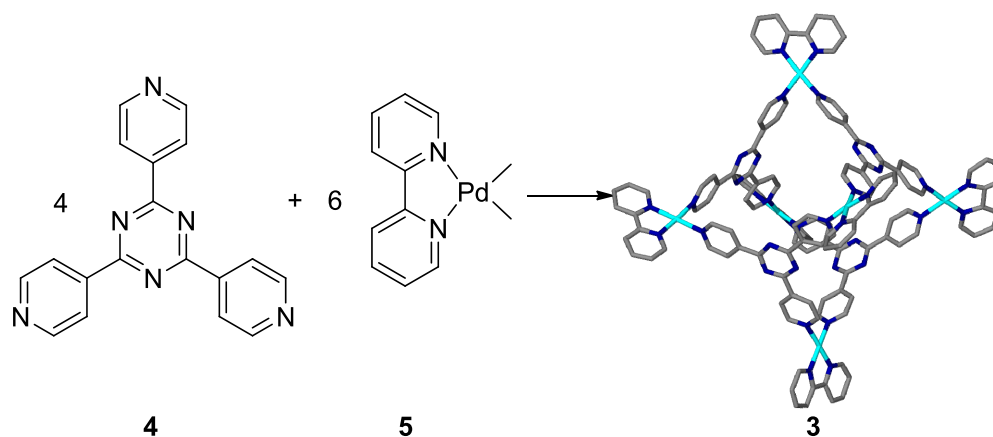


**Figure 3.** Metal-directed assembly of triangular ligand **4** with directing metal centres **5** to form assembly **3**. Hydrogen atoms are omitted for clarity.<sup>4</sup>

### 1.1 Common interactions observed in supramolecular chemistry

As mentioned above, there are many different interactions involved in the formation of supramolecular assemblies. These differ in their strength and nature, those most commonly observed are non-covalent interactions.<sup>1</sup> The strongest of these is the ion-ion interactions. Its strength is similar to that of a normal covalent bond, a very good example of this is sodium chloride. Although this is not a supramolecular assembly, it illustrates the strength of this interaction and the concept very well. In the cubic lattice, which is adopted in the crystal structure of sodium chloride, each sodium ion is interacting with six chlorine anions and *vice versa* to form the solid state structure. An example of this in supramolecular chemistry is the interaction between 2,4,6-tris(DABCO-*N*-methyl)mesitylene and  $[\text{Fe}(\text{CN})_6]^{3-}$  (Figure 4 a).<sup>1,7</sup>

Another strong interaction is the ion-dipole interaction between an ion and a polar molecule. An example of this is the sodium ion dissolved in water, where six water molecules coordinate around the ion.<sup>1</sup> In supramolecular chemistry, a famous example of this is the interaction of the family of crown ethers with different alkali metal cations (Figure 4 b) to afford varied degrees of binding depending on the complementarity of host-to-guest size.<sup>1</sup>

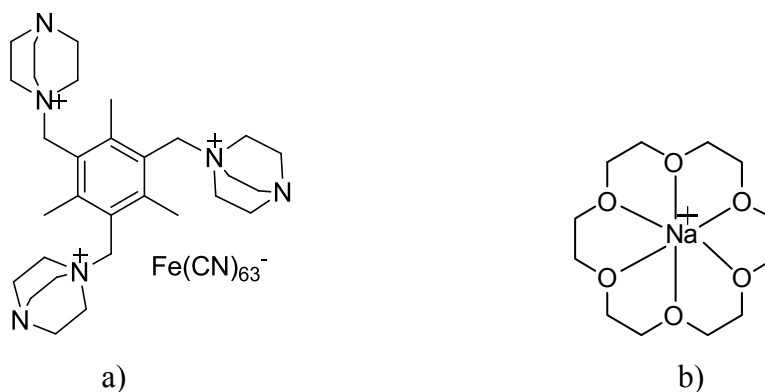


**Figure 4.** a) Schematic representation of an ion-ion interaction in supramolecular chemistry.<sup>7</sup> b) sodium 18-crown-6 complex representing an ion-dipole interaction.<sup>1</sup>

Dipole-dipole interactions are commonly observed in crystal structures. There are two different alignments of dipoles for this interaction. One is where a single pair of dipoles on adjacent molecules are orthogonal (Figure 5a), while the other is where the two opposing dipoles align themselves as shown in Figure 5b. This interaction can be observed with carbonyl compounds.<sup>1</sup>

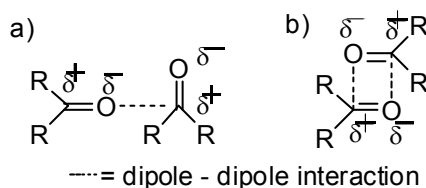


**Figure 5.** Schematic representation of a pair of a) orthogonal dipoles,<sup>1</sup> and b) opposing aligned dipoles.<sup>1</sup>

The hydrogen bonding interaction is a very widely spread and important interaction in supramolecular chemistry. This interaction normally occurs when a hydrogen (H) atom is connected to an electronegative atom donor (D) and usually a similar electronegative atom with a lone pair of electrons as an acceptor (A), commonly written as D-H...A.<sup>1</sup> There are many different geometries of hydrogen bonding known, *e.g.* linear, bent, donating bifurcated, accepting bifurcated, trifurcated and three centred bifurcated.<sup>1</sup> One of the best examples of this type of interaction is in the base pairing in DNA (Figure 6a).<sup>1</sup> Secondary interactions can also occur in hydrogen bonding and can be either attractive or repulsive (Figure 6b).

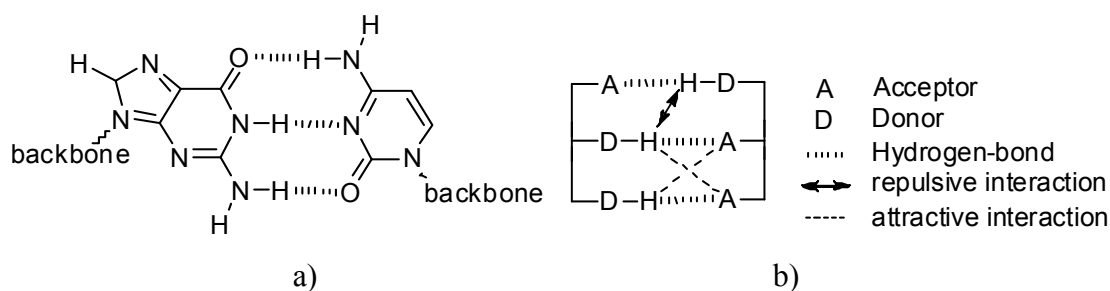


**Figure 6.** Schematic showing **a)** hydrogen bonding interactions found between guanine and cytosine in DNA,<sup>1</sup> and **b)** repulsive and attractive secondary interactions found in hydrogen bonded arrangements.<sup>1</sup>

Another commonly observed and important phenomenon is the  $\pi$ -stacking interaction. This interaction often occurs between an electron-rich and an electron-poor aromatic ring. There are two different ways by which this interaction can occur: face-to-face and edge-to-face as shown in Figure 7a.<sup>8</sup> An aromatic ring has a negative cloud of electrons above and below the plane of the ring, and a positively charged area between them (Figure 7b). Due to the negatively charged electron cloud, the face-to-face stacking is typically off-centred, as it would otherwise be a strong repulsive interaction. Cation<sup>9</sup>- and anion- $\pi$ -interactions<sup>10</sup> are related and as the names imply, there is a cation or anion interacting with the aromatic ring respectively.

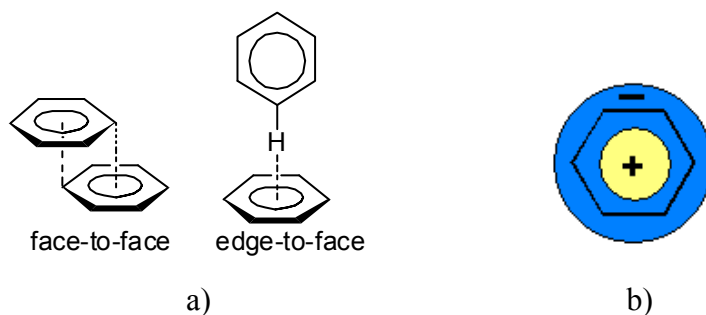


**Figure 7.** Schematic showing **a)** representation of  $\pi$ -stacking using benzene in the face-to-face and edge-to-face arrangements, and **b)** a top down view of the electron cloud found in a benzene ring indicating slightly negative and positively charged area.

The last of the intermolecular interactions commonly involved in supramolecular chemistry are van der Waals forces, close packing and closed shell interactions. All of those interactions are relatively small and weak. Van der Waals forces arise when an electron cloud is polarised due to the proximity of an adjacent nucleus. Crystal close packing, according to the theory of Kitaigorodskii,<sup>11</sup> is the maximisation of favourable isotropic van der Waals interactions. The presence of a large number of van der Waals

forces has been shown to dominate the assembly of molecules that contain long alkyl chains.

Closed-shell interactions are not normally expected, because they occur with the closed shell of neutral or like-charged atoms. Examples of this phenomenon are secondary bonding interactions, halogen bonding and metalophilic interactions.<sup>12</sup>

## 1.2 Calixarenes

The name calixarene comes from the Latin word '*calix*' meaning vase or cup, and '*arene*' representing an aromatic unit (Figure 8a).<sup>13,14</sup> This can be taken literally because it has a cavity like a cup and the backbone is made predominantly of aromatic rings. Calix[4]arenes are commonly encountered in supramolecular chemistry and their basic structure can be seen below in Figure 8b. The aromatic rings in the backbone of the calix[4]arene are connected through bridging methylene groups. The molecular skeleton of the calix[4]arene is divided into three different areas; the upper-rim, the lower-rim and the annulus (Figure 8b). Calix[4]arenes often possess lower-rim OH groups that form hydrogen-bonded rings at the base, holding the calixarene in a cone-conformation.<sup>13,14</sup> Functionalisation at the 'lower rim' with different groups is also possible and this is discussed in section 1.3.1. The top of the molecule (the upper rim) can be functionalised with various groups possessing different properties, and examples of such functionalisation are shown in section 1.3.2. The bridging methylene groups constitute the '*annulus*', and it is possible to replace these with sulfur atoms or sulfinyl groups for example.<sup>13-15</sup>

---

**Figure 8.** a) A vase illustrating a calix[4]arene shape. b) General nomenclature associated with calix[4]arenes.<sup>13,14</sup>

Calix[4]arenes have four main isomers as shown in Figure 9. Some calix[4]arenes can have distorted structures, an example of which exists in the cone conformer. In this conformation, two phenyl rings in opposite positions within the framework can be bent inwards towards each other while the remaining two splay outwards to afford a ‘pinched cone’.<sup>16</sup> Despite this feature, the ‘cone conformation’ is used to describe any situation where all four upper-rim **R**-groups are pointing in the same direction, which forms a very useful cavity in between the **R**-groups. The ‘partial-cone’ occurs when one of the groups is switched around. The other two conformations are where two of the **R**-groups are pointing in the opposite direction. The ‘1,2-alternate’ is where neighbouring units are pointing in the same direction, and the ‘1,3-alternate’, the two opposite are pointing in the same direction.<sup>13-15</sup>

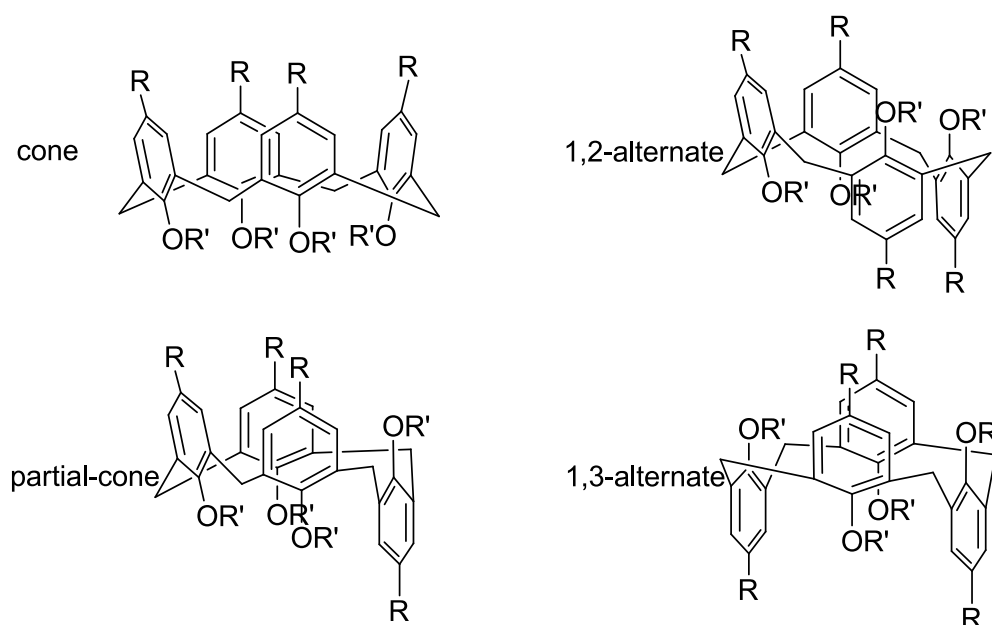


**Figure 9.** The four main conformations found for calix[4]arenes where R and/or R' can be H, aromatic, aliphatic or combinations thereof.<sup>13-15</sup>

Resorcinol[4]arenes and pyrogallol[4]arenes are another type of calix[4]arene and their structures are shown in Figure 10. Both of these types of molecule have similar lower rim characteristics (generally alkyl chains) which differ from typical calix[4]arenes by the absence of the hydroxyl or alkoxy groups at the lower rim. The upper rim has two or three hydroxyl groups present for the resorcinol[4]arenes<sup>17-19</sup> and pyrogallol[4]arenes respectively.<sup>20,21</sup>

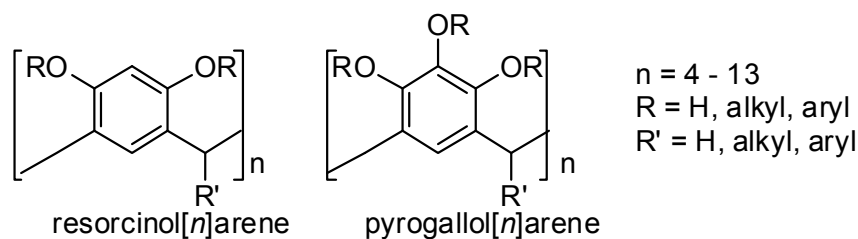
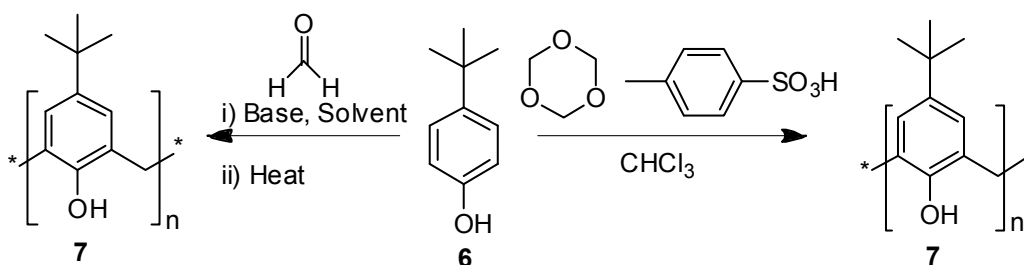


**Figure 10:** Resorcinol[ $n$ ]arene and pyrogallol[ $n$ ]arene.<sup>22</sup>

These molecules are versatile building blocks and have been shown to have very interesting supramolecular properties in the formation of a wide range of different structures. Same examples are discussed later in this chapter.

### 1.3 Synthesis of calixarenes

There are two main synthetic routes for the synthesis of calixarenes, these being base and acid induced reactions. The base reaction is commonly used to make smaller calix[ $n$ ]arenes ( $n = 4 - 8$ ) (Scheme 1). The size of the macrocycle made is highly dependent on the reaction conditions employed. For example, in order to make *p*-tert-butylcalix[4]arene, *p*-*tert*-butylphenol (**6**) formaldehyde and NaOH are used to produce a polymer intermediate, which is heated at reflux in diphenyl ether at 260°C for 4 h. This process cracks the polymer to smaller ring structures (calix[ $n$ ]arenes) and forms a small percentage of different isomers. Although this is the case, the main isomer obtained is the tetramer, and this is purified by recrystallisation. The acid-induced reaction can be used to make calix[ $n$ ]arenes where  $n = 4 - 20$  (Scheme 1). This less frequently employed reaction route produces a mixture of various isomers, which can then be separated by column chromatography.<sup>13,14,23</sup>

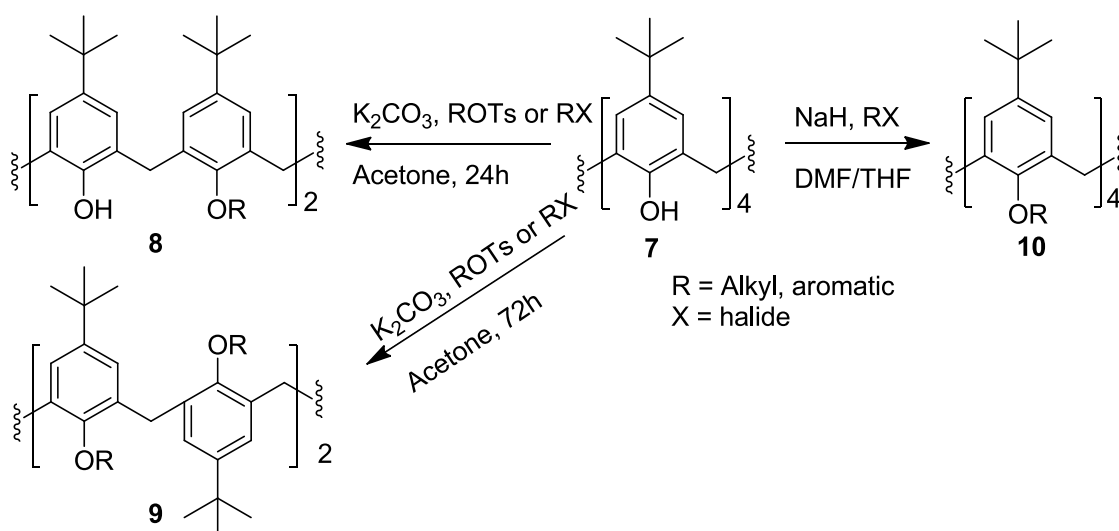


**Scheme 1.** Base and acid induced syntheses of *p*-tert-butylcalix[ $n$ ]arenes where  $n = 4-8$  (**7a – e**) and 4–20 (**7a – q**) respectively.<sup>14,23</sup>

The selective production of calix[*n*]arenes is an area of great interest but it is beyond the scope of this study to describe all of the routes investigated to this end.

### 1.3.1 Manipulation of the lower rim

The hydroxyl group at the lower rim of calix[4]arene can be readily converted into ethers by literature methods (Scheme 2).<sup>14,23,24</sup> Variation in reaction conditions can afford calix[4]arenes that are di-, tri- or tetra-substituted at the lower rim.<sup>14,23</sup> Again the synthetic chemistry associated with the manipulation of the lower rim is wide ranging and only limited numbers of examples are discussed below.

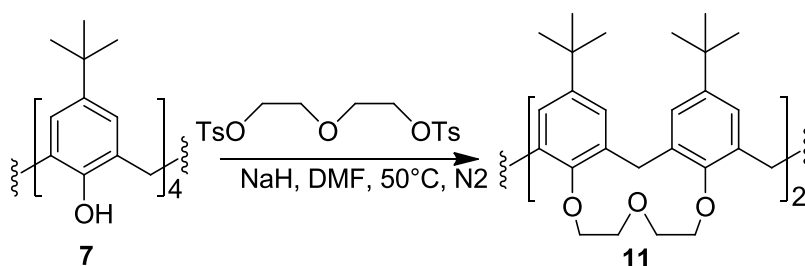


**Scheme 2.** Reaction conditions employed in the selective alkylation of calix[4]arene. The use of a weak base and different reaction times affords the di- or tetra-ether in cone and 1,3-alternate conformations respectively. The use of a stronger base readily affords the tetra-ether in the cone-conformation.

As seen in Scheme 2, di-ether **8** can be obtained under mild, basic conditions within a 24 h period.<sup>23</sup> In the presence of a higher concentration of base and alkyl halide, the tetra-ether **9** is formed in the 1,3-alternate conformation over a period of 72 h.<sup>15</sup> Under more forcing conditions (with sodium hydride as the base), tetra-ether **10** can be synthesised in a cone conformation within approximately 4 h.<sup>25,26</sup> An important feature of ester formation at the lower rim of the calix[4]arene framework is that alkyl chain length must be sufficient to prevent inversion of the molecule through the annulus.<sup>3,27</sup> It is known from literature that a propyl chain is necessary to prevent this inversion in a calix[4]arene. Although this is the case, the resulting tetra-

propoxycalix[4]arene retains some degree of flexibility, and this general calixarene framework often adopts the pinched cone conformation in the solid state.

Bis-crown-ethers can also be formed at the lower rim of the calix[4]arene framework. This locks the molecule into a relatively rigid cone conformation. The general synthesis of this bis-crown-ether is shown in Scheme 3.<sup>28,29</sup> Reaction of compound **7** with sodium hydride (acting as a base and template) and diethylene glycol ditosylate results in the formation of the bis-crown ether derivative that possesses pseudo C<sub>4</sub>-symmetry within the resulting molecule (when ignoring the lower rim).



**Scheme 3.** Synthesis of biscrown-ether calix[4]arene.<sup>28,29</sup>

By comparing the single crystal X-ray structures of a bis-crown-ether calix[4]arene (**12**) and tetra-nitro-tetrapropoxycalix[4]arene (**13**), it is clear that crown ether derivative adopts a true cone conformation (Figure 11). Tetra-nitro-tetrapropoxycalix[4]arene adopts the pinched cone conformation, with two NO<sub>2</sub> groups pointing outwards and the remaining two are pushed towards the centre of the calixarene cavity. This comparison stresses how a small change to the lower rim can affect the conformation and this will be utilised in this study through the synthesis of systems based on both framework types.

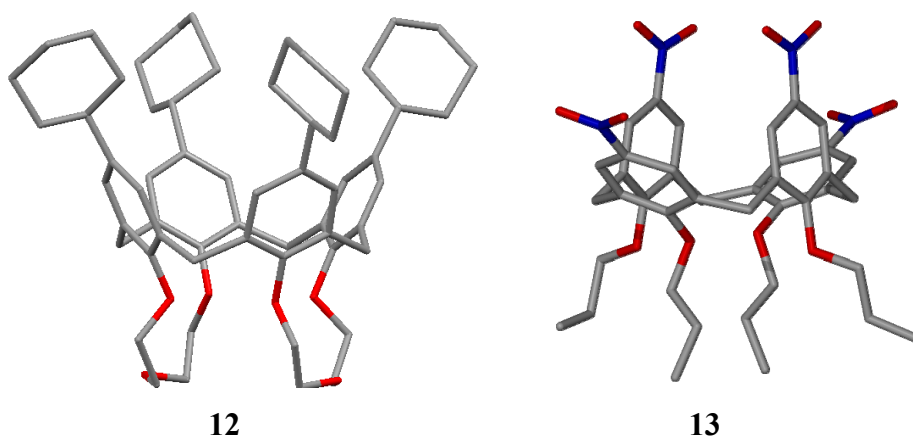
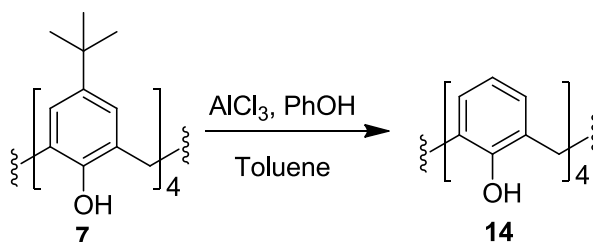


**Figure 11.** Single crystal X-ray structures of tetrakis(*p*-cyclohexyl)-biscrown-3-calix[4]arene (**12**)<sup>28</sup> and tetra-nitro-tetrapropoxycalix[4]arene (**13**).<sup>30</sup>



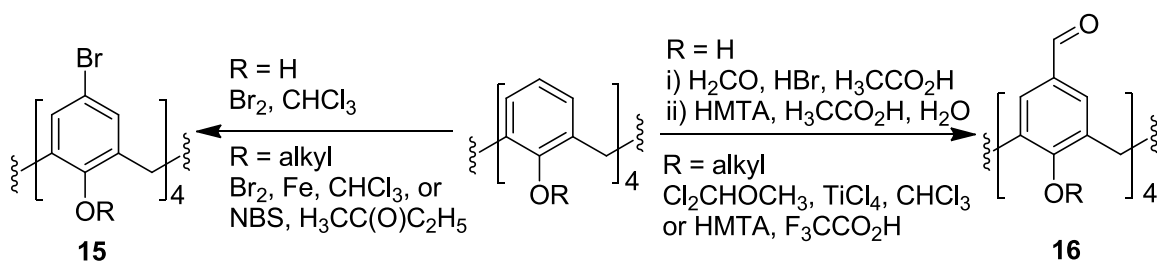
### 1.3.2 Manipulation of the upper rim

As the majority of calix[*n*]arene starting materials possess *p*-*tert*-butyl functionality (due to ease of synthesis), the first reaction typically performed on the upper-rim is de-*tert*-butylation (Scheme 4).<sup>31</sup> By removing this group, the *para*-position is open to manipulation and introduction of different functional groups.<sup>1,14</sup> Such synthetic alteration can dramatically change the supramolecular properties of these ligands, including the size of the internal cavity, and the selectivity towards various ions and small molecules for example.<sup>1,14,32,33</sup> This can be achieved by changing the electronegativity of the upper-rim *e.g.* by introducing atoms such as oxygen, nitrogen and sulfur.<sup>1,3,14,34</sup> These atoms have lone pairs of electrons which can be donated to a metal centre, take part in the formation of hydrogen bonds with small molecules, or interact with other ions.<sup>1-3,18,34,35</sup> The associated chemistry at the upper rim is also wide ranging, and although some of the possible synthetic modification can be found in this section, there are many more examples to be found in the literature.<sup>31,36-46</sup>



**Scheme 4.** De-*tert*-butylation of **7** to produce **14**.

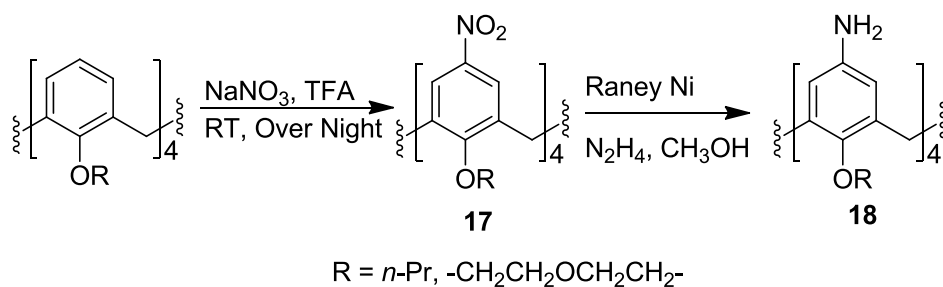
The de-*tert*-butylation (Scheme 4) involves **7**, phenol and aluminium trichloride dispersed in toluene. The reaction normally achieves high yields of the desired material within 3 – 4 h after workup.<sup>31</sup> Scheme 5 shows the introduction of bromine to the upper-rim of the calix[4]arene framework. Compound **15a** can be reacted under the lithium-halogen exchange reaction conditions to introduce a variety of different functional groups.<sup>36</sup> It is also worth noting that the protected calixarene **15b** requires harsher reaction conditions to introduce the bromine, requiring the addition of iron or NBS, compared to just elemental bromine for the synthesis of unprotected calixarene **15a**.<sup>37</sup>



**Scheme 5.** Bromination and formylation of calix[4]arene to afford *p*-bromo and *p*-formyl calix[4]arene derivatives **15**(a R = H, b R = alkyl) and **16**(a R = H, b R = alkyl) respectively.

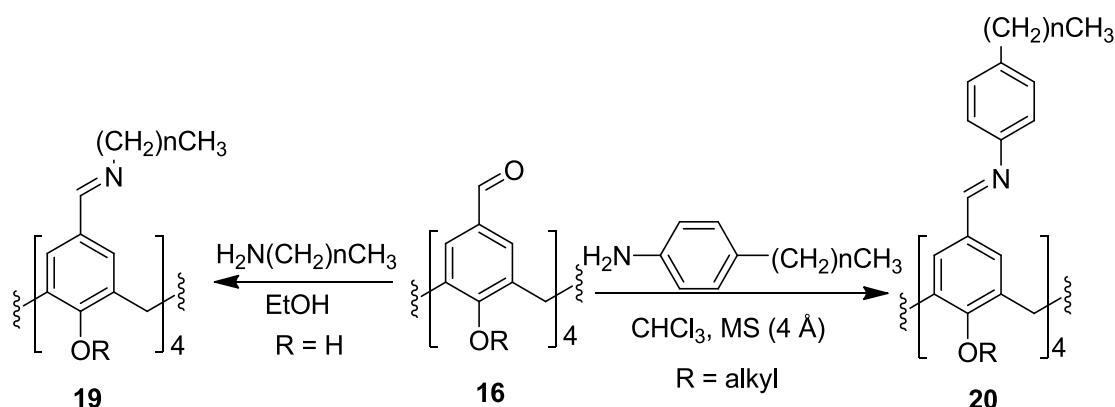
Formylation of both protected and unprotected calixarenes is also shown in Scheme 5. The formylation of protected calixarenes can be carried out as a one pot reaction with titanium(IV) chloride and 1,1-dichloromethyl methyl ether.<sup>38</sup> By performing this formylation reaction at different temperatures, or by substituting titanium(IV) chloride with tin chloride, different formylation compounds can be synthesised to form selectively mono-, di-, tri- or tetra-formylcalix[4]arenes.<sup>38-42</sup> If tetra-formyl derivatives are required, formylation can be carried out by reacting lower-rim protected calix[4]arenes with hexamethylenetetramine (HMTA) in trifluoroacetic acid.<sup>38,43</sup> In order to introduce formyl functionality to the upper-rim of a lower-rim hydroxyl calix[4]arene, it is first necessary to bromo-methylate the upper-rim by reaction with hydrogen bromide and *p*-formaldehyde.<sup>24,37</sup> Subsequent reaction with HMTA in acetic acid affords *p*-formylcalix[4]arene (**16**) in good yield.<sup>24,39</sup>

Scheme 6 shows the synthesis of lower-rim protected tetra-amino-calix[4]arene first by the nitration of the *p*-position with sodium nitrate in trifluoroacetic acid to afford compound **17**. Subsequent reduction with Raney nickel and hydrazine affords the desired tetra-amino derivatives in good yield.



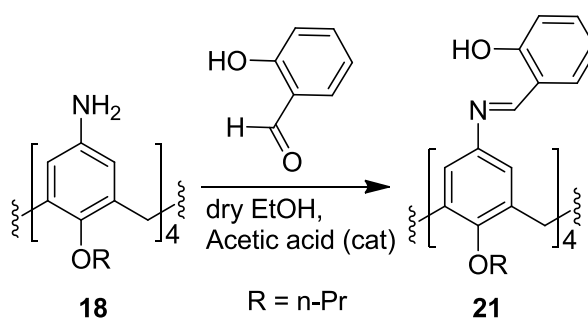
**Scheme 6.** Synthesis of tetra-aminocalix[4]arenes **18**(a R = *n*-Pr, b R = CH<sub>2</sub>CH<sub>2</sub>OCH<sub>2</sub>CH<sub>2</sub>) via the tetra-nitrocalix[4]arene intermediates **17**(a R = *n*-Pr, b R = CH<sub>2</sub>CH<sub>2</sub>OCH<sub>2</sub>CH<sub>2</sub>).<sup>43,44</sup>

Uses of tetra-*p*-formylcalix[4]arenes include their oxidation to afford *p*-carboxylatocalix[4]arenes as another type of building block for self-assembly,<sup>45</sup> or as starting materials in Schiff-base reactions such as those shown in Scheme 7. The condensation reaction introduces an aromatic amine compound to a calix[4]arene upper-rim. The Schiff-base reactions are carried out at either RT or at reflux in ethanol or chloroform.<sup>38,46</sup> Literature examples of this reaction include the use of alkylamines with lower-rim hydroxycalix[4]arene (**19**),<sup>39</sup> and aryl amines with a lower-rim *O*-alkyl ester calix[4]arene (**20**, Scheme 7).<sup>38</sup>



**Scheme 7.** Synthesis of Schiff base calix[4]arenes. **19** is an example of an unprotected **16** and **20** for the protected calixarene.

Another literature example of Schiff-base reaction at the upper-rim of a calix[4]arene-*O*-alkyl ester is the reaction shown in Scheme 8.<sup>44</sup> Here the aldehyde and amine are switched around relative to the reaction route shown in Scheme 7.



**Scheme 8.** Reaction used to generate Schiff-base calix[4]arenes in this study.

Although literature precedent exists for these types of reaction at the upper-rim of a calix[4]arene, variation in the types of aryl unit (in the example in Scheme 7) or the introduction of functional groups to the ring of the sicaldehyde starting material

(Scheme 8) has not been explored. This variation is carried out as part of this study in order to produce a library of potentially useful building blocks.

#### 1.4 Hydrogen- bonded calixarene structures

An example of a small assembly (the ‘tennis ball’) held together by complementary hydrogen bonds was described in an earlier section of this chapter.<sup>2,3</sup> In just the same way as with small building blocks, the introduction of different functionality to the upper- or lower-rim of a calixarene allows for the programmed isolation and characterisation of different-sized non-covalent molecular capsules<sup>3,20,32,34,35</sup> and nanotubes.<sup>47-51</sup> Calixarene **22a** (Figure 12) is an example of a self-assembling building block that produces a small dimeric capsule with an internal cavity volume of around 180 Å<sup>3</sup>.<sup>3</sup> This array is held together by 16 complementary hydrogen bonds around the seam of the capsule, which are formed when the secondary ureas at the upper-rim of both calixarenes interact favourably with each other. Synthetic adaptation of this calixarene system allows for the assembly of a hetero-dimeric capsule **23** by combining ligands **22a** and **22b**.<sup>2,3,35</sup>

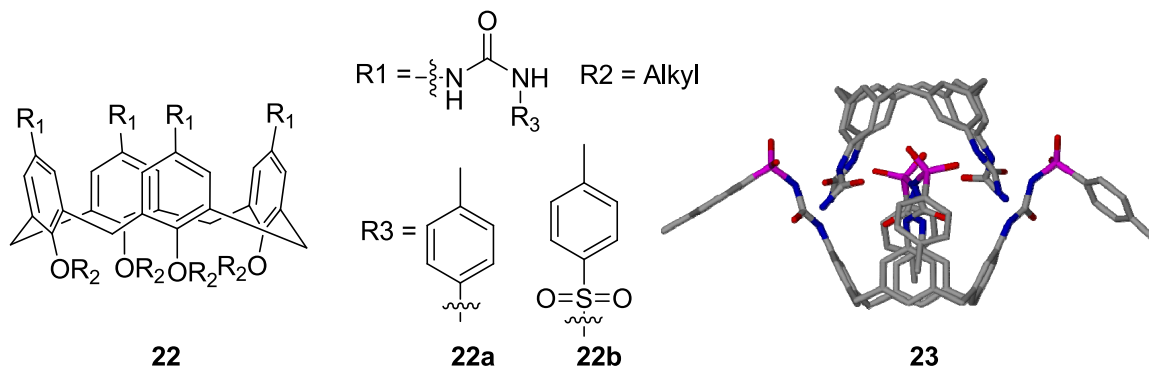


**Figure 12.** Calix[4]arene building blocks based used in the assembly of homo- and hetero-dimeric hydrogen-bonded capsules.<sup>2,3</sup> Hydrogen atoms, lower-rim functionality and the tolyl groups of the urea units are omitted for clarity.

Another interesting hetero-dimeric hydrogen-bonded capsule system has been investigated by Schrader and co-workers.<sup>52</sup> These dimeric-capsules are held together by both ionic and hydrogen bonding interactions. This was achieved by substituting the upper rim of one calixarene with aniline groups and the other with either phosphonate or carboxylate groups.<sup>52</sup>

Relatively small systems have been described above, and one of the first structures to be constructed with an cavity greater than 1000 Å<sup>3</sup> was composed of *C*-methylresorcinol[4]arene (CMRC, **24**, Figure 13).<sup>53</sup> Six CMRC subunits and eight structural water molecules to produce the hexameric structure **25** that encapsulates nitrobenzene molecules on the capsule interior, that is estimated to have a cavity volume of ~ 1375 Å<sup>3</sup>.<sup>53</sup> The whole structure is held together by 60 intermolecular hydrogen bonds and this system has been extensively studied by Atwood,<sup>54-56</sup> Rebek<sup>57,58</sup> and others<sup>59</sup> in both solution and the solid state with various different experimental techniques such as X-ray diffraction, NMR and MS. Using different organic solvents, the stability of the capsule with respect to the resorcinolarene monomer exchange was analysed, and it was found that the most stable hexameric capsule was achieved when chloroform was used compared to DCM or benzene.<sup>58</sup>

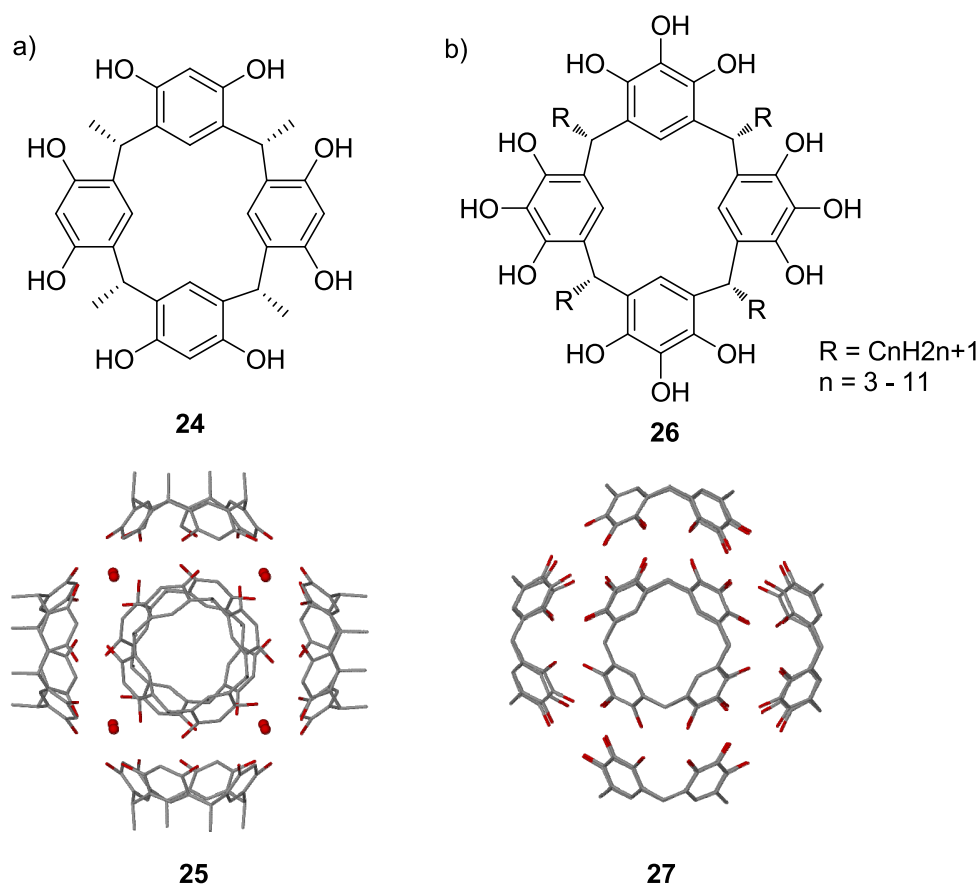


**Figure 13.** The assembly of **a)** CMRC into a hexameric hydrogen-bonded nano-capsule with structural water molecules, and **b)** *C*-alkylpyrogallol[4]arenes into related self-assembled capsules in the absence of structural water molecules. Water molecules are shown as red spheres, and hydrogen atoms and lower rim alkyl chains have been removed for clarity.

The *C*-alkylpyrogallol[4]arenes (general formula shown as **26** in Figure 13) are closely related to CMRC. Crystallisation of these building blocks from various solvents results in the formation of similarly sized, hexameric, hydrogen-bonded capsules that are estimated to have an internal cavity volume of  $\sim 1250 \text{ \AA}^3$ .<sup>54,60-62</sup> The introduction of additional upper-rim hydroxyl groups results in the formation of 72 intermolecular hydrogen bonds in the capsule seam, and removes the need for structural water molecule in the capsule formation. No water molecules are present in this structure but 10 acetonitrile molecules are present inside the assembly. Due to the increased number of hydrogen bonds present in the capsule, this assembly is more stable than assembly **25**, and the capsule is stable towards various species that would disrupt the key hydrogen-bonded capsule seam.<sup>20</sup>

The final example of hydrogen-bonded calixarene structures in this section describes the assembly of Schiff-base compound **28** (Figure 14).<sup>63</sup> Due to the synthetic route employed to reach compound **28**, the calixarene exists in the 1,3-alternate conformation with subsequently divergent 4-pyridyl Schiff-base functionality. When crystallised from nitromethane with 4,4'-biphenol, a hydrogen-bonded quintuple helix structure is formed. This network consists of a 1:1:1 ration of solvent:**28**:biphenol and stresses the importance of control over calixarene conformation through synthesis.<sup>63</sup>

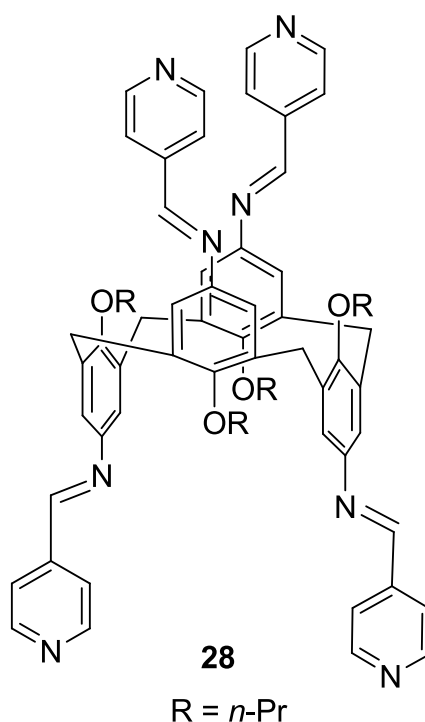


**Figure 14.** Schematic of upper-rim Schiff-base calix[4]arene **28** showing 4-pyridyl functionality.

## 1.5 Metal templated calixarene structures

As stated earlier, metals can be introduced into systems in order to give some degree of flexibility to supramolecular assemblies if the ligands are very rigid. These metals can act as hinges and give the components the necessary movement to assemble into a structure.<sup>3,4-6,64,65</sup> In some literature examples, ligands used in the formation of metal-organic capsules are rather rigid and need the metal centres to act as hinges.<sup>3</sup> An advantage of using metals to form supramolecular assemblies is that the resulting structures often have greater stability and rigidity when compared to hydrogen-bonded analogues (should they exist). Alternatively, and depending on the required function of a system, hydrogen-bonded analogues of some metal-organic systems complexes can be used if reversible encapsulation of guest molecules is preferred.<sup>61,66</sup>

There are numerous examples of metal-templated assemblies and it is beyond the scope of this document to describe all of these. One such example was reported by Hunter and co-workers, and is a system based on calix-tetraporphyrin (**29**, Figure 15) that assembles with zinc metal centres.<sup>67</sup> By changing the stoichiometry of the ligand and a bidentate spacer (1,4-diazabicyclo[2.2.2]octane), various supramolecular diametric-capsules can be synthesised that possess cavities of varied size. The ability to change the volume of encapsulated space allow for the tuning of host properties towards different ions and molecules.<sup>67</sup>

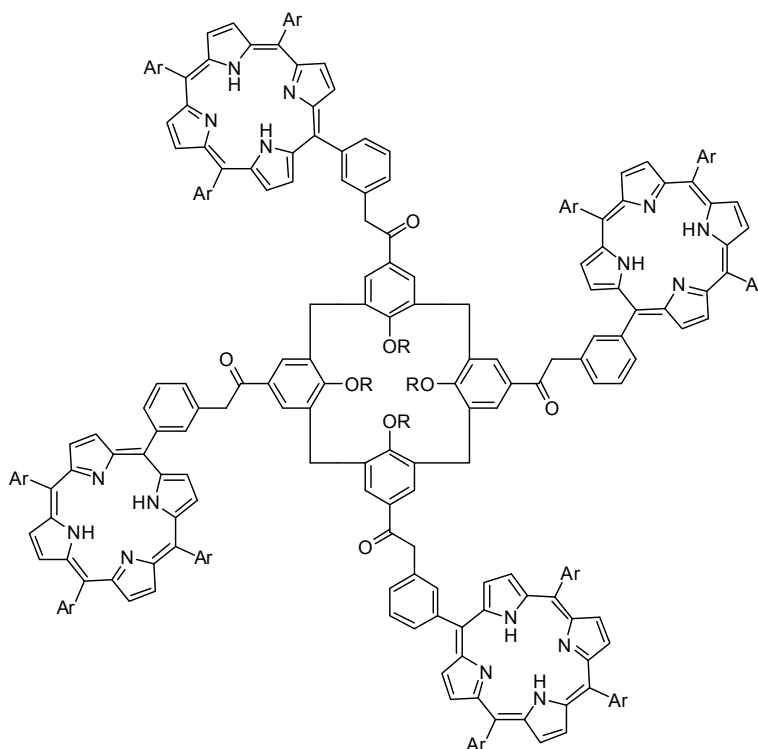


**Figure 15.** Schematic of calix-tetraporphyrin **29**.

A *p*-functionalised calix[4]arene that shows interesting supramolecular assembly properties is *p*-sulfonatocalix[4]arene (**30**, Figure 16).<sup>3,48,49</sup> The assembly chemistry of this building block is well explored and although it typically forms anti-parallel bi-layer arrays containing guest molecules, a number of particularly notable structures are discussed here. When the sodium salt of **30** is crystallised in the presence of one equivalent of pyridine-*N*-oxide and half an equivalent of La(NO<sub>3</sub>)<sub>3</sub>, the molecular components spontaneously assemble into a spherical structure.<sup>48</sup> The spherical assembly conforms to icosahedral symmetry and twelve molecules of **30** occupy the vertices of this arrangement. The resulting structure is held together by numerous intermolecular interactions including hydrogen bonds, van der Waals forces, metal-ligand interactions and electronic contacts. A key feature of the assembly is that lanthanide ions act as hinges between neighbouring calixarene clusters. The assembly has an internal volume of ~ 1700 Å<sup>3</sup>, which is occupied by 30 ordered water molecules and 2 hydrated sodium ions. When the pyridine-*N*-oxide guest is exchanged for 18-crown-6, an alternative type of structure is formed.<sup>49</sup> Sodium or lanthanide metals occupy the crown ether cavities and the molecular components assemble into what has been termed ‘*Russian dolls*’ (**31** in Figure 16).<sup>3,49,68</sup> This is best described as a host within a host, and by varying stoichiometries in this system, it is possible to assemble spherical structures based on the cuboctahedron Archimedean solid.<sup>49</sup> Twelve molecules occupy the vertices of the polyhedron, and these are linked by ‘*Russian dolls*’.

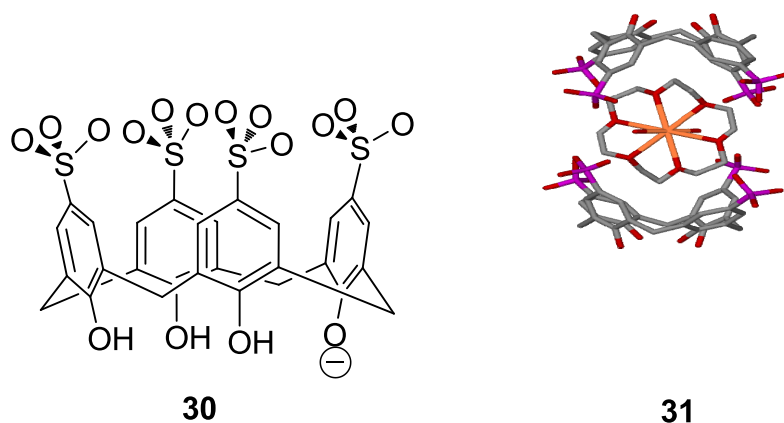


**Figure 16.** *p*-Sulfonatocalix[4]arene **30** and the encapsulation of a sodium 18-crown-6 complex by two molecules of **30**, resulting in the formation of the “*Russian doll*” assembly **31**.<sup>68</sup> Hydrogen atoms are omitted for clarity.



Compound **30** can also be used to form nanotubular arrays by simply changing the stoichiometries of **30** to lanthanum nitrate to pyridine-*N*-oxide.<sup>48</sup> Each nanotube is linked to a neighbouring assembly by lanthanum hinges that coordinate to calixarene upper-rim sulfonate groups. This is an excellent example of how crystallisation conditions and reactant ratios can influence supramolecular assembly formation.

There are a number of examples in which calixarenes or resorcinolarenes appended with upper-rim pyridyl or extended pyridyl functionality have been used in the formation of metal-organic structures.<sup>18,21,69,70</sup> These ligands are generally rigid due to the presence of extended aromatic systems, and as shown in Figure 17, directing palladium or platinum ions can be used as hinges to construct different supramolecular capsules.

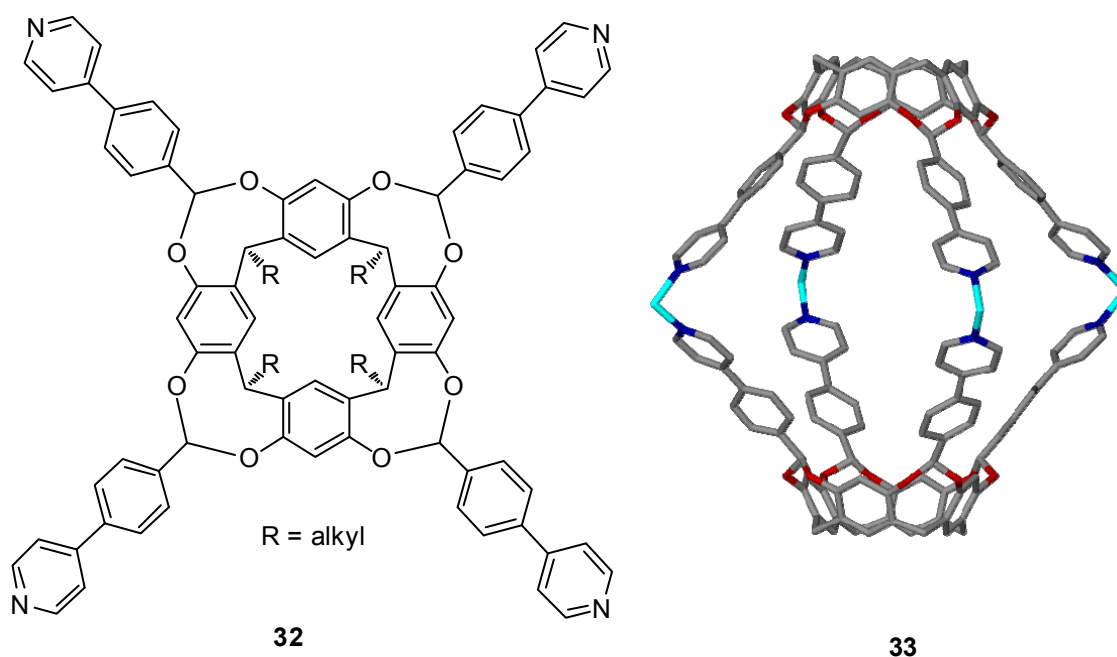
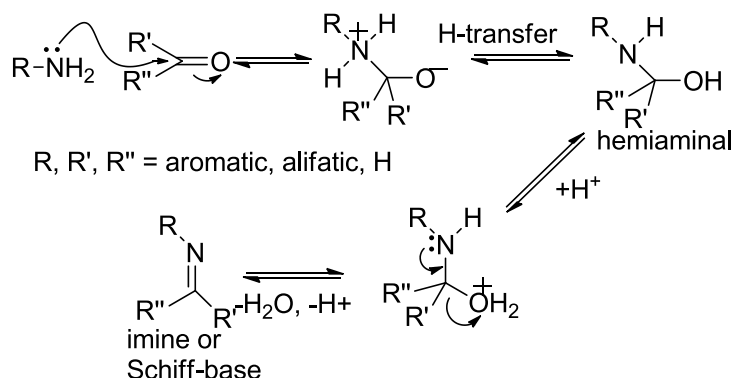


**Figure 17.** Extended pyridyl functionalised resorcinol[4]arene **32** that assembles in a directed fashion with either palladium or platinum ions to form into the metal-organic capsule **33**.<sup>18</sup> Hydrogen atoms, lower-rim R groups and additional ligands on metal centres are omitted for clarity.

### 1.6 Formation of Schiff bases and common metal coordination modes

A Schiff-base reaction is a condensation reaction. A primary amine reacts with an aldehyde or ketone to produce a hemi aminal intermediate which then loses a molecule

of water to form an imine or Schiff-base product. The reaction mechanism can be seen in Scheme 9.<sup>71</sup>



**Scheme 9.** General Schiff-base reaction mechanism.<sup>71</sup>

The aldehydes used for the Schiff-base reactions described in this section are all based on salicylaldehyde. This basic structure has been used in the literature extensively, especially in the formation of ligands for use with different transition metals to afford catalytic species and in supramolecular complexes.<sup>72-79</sup> Metals often used to form these assemblies include zinc, nickel, iron, molybdenum, copper, cobalt, and vanadium although this is not an exhaustive list. In this section, a small number of the supramolecular assemblies synthesised to date and some binding modes with the basic Schiff-base structure are described. Figure 18 shows the core of a typical Schiff-base product compound **34** that is formed via the condensation of aniline with salicylaldehyde.

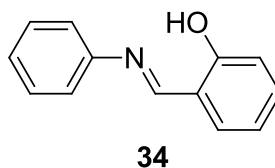


**Figure 18.** Schiff base formed by the condensation of aniline with salicaldehyde to afford compound **34**.<sup>72</sup>

Albrecht *et al* have used this basic unit in the synthesis of the tridentate ligand shown in Figure 19.<sup>73,74</sup> This ligand **34** was subsequently reacted with titanium oxide and potassium carbonate in a 1:1:1 ratio to produce a tetrahedral molecular assembly. Four titanium centres are located at the vertices of the tetrahedron and the four ligands constitute the panels that represent the sides of the polyhedron. The large cavity in the

structure is occupied by four potassium counter ions and approximately three DMF solvent molecules. Although the ligand forms the panels of the tetrahedral array, large pores suggest that guest exchange should be possible in solution.<sup>73,74</sup>

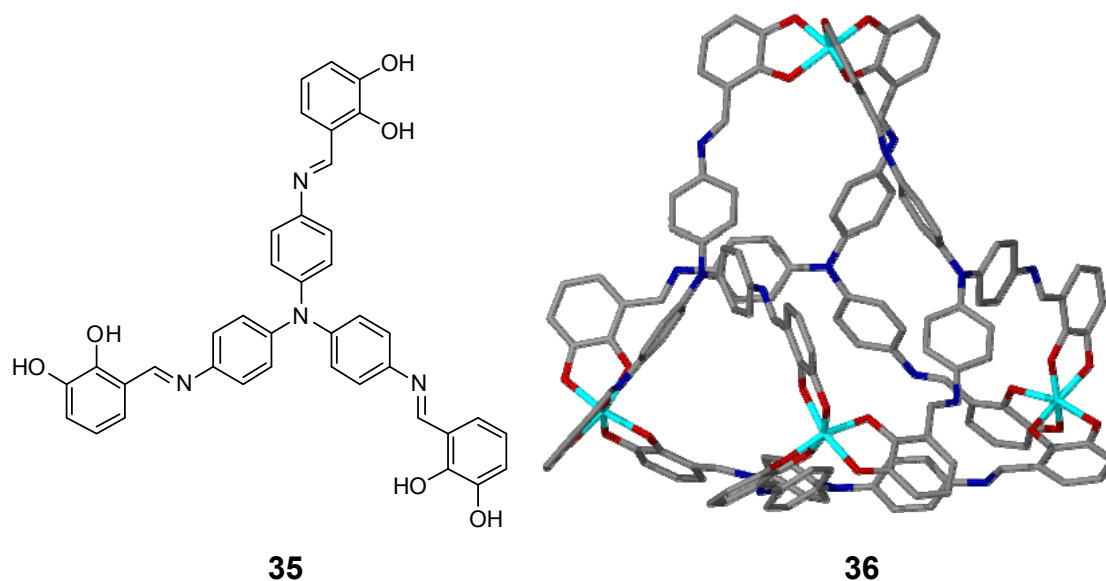


**Figure 19.** Ligand **35** and the tetrahedral supramolecular assembly **36** resulting from metal-directed assembly.<sup>73,74</sup> Hydrogen atoms are omitted for clarity.

Lacroix *et al* have synthesised and crystallised transition metal complexes with ligand **37** (Figure 20).<sup>75</sup> Reaction of the ligand with  $\text{Ni}(\text{AcO})_2$  affords a  $\text{NiL}_2$  complex (**38**) that is in square-planar geometry around the metal centre. An analogous reaction with  $\text{Cu}(\text{AcO})_2$  also produces a  $\text{CuL}_2$  complex (**39**), but in this case, the geometry around the metal centre is between square planar and tetrahedral, and is the result of both steric and electronic effects. The geometry of the corresponding  $\text{CoL}_2$  complex (**40**) is pseudo-tetrahedral, indicating that the metal centres are playing a key role in assembly. All of these complexes are formed with the nitrogen of the imine group and the phenol oxygen coordinating to the metal centre as expected.<sup>75</sup>

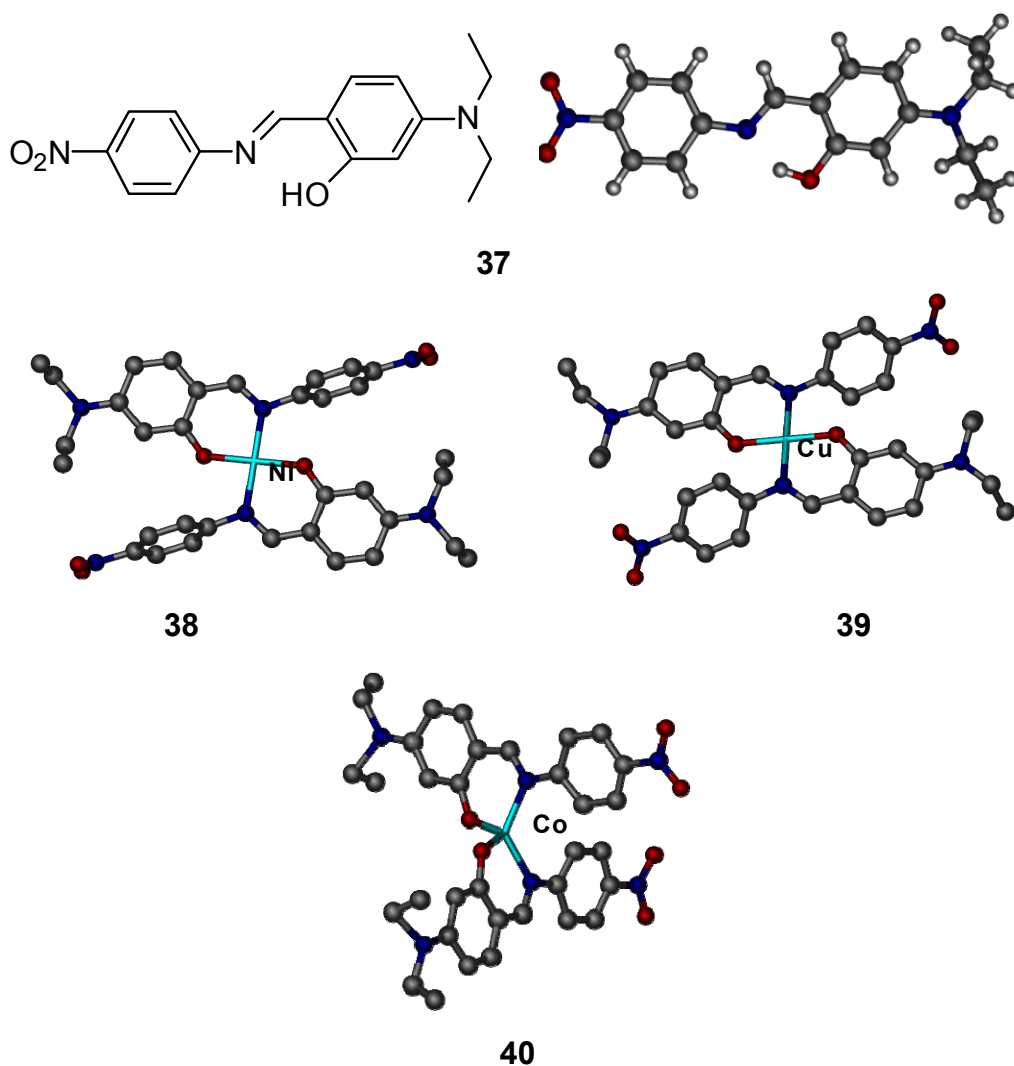


**Figure 20.** Ligand (**37**, L) used to synthesise complex **38** (Ni), **39** (Cu) and **40** (Co).<sup>75</sup> Hydrogen atoms are omitted for clarity.

Kleij *et al* used the Schiff-base reaction to synthesise the supramolecular building block **41**.<sup>76</sup> This monomer already contains a zinc centre coordinated to two nitrogen and two oxygen atoms, as seen in Figure 21. This building block self-assembles into an open vase tetramer (**42**, Figure 21), which is held together by four pyridine nitrogen – zinc interactions. This assembly has an internal volume of  $\sim 3100 \text{ \AA}^3$ , and generates channels in the crystal structure that are occupied with disordered solvent molecules.<sup>76</sup>

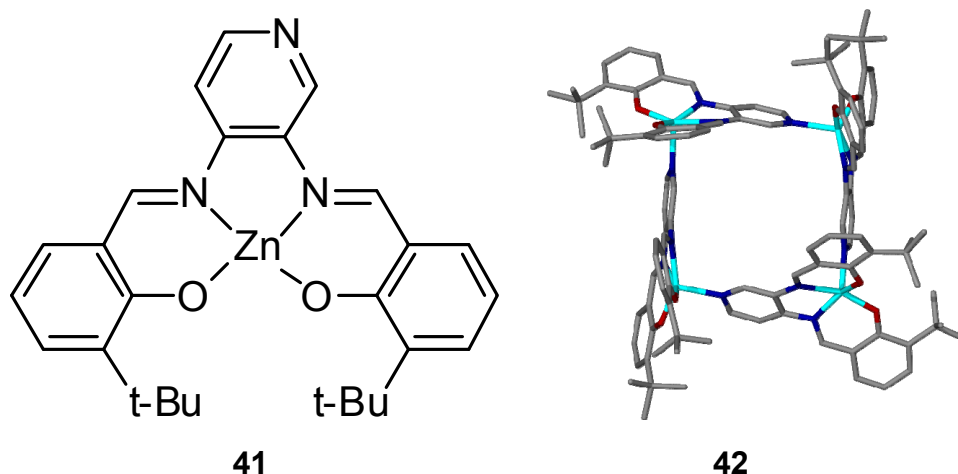


**Figure 21.** Supramolecular building block **41** which self-assembles into **42** through the pyridine-nitrogen – zinc interaction.<sup>76</sup> Hydrogen atoms are omitted for clarity.

The same group has also synthesised **43** (Figure 22), which is a supramolecular building block related to **41**, but which contains two zinc centres.<sup>77</sup> By reacting this new building block with different bipyridines, open-box assemblies of varied size were synthesised and characterised. When simple bipyridine is used, the resulting supramolecular box has a diameter of  $\sim 14$  Å. This assembly forms channels through the crystal in one dimension only, and these are also occupied with solvent molecules. When an elongated bipyridine was employed, where two pyridine units are separated by a  $\text{CH}_2\text{CH}_2$  spacer, the diameter of the box increased to  $\sim 16$  Å. A diameter of  $\sim 17.5$  Å can be achieved when the spacer length is increased by use of a benzene ring between the two pyridine units.<sup>77</sup>

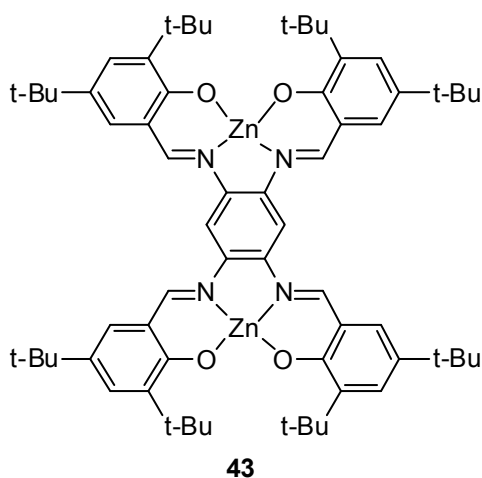


**Figure 22.** Building block **43** used to form box shaped supramolecular assemblies.<sup>77</sup>

Shaabani and Alemi have used salicylaldehyde and a mono-aminocalix[4]arene to produce a mono-Schiff-base calix[4]arene (**44**) as shown in Figure 23.<sup>78</sup> This ligand has subsequently been used in the synthesis of a supramolecular complex with a copper cation based on the motif shown in Figure 23. The resulting complex was made up of two calix[4]arene units for each copper ion, **45** shows the metal-ligand interaction of the resulting complex. This structure was analysed by UV/vis spectrometry, and showed that the spectra of both the monomer and the complex are solvent dependent. Both the nitrogen and oxygen of the salicylaldehyde are coordinating to the copper ion to form a stable tetrahedral coordination complexes. Cobalt and nickel have been used with **44** to obtain supramolecular assemblies, but due to steric hindrances and that those metals often prefer square planar or octahedral geometries, no complexes with **44** were reported.<sup>78</sup>

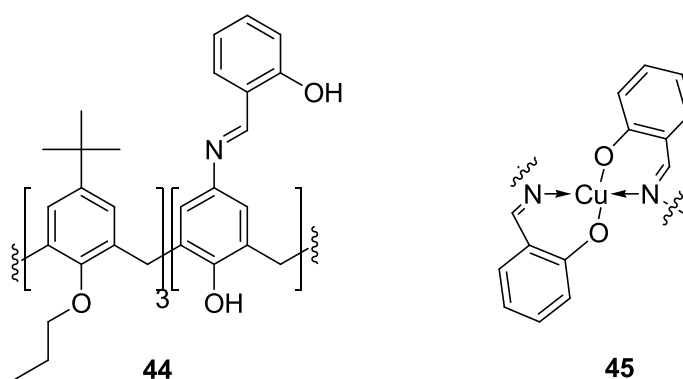


**Figure 23.** Schematic of the mono-Schiff-base calixarene **44**, and the assembly mode formed with cupric ions.<sup>78</sup>

The final type of building block highlighted here, and that involves Schiff-base reactions, is the series of calix[6]arene based ligands shown in Figure 24.<sup>79</sup> The calix[6]arene framework of **46** has four Schiff-base units at the upper-rim while two *p-tert*-butyl groups occupy the remaining positions. Copper and nickel ions were used to synthesise supramolecular complexes **47**, and analysis showed the metal to ligand ratio to be 2:1.

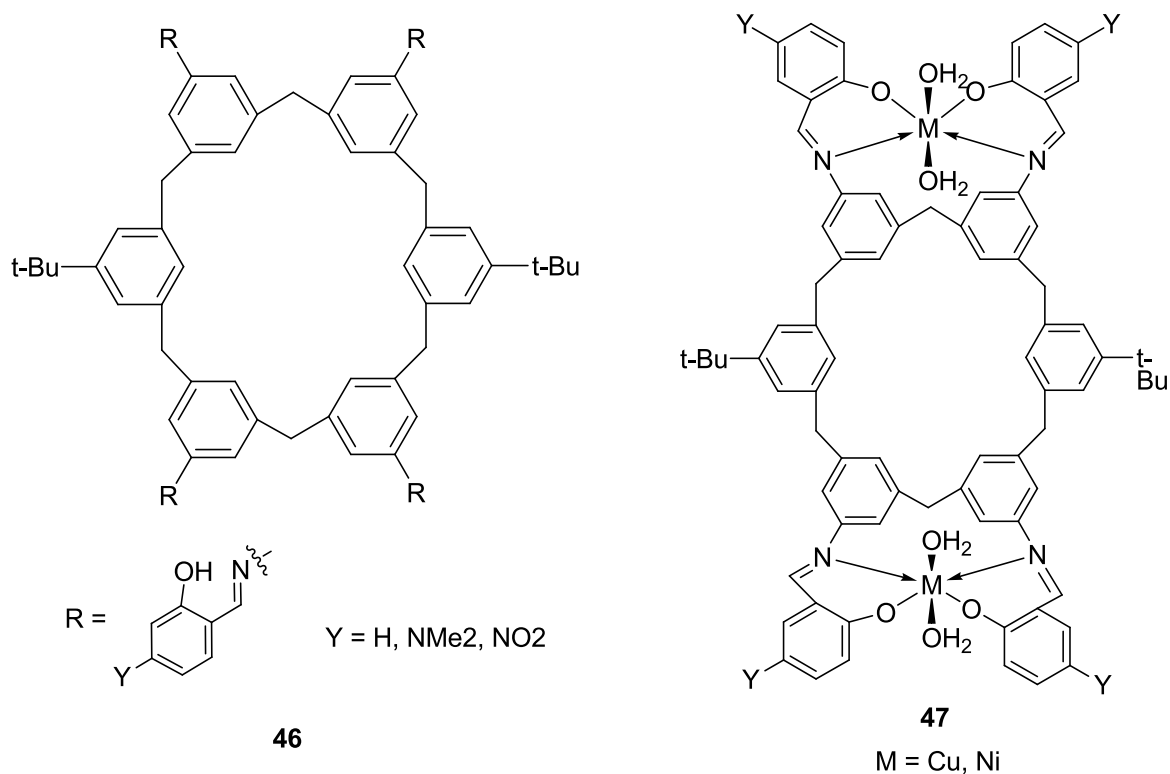


**Figure 24.** Schematic of the Schiff-base calix[6]arenes based on structure **46** that were used to form complexes **47** with copper or nickel metal ions.<sup>79</sup>

### 1.7 Project aims

The aim of this project is to synthesise a library of different Schiff-base calix[4]arenes that can subsequently be used in self- or metal-assisted assembly processes or in transition/lanthanide metal complexation. In general, the synthetic routes chosen start from either *tetra*-aminocalix[4]arenes or *tetra*-formylcalix[4]arenes. In the case of the *tetra*-formyl derivatives, this chemistry also focuses on the use of both protected and unprotected lower-rim calix[4]arenes (Figure 25).

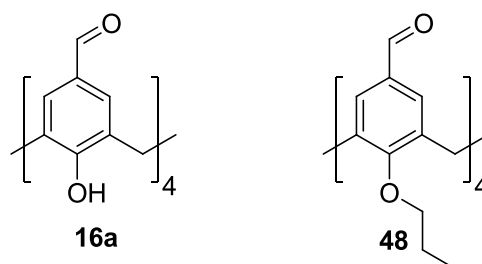


**Figure 25.** Protected and un-protected *p*-formylcalix[4]arenes to be used as starting materials in this study.

In addition to the aforementioned approach, calix[4]arenes that are flexible or rigid can be formed by protection at the lower-rim with either *n*-propyl groups or bis-crown-ether formation respectively. This control over rigidity should afford ligands that behave differently towards guest species and/or metal centres in future studies.

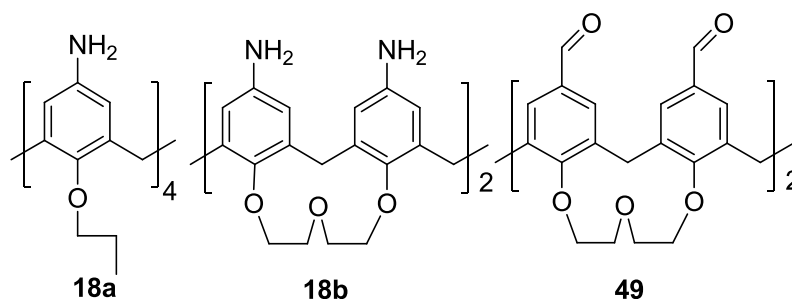


**Figure 26.** Other *p*-amino and *p*-formylcalix[4]arenes to be used as rigid or flexible starting materials in this study.

A number of different amines and aldehydes (shown in Figure 27) were selected for Schiff-base formation with the starting materials shown in Figures 25 and 26. This was in a bid to isolate a broad library of related, yet slightly different supramolecular building blocks that may behave differently towards guest molecules due to the location of donor atoms for example. This feature is especially important when the flexibility in the system is also considered as cavity conformation can respond to chemical stimuli.

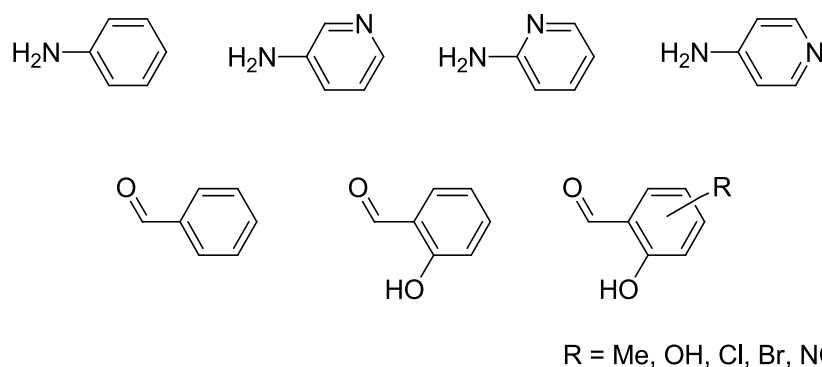


**Figure 27.** Amines and aldehydes selected for Schiff-base formation with *p*-formyl and *p*-aminocalix[4]arenes in this study.

With respect to the substitution of the salicaldehydes shown in Figure 27, variation in the location of methyl, hydroxyl, halo and nitro functionality was performed with a view to altering steric and electronic influences within the resulting ligands. For the resulting ligands containing pyridyl functionality, these can be combined with



assembly directing metal centres to afford metallo-supramolecular systems akin to those shown in Figure 17, but that may contain an additional degree of flexibility depending on the chosen calix[4]arene starting material. The result of the syntheses relating to these new ligands is described in the following chapter.

## ***CHAPTER II***

### ***Results And Discussion***

## 2 Results and Discussion

This chapter is split into two major sections based on the reaction between amino-pyridines and *p*-formylcalix[4]arenes, and the reaction of functionalised hydroxybenzaldehydes with *p*-aminocalix[4]arenes. In both sections this has been carried out with different calix[4]arenes with a view to isolating various families of new supramolecular building blocks for use in future studies.

### 2.1 *Amino-pyridine Schiff-base and reductive amination reactions with p-formylcalix[4]arenes*

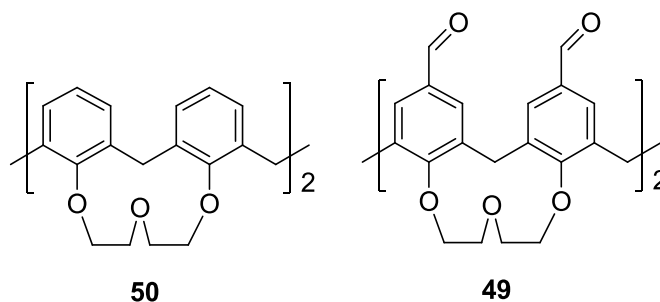
Pyridine-containing supramolecular building blocks have shown interesting properties with respect to the formation of capsules and coordination polymers with metals centres.<sup>18,63,80,81</sup> In this regard, the formation of some supramolecular complexes using pyridines and directing metal centres has been described in the introductory chapter. In order to be able to controllably assemble supramolecular capsules (for example), a prior degree of control must be obtained over the conformation of the ligand to be combined with directing metal centres. The two different ligand series synthesised in the following sub-sections are based on Schiff-base products formed using a tetra-formyl bis-crown-ether calix[4]arene with different amino-pyridines, and the products of a reductive amination reaction with tetra-formylcalix[4]arene with the same amino functionalised starting materials. The products obtained by reductive amination are predicted to be more flexible than their imino analogues due to the presence of single and double C-N bonds respectively. In addition to this, the Schiff-base calixarenes will possess conjugation with the annulus of the framework and the appended pyridine, adding to the rigidity of the system.

This project was initiated by a project student working in this group in 2008. Progress made in that mini-project towards the synthesis of a library of Schiff-base products starting from tetra-formylcalix[4]arene (**16a**). Although the syntheses were successful in the majority of cases, the products obtained were difficult to isolate and were found to readily decompose in solution. The reason for this was thought to be due to the presence of the acidic hydroxyl-groups at the calix[4]arene lower-rim that were then cleaving the imine bond formed during synthesis. Given this, tetra-propoxycalix[4]arene analogues were employed so as to afford stable products. This was found, however, to have the effect of distorting the cone conformation in the solid state

to afford the ‘pinched cone’ in the resulting Schiff-base building blocks synthesised. In order to achieve a similar ‘protection’ effect, and in order to maintain the rigid cone structure of the calix[4]arene, crown-ether links were introduced to the lower-rim prior to Schiff-base reaction formation. Structural analysis of this ligand series could then be compared those prepared in the previous study. As stated above, the two ligand series described in this section involve reaction with amino-pyridines. Specific results of these reactions are outlined below.

### 2.1.1 Schiff-base imino products

The bis-crown-ether calix[4]arene is synthesised by de-protonation of calix[4]arene with sodium hydride in DMF, followed by the addition of diethylene glycol di(*p*-toluenesulfonate).<sup>28,29</sup> This reaction is carried out in high dilution to obtain moderately high yields of compound **50** (Figure 28) that is isolated by column chromatography. The crown-ether was subsequently formylated by reaction with hexamethylenetetramine (HMTA) in trifluoroacetic acid to afford a starting material for use in Schiff-base formation (compound **49**, Figure 28). The crystal structure of compound **49** was obtained, and this is discussed later in section 2.3. This reaction was also carried out according to a literature procedure for the synthesis of tetra-formyl-tetrapropoxycalix[4]arene,<sup>43</sup> although this proved to be more difficult during workup with bis-crown-ether derivative **49**. Purification of compound **49** was achieved by pouring the reaction mixture onto ice and extracting with dichloromethane. Concentration of this solution and addition dropwise to hexane resulted in precipitation of the pure product.



The pyridine Schiff-bases were synthesised by reacting the formulated crown-ether calix[4]arene with aniline or the appropriate amino-pyridine in the presence of molecular sieves in order to remove any water which formed during the reaction (Figure 29). Following concentration of the solution, hexane was added to precipitate the product, which was then filtered off and dried. Aniline was used as a Schiff-base test-reaction, before exploration of the pyridine based analogues. Full characterisation of compounds **51-54** was not possible due to the products having extremely low signal to noisy ratios in there NMR spectra. This is perhaps related to the formation of various isomers, at the upper rim but is unexplained at this point. The IR of compound **54** is indicative of reaction completion with the presence of a characteristic C=N bond stretch at  $1601\text{ cm}^{-1}$ . Due to the lengthy synthesis of these compounds, their associated problematic analyses and time constraints, this ligand series was ultimately abandoned.

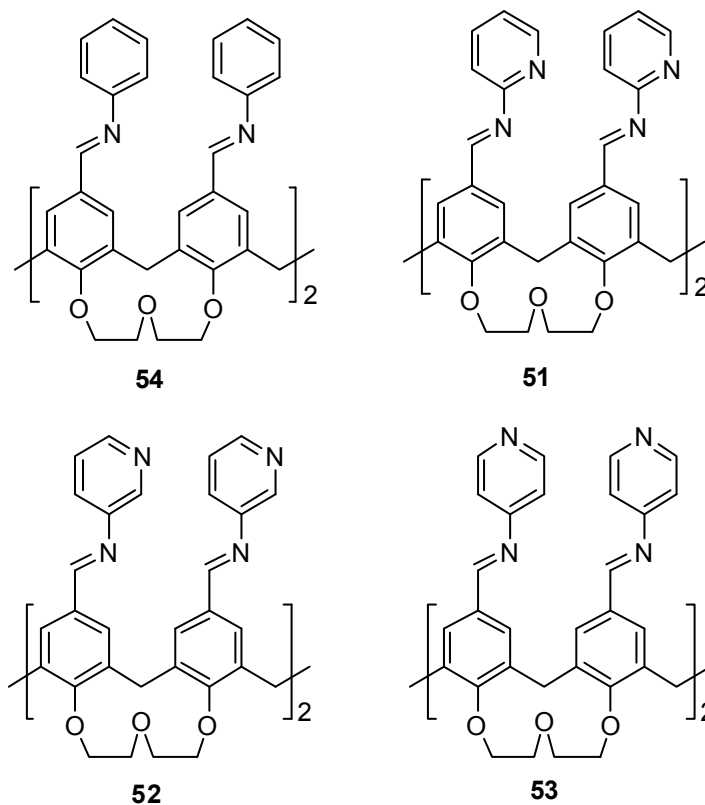


**Figure 29.** Compounds **51-53** and **54** obtained from reaction of tetra-formyl bis-crown-ether calix[4]arene with the three isomers of amino-pyridine or aniline.

### 2.1.2 Reductive amination products with *p*-formylcalix[4]arene

Tetra-formylcalix[4]arene (**16a**, Figure 30) was synthesised *via* the bromomethyl compound **55**. This calixarene was synthesised from calix[4]arene, *p*-formaldehyde and hydrogen bromide, and after purification, compound **55** was reacted with HMTA and TFA according to literature procedure to afford **16a**.<sup>39</sup> Both reactions yielded the desired products in high yield, and the subsequent reductive amination steps were carried out by literature adapted methods.<sup>82</sup> Compound **16a** was reacted with either aniline or an amino-pyridine in the presence of sodium triacetoxyborohydride that acts as a mild reducing agent. Following workup, compounds **56** - **59** were isolated in good yield (Figure 31).

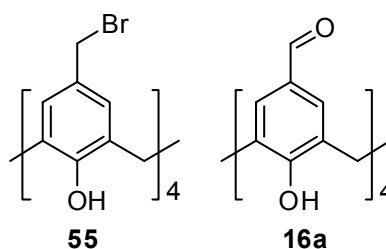


**Figure 30.** Compound **16a** synthesised by bromo-methylation of calix[4]arene and subsequent reaction with HMTA in TFA.<sup>39</sup>

The reaction of compound **16a** with aniline was carried out as a test reaction to determine the optimal reaction conditions for the reductive amination with this system. Unfortunately it was subsequently found that the amino-pyridines reacted differently to aniline in this reaction, and modified reaction conditions were required. Characterisation of compound **56** was performed with MS, NMR and IR. The absorption peaks at  $1149\text{ cm}^{-1}$  and  $3422\text{ cm}^{-1}$  in the IR spectrum correspond to the N-C and N-H bond stretches respectively. Notably the C=O stretch of the starting material was not observed. The NMR spectra showed all signals that are indicative of product formation, and MALDI-MS analysis showed a peak at  $m/z = 867.4$  corresponding to the expected molecular mass with an additional sodium ion  $[M+\text{Na}]^+$ .

Compound **57** was found to be poorly soluble in organic solvents including DMSO and, as such no meaningful NMR data was obtained. Alternative characterisation by MS and IR confirmed successful isolation of the product. A peak at  $m/z = 849.3$  corresponds to the molecular weight with an extra hydrogen atom, while a second observed peak at  $m/z = 871.2$  showed the expected molecular weight and an

additional sodium ion. Characteristic C-N and N-H stretches were observed in the IR spectrum at  $1150\text{ cm}^{-1}$  and  $3400\text{ cm}^{-1}$  respectively.

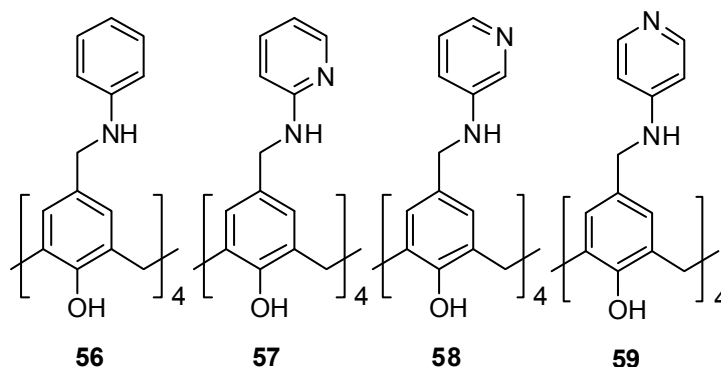


**Figure 31.** Compounds **56** - **59** synthesised by reductive amination of compound **16a** with aniline and the three isomers of amino-pyridine.

The next compound in this series is **58**, which has also only been characterised with MS and IR due to solubility problems. The N-C bond peak is at  $1148\text{ cm}^{-1}$  and at  $3378\text{ cm}^{-1}$  for the N-H bond in the IR spectra. The two peaks in the MS at  $m/z = 849.4$  and  $871.3$  correspond to the molecular mass and an extra hydrogen or sodium ion respectively.

The last compound in this series is **59** this was only characterised by IR. In the spectra the C=O peak has disappear, the N-C peak appeared at  $1147\text{ cm}^{-1}$  and the N-H bond at  $3434\text{ cm}^{-1}$ .

Despite solubility issues associated with compounds **57** - **59**, alternative characterisation methods indicate the successful synthesis of the desired products. Attempts to grow single crystals of these calix[4]arenes from various solvents amongst others acetone and DMF failed, with the production of only micro-crystalline material.

## 2.2 *Schiff-base reactions between lower-rim protected p-aminocalix[4]-arenes and selected benzaldehydes*

Due to the problems encountered in the synthesis and analysis of the amino-pyridine complex series highlighted above, in addition to resulting time constraints, it was decided that a new series of Schiff-base compounds should be synthesised from *p*-aminocalix[4]arenes **18a** and **18b** and a series of functionalised benzaldehydes (Figure 32). The two ligand series discussed in this part can potentially be used to investigation

the supramolecular behaviour of rigid and flexible calix[4]arenes that may give very different results with regard to the stability and volume of any resulting supramolecular assemblies. As described in the project aims section of the introductory chapter, the functionalities introduced at the aromatic ring of the benzaldehyde could potentially form different intramolecular interactions with specific chemical moieties.

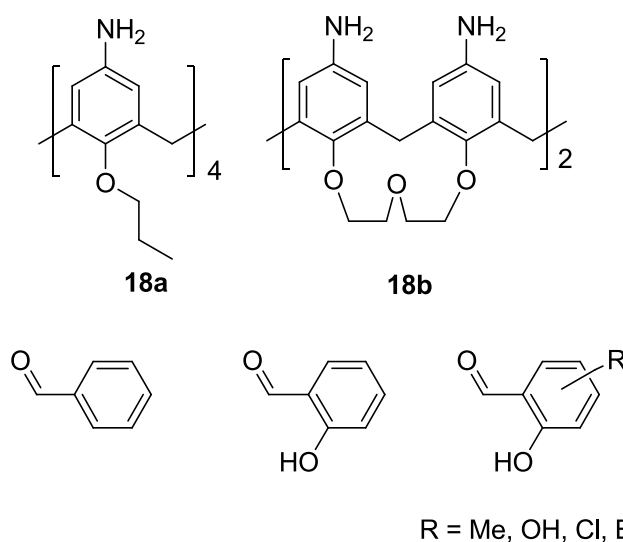


**Figure 32.** Compounds **18a** and **18b** to be used in Schiff-base formation with the selection of benzaldehydes shown.

Test reactions were carried out with both types of *p*-aminocalix[4]arene and either benzaldehyde or 2-hydroxybenzaldehyde. Based on the literature examples of metal-binding by Schiff-bases in the introductory chapter, the materials from this study should be very useful in binding a range of different metal ions and therefore have potential in metal-directed assembly. New Schiff-base calix[4]arenes were synthesised with all of the benzaldehydes shown except for 2,3-hydroxybenzaldehyde due to a problem with commercial supply.

### 2.2.1 Tetra-propoxycalix[4]arene Schiff-bases

Propylation of calix[4]arene to afford tetra-propoxycalix[4]arene was carried out according to literature procedure.<sup>83</sup> Calix[4]arene was de-protonated with sodium hydride prior to the addition of iodopropane. Compound **60** was isolated in high yield following crystallisation. Upper-rim nitration to afford compound **17a** was carried out by reacting **60** with sodium nitrate in trifluoroacetic acid overnight.<sup>43</sup> Subsequent reduction to afford the corresponding aminocalix[4]arene was then performed with



Raney nickel and hydrazine by heating at reflux to afford compound **18a** in near quantitative yield.<sup>44</sup>

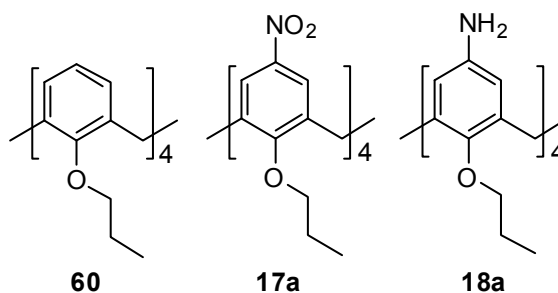


**Figure 33.** Compounds **17a**, **18a** used in the synthesis of **60**.

As in previous sections, reactions of compound **18a** with benzaldehyde and 2-hydroxybenzaldehyde were carried out as tests or blanks. The aldehydes were reacted with the compound **18a** in ethanol in the presence of acetic acid as a catalyst. Compound **61** (Figure 34) was isolated by evaporating the reaction mixture and the re-crystallising from MeOH and DCM. The crystals formed of this product were of limited quality and were found upon examination to require a stronger X-ray source such as that of a synchrotron. Compound **62** (that precipitated during reaction, Figure 34) was isolated by filtration, and was purified by washing with hot ethanol. Various attempts to obtain single crystals for both compounds were unsuccessful.

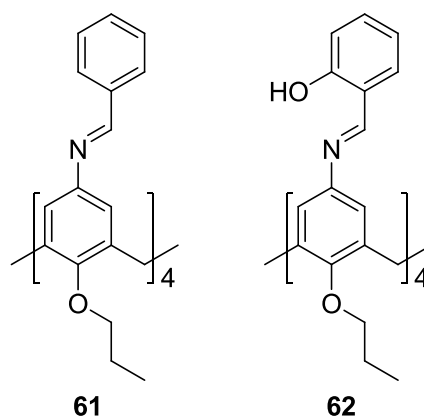


**Figure 34.** Compounds **61** and **62** synthesised by the reaction of compound **18a** with benzaldehyde and salicaldehyde respectively.

Compound **61** was characterised by NMR and IR spectroscopic analysis. Both methods showed that the reaction was successful with the characteristic signals of the imine hydrogen at  $\delta$  8.05 ppm in the  $^1\text{H}$ -NMR and the C=N stretch at  $1627\text{ cm}^{-1}$  in the IR spectra. Compound **62** was identified using NMR, IR and MS spectroscopic analysis. In the  $^1\text{H}$ -NMR of **62**, both the hydroxy and imine hydrogens are present at  $\delta$  13.22 and  $\delta$  8.25 ppm respectively. The characteristic signals in the IR spectra for the OH and C=N bonds were also observed at  $3448\text{ cm}^{-1}$  and  $1618\text{ cm}^{-1}$ . In the MS the expected molecular ion peak at  $m/z = 1069.5$  was observed with an additional peak at  $m/z = 1091.4$  which corresponded to a sodium ion coordinating to **62**. All of the characterisation methods indicate the formation of **62**.

The same reaction conditions were employed for Schiff-base formation between compound **18a** and the three isomers of methyl salicaldehyde to afford compounds **63** - **65** (Figure 35). The three compounds were analysed using NMR, IR and MS spectroscopic methods. All showed the characteristic N=C and O-H stretches at around  $1625\text{ cm}^{-1}$  and  $3300\text{ cm}^{-1}$  respectively. In all cases, the aldehyde C=O stretch between  $1750 - 1675\text{ cm}^{-1}$  was not been observed in the IR spectra. The expected molecular ion peak for this series of compounds was  $m/z = 1125$ . This was observed in all cases, and for compound **63** an additional peak is observed at  $m/z = 1147.47$ , corresponding to the molecular weight of **63** and a sodium ion replacing one hydrogen atom. It was possible to grow single crystals of compound **63** - **65**, but these were also found to be too weakly diffracting to obtain a structure solution. These samples also require a stronger X-ray source such as synchrotron radiation.

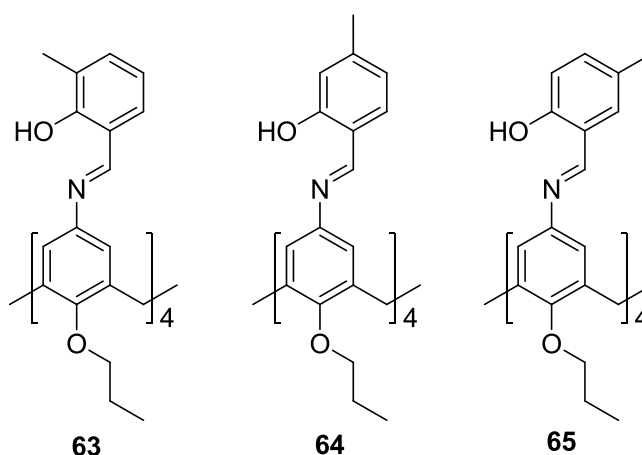


**Figure 35.** Compounds **63**, **64** and **65** synthesised by the reaction of compound **18a** with the three isomers of methyl salicaldehyde.

Compound **66** (Figure 36) was synthesised by reaction of **18a** with 2-hydroxy-5-nitrobenzaldehyde. The  $^1\text{H}$  and  $^{13}\text{C}$  NMR spectrum of this compound showed a high level of noise, and for this reason satisfactory characterisation by this method was not possible. This was attributed to the low solubility of the product, and, although this is the case, IR and MS spectra both indicate formation of the product. The characteristic N=C and O-H stretches in the IR spectra are shown at  $1617\text{ cm}^{-1}$  and  $3448\text{ cm}^{-1}$  respectively, and the peak observed at  $m/z = 1249.47$  in the mass spectrum matches the expected molecular mass of the product.

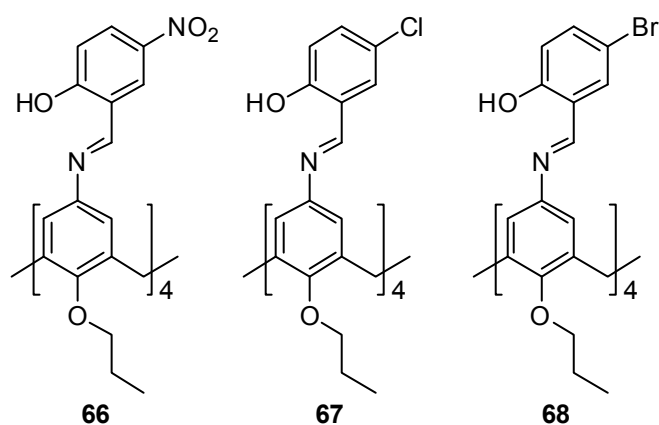


**Figure 36.** Compounds **66**, **67** and **68** synthesised from the reaction of **18a** with 2-hydroxy-5-nitrobenzaldehyde, 2-hydroxy-5-chlorobenzaldehyde and 2-hydroxy-5-bromobenzaldehyde respectively.

The halo derivatives **67** and **68** (Figure 36) were successfully synthesised, as suggested by NMR, IR, and MS spectral analysis. The  $^{13}\text{C}$ - and  $^1\text{H}$ -NMR spectra of **67** show no evidence of aldehydic carbon or hydrogen signals, and no signals for the *p*-amino functionality of compound **67**, indicating that the reaction has reached completion. There is a single peak in the  $^1\text{H}$ -NMR at  $\delta$  8.2 ppm, which corresponds to the hydrogen at the carbon of the newly formed imine bond, while another peak at  $\delta$  13.27 ppm corresponds to the phenolic hydrogen. The  $^1\text{H}$  NMR spectrum of **68** was also found to be very noisy, a feature that hindered identification in the solution phase. The IR and MS spectra of both compounds show the characteristic stretches of the phenolic O-H at  $3435\text{ cm}^{-1}$  and  $3436\text{ cm}^{-1}$  and the N=C of the imine bond at  $1619\text{ cm}^{-1}$  and  $1615\text{ cm}^{-1}$  respectively. The molecular ion peaks in the MS at  $m/z = 1207$  and  $m/z = 1385$  correspond to the respective molecular masses of compounds **67** and **68**.

Crystallisation of these molecules was attempted from various solvents, but as in previous attempts with similar derivatives, this was also unsuccessful.

The last set of compounds synthesised with the amino-functionalised tetra-propoxycalix[4]arene is based on the Schiff-base reaction with hydroxyl salicaldehydes. The solubility of compound **69** (Figure 37) was again an issue resulting in poor NMR spectra, but product formation was confirmed by IR and MS. The IR spectrum displays the characteristic peaks at  $3414\text{ cm}^{-1}$  and  $1620\text{ cm}^{-1}$  corresponding to the O-H and C=N stretches respectively. The expected molecular mass of  $m/z = 1133$  was observed in the mass spectrum. The isolation of compound **70** (Figure 37) was not possible due to difficult workup and recrystallisation procedures.

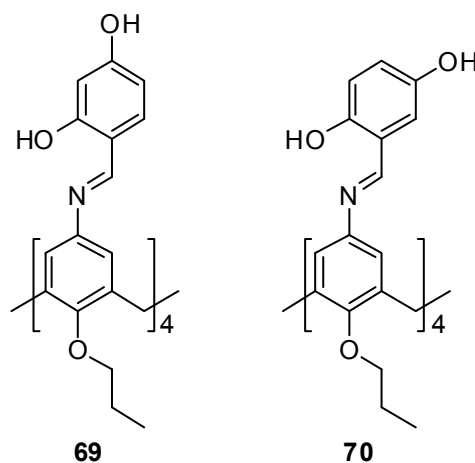


**Figure 37.** Compounds **69** and **70** synthesised from the reaction of **18a** with two isomers of hydroxy-salicaldehyde.

### 2.2.2 Bis-crown-ether calix[4]arene Schiff-bases

Literature examples of bis-crown-ether calix[4]arenes show these molecules to exist in the expected cone conformation, rendering them very rigid compared to their propylated analogues. Based on the improved stability of Schiff-base calix[4]arenes isolated from *p*-amino rather than *p*-formyl precursors, it was anticipated that the upper-rim amino bis-crown-ether would afford rigid Schiff-bases for use in future supramolecular studies. Bis-crown-ether calix[4]arene **50** was synthesised according to the procedure described in section 2.1.1. Following the isolation of compound **50**, the next step towards the synthesis of the *p*-amino-bis-crown-ether calix[4]arene is nitration at the upper-rim (Figure 38). This was carried out in the same way as for calix[4]arene

**17a.** Reduction of **17b** was also carried out according to the literature procedure for the synthesis of **18a**. Both **17b** and **18b** are obtained in high yield, and the same general reaction conditions employed in the synthesis of the tetra-propoxycalix[4]arene Schiff-base ligands discussed in section 2.2.1 were employed for the synthesis of the products described below.

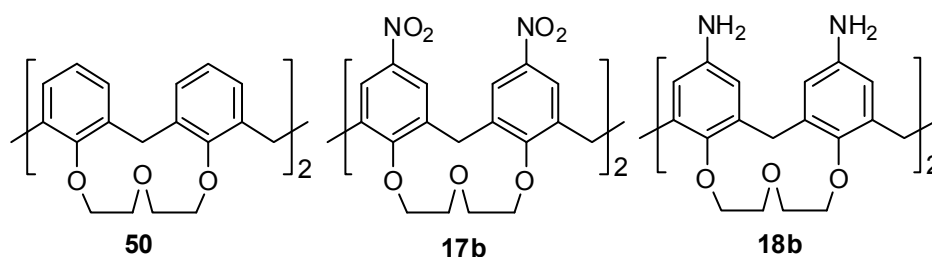


**Figure 38.** Compounds **50**, **17b** and **18b**.

Two test reactions were performed by reacting compound **18b** with benzaldehyde and salicaldehyde to produce bis-crown-ether calix[4]arenes **71** and **72** respectively (Figure 39). In a bid to determine the orientation of the upper rim appendages in compounds **71** and **72**, several attempts were made to grow single crystals of both host molecules. Unfortunately it was only possible to obtain micro crystalline material by crystallisation from several solvents. Compounds **71** and **72** were characterised by NMR, IR and MS spectra methods. The  $^1\text{H}$  and  $^{13}\text{C}$  NMR spectra of both compounds show a singlet peak at around  $\delta$  8.3 ppm, which corresponds to the hydrogen of the imine bond. In addition, the spectrum of compound **72** shows a broad singlet at around  $\delta$  13.1 ppm, corresponding to the phenolic hydrogen atom at the upper-rim. The IR spectra of both show a peak at around  $1620\text{ cm}^{-1}$ , corresponding to the imine  $\text{N}=\text{C}$  bond, with concomitant disappearance of the aldehyde signals at higher wavenumber. For compound **72**, an additional peak at  $3448\text{ cm}^{-1}$  correlating to O-H stretching was also observed. The molecular ion peaks of both compounds were also observed at corresponding molecular mass peaks of  $m/z = 977$  and  $m/z = 1041$  respectively. For compound **72**, a peak at  $m/z = 1064$  was observed corresponding to the molecular mass with an additional sodium ion coordinating to this ligand.

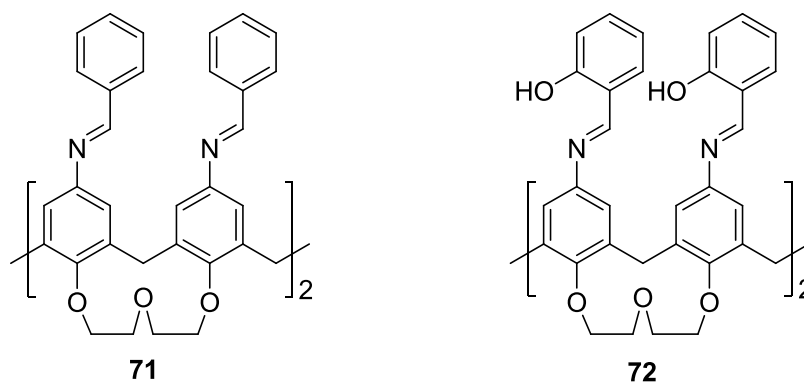


**Figure 39.** Compounds **71** and **72** synthesised from the reaction of **18b** with benzaldehyde and salicaldehyde respectively.

The series of methyl-substituted 2-hydroxybenzyl-imino-biscrown-ether calix[4]arenes **73** - **75** (Figure 40) were isolated in good yield and were identified by NMR, IR and MS. All NMR spectra have the characteristic phenolic and imino hydrogen signals at around  $\delta$  13 ppm and  $\delta$  8.3 ppm respectively, in addition to the expected methyl signal of the phenolic ring at the upper rim of the calixarene at around  $\delta$  2.2 ppm. The two characteristic stretches in the IR spectra, at around  $1620\text{ cm}^{-1}$  and  $3400\text{ cm}^{-1}$ , for O-H and C=N stretches respectively, were observed for compounds **73** - **75**, indicating the successful completion of the Schiff-base reaction. In the MS spectra, all the compounds have a signal relating to the molecular mass at  $m/z = 1097$ . In addition to this peak, compounds **73** and **74** both have a peak at about  $m/z = 1119$ , which can be identified as the molecular mass with loss of one hydrogen atom and complexation of a sodium ion. Compound **75** has a peak at  $m/z = 1120$ , corresponding to the expected molecular mass with an additional sodium ion.

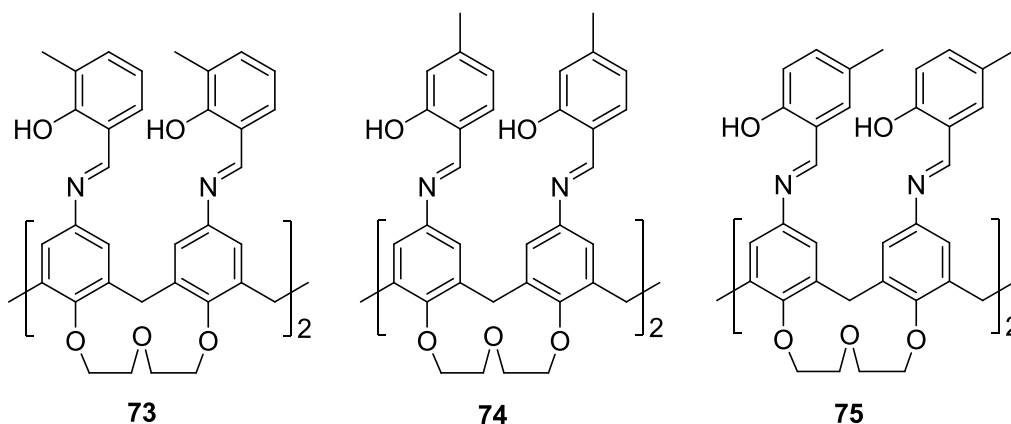


**Figure 40.** Compounds **73**, **74** and **75** synthesised from the reaction of **18a** with the three isomers of methyl-salicaldehyde.

Compound **76** (Figure 41) was synthesised using 2-hydroxy-5-nitrobenzaldehyde. Routine characterisation methods show that compound **76** has been successfully synthesised. The signals at around  $\delta$  12.9 ppm and  $\delta$  8.4 ppm in the proton NMR spectrum correspond to the expected phenolic hydroxy and imino hydrogen respectively. The characteristic bond stretches in the IR spectra can also be recognised, with C=N and OH stretches at  $1617\text{ cm}^{-1}$  and  $3435\text{ cm}^{-1}$  respectively. The molecular ion peak at  $m/z = 1223$  corresponds to the expected molecular weight of compound **76**.

The successful synthesis of halogenated crown-ether Schiff-base products **77** and **78** (from reaction of compound **18b** with 2-hydroxy-5-chlorobenzaldehyde and 2-hydroxy-5-bromobenzaldehyde respectively) was also confirmed by NMR, IR and MS spectral methods. Both compounds display the phenolic and imino hydrogen signals at about 13 ppm and 8.5 ppm respectively. The IR spectra of both show O-H stretches at  $3448\text{ cm}^{-1}$  and  $3435\text{ cm}^{-1}$ , and N=C stretches at  $1620\text{ cm}^{-1}$  and  $1618\text{ cm}^{-1}$ . In both the NMR and IR spectra, the aldehyde signals are not observed, further indicating successful completion of the reaction. The molecular ion peaks at  $m/z = 1179$  and  $1357$  correspond to the expected molecular weights of compounds **77** and **78** respectively. In the MS of compound **77**, a second peak at  $m/z = 1201$  corresponds to the replacement of a hydrogen atom with a sodium ion.

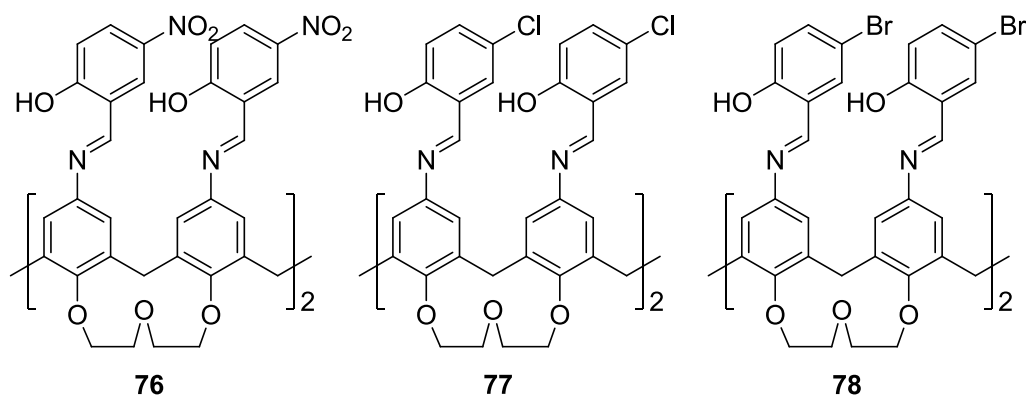


**Figure 41.** Compounds **76**, **77** and **78** synthesised from the reaction of **18b** with 2-hydroxy-5-nitrobenzaldehyde, 2-hydroxy-5-chlorobenzaldehyde and 2-hydroxy-5-bromobenzaldehyde respectively.

The last compounds to be synthesised in this series are **79** and **80**, which possess an extra hydroxyl group at the four or five position of the phenolic ring respectively. It was only possible to characterise compound **79** by MS and IR spectral methods due to a

high signal to noise ratio, and time constraints that prevented further drying of the material. The MS shows a peak matching the expected molecular mass of **79** at  $m/z = 1104.47$ . The typical C=N and OH stretches were observed at  $1625\text{ cm}^{-1}$  and  $3428\text{ cm}^{-1}$  respectively, indicating successful completion of the reaction. The proton NMR for compound **80** was also noisy, but showed the presence of two phenolic hydrogens at  $\delta$  12.31 ppm and the imino hydrogen at  $\delta$  8.64 ppm. The  $^{13}\text{C}$ -NMR could not be interpreted due to poor solubility a very weak signal despite the collection of many scans. The MS shows the expected molecular mass and additional peaks corresponding to the loss of one hydrogen atom and the presence of an additional sodium ion at  $m/z = 1105.5$  and  $m/z = 1127.8$  respectively. Again, the IR spectra show the expected N=C and O-H stretches at  $1618\text{ cm}^{-1}$  and  $3428\text{ cm}^{-1}$ , indicating successful completion of the reaction. Unfortunately it was not possible to obtain the third isomer of dihydroxybenzaldehyde to complete this ligand set due to problems with the chemical shipment.

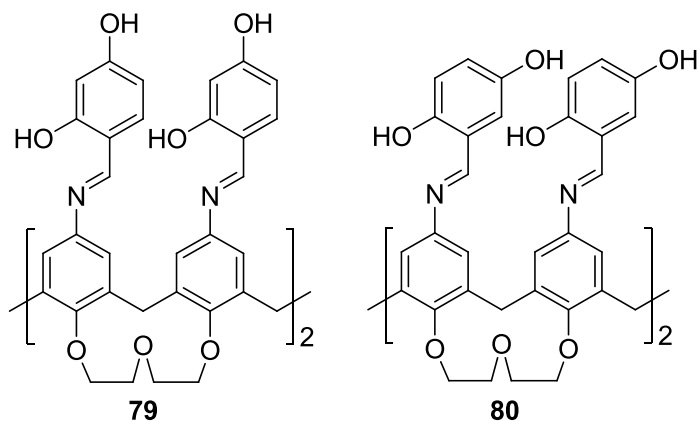


**Figure 42.** Compounds **79** and **80** synthesised from the reaction of **18b** with 2,4-dihydroxybenzaldehyde and 2,5-dihydroxybenzaldehyde respectively.

From the reactions and analyses described above, all compounds in this series were successfully synthesised and isolated. Unfortunately none have been successfully crystallised, despite the use of several different solvents for use in a slow evaporation method. Alternative crystallisation methods such as vapour diffusion may be explored in future to confirm the orientation of the upper-rim appendages on the bis-crown-ether calix[4]arene framework.



### 2.3 Crystallographic studies

During this study the single crystal X-ray structure of one compound was obtained. Single crystals of compound **49** were grown by slow evaporation of an ethyl acetate/hexane solvent mixture (in a ratio of 60:40) following purification via column chromatography. The crystals are in a monoclinic cell and structural analysis was performed in the space group  $P2_1/c$ . The asymmetric unit contains one molecule of compound **49** and a molecule of ethyl acetate, as solvent of crystallisation, that resides in the cavity presented by the rigid bis-crown-ether calix[4]arene. Two of the aldehyde groups at the upper rim are disordered over two positions and this has been modelled accordingly with the use of partial occupancies. The methyl group of the ethyl acetate guest molecule points to the centre of the calixarene cavity and forms a  $\text{CH}\cdots\pi$  interaction with a  $\text{CH}\cdots\text{aromatic centroid}$  distance of 2.785 Å.

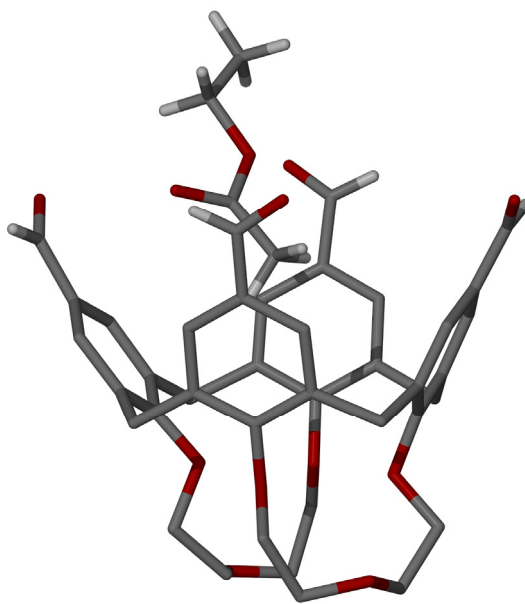


**Figure 43.** Stick representation of the single crystal X-ray structure of compound **49** with a molecule of ethyl-acetate occupying the cavity of the bis-crown-ether calix[4]arene. Hydrogen atoms, except those associated with upper-rim formyl groups and the ethyl acetate guest are omitted for clarity. The two disordered formyl groups are shown in only one of two positions.

Examination of the extended structure shows that although compound **49** forms a complicated packing diagram (Figure 44), the molecule packs so as to form anti-parallel

layers in much the same way as *p*-sulfonatocalix[4]arene. Full crystallographic data for this analysis are available in the appendix section.

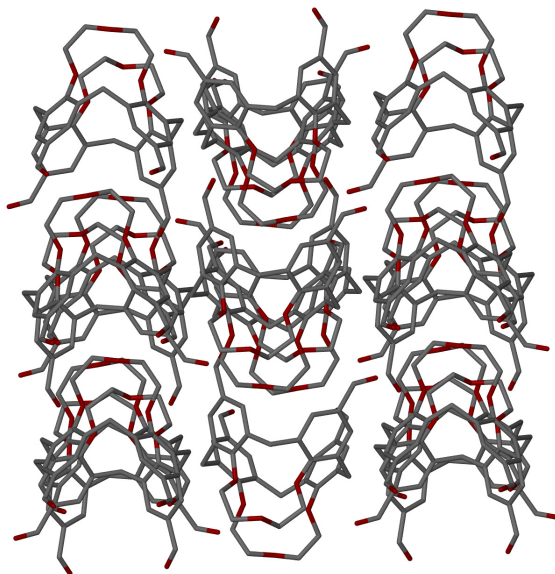


**Figure 44.** Packing diagram for compound **49** showing anti-parallel packing. Hydrogen atoms and ethyl acetate molecules are omitted for clarity.

## ***CHAPTER III***

### ***EXPERIMENTAL***

### 3 Experimental

#### *General Information*

IR spectra were recorded on a Perkin Elmer 1600 FT IR spectrometer. Spectra were recorded as potassium bromide discs. Mass spectra were obtained on Kratos Concept IS EI (electron impact) and Fisons VG Quattro (electrospray) spectrometers.  $^1\text{H}$  NMR spectra were recorded at 200 and 400 MHz on Bruker AC200 and DPX400 spectrometers;  $^{13}\text{C}$  NMR spectra were recorded at 50 and 101 MHz on the same instruments. Chemical shifts are recorded in parts per million ( $\delta$  in ppm).

The numbering for the systematic nomenclature of calixarenes can be seen in Figure 45. The sample given is for *p*-*tert*-butylcalix[4]arene where its systematic name is 5,11,17,23-tetra-*tert*-butyl-25,26,27,28-tetrahydroxycalix[4]arene.<sup>2</sup>

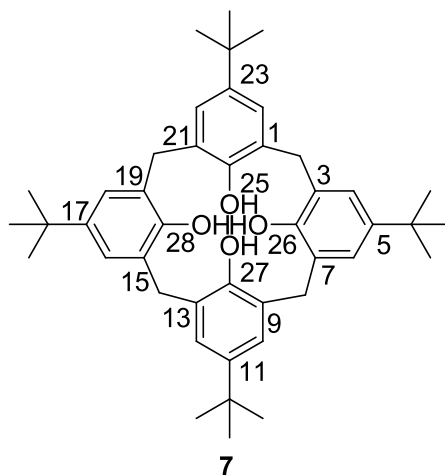
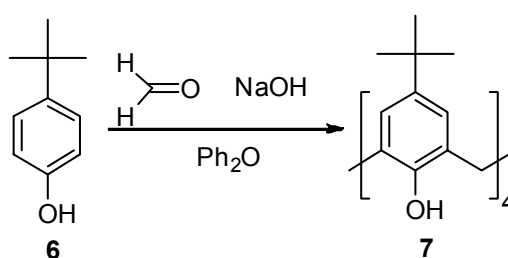


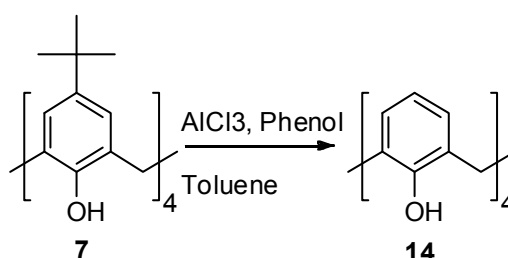
**Figure 45.** Example of the systematic numbering of calix[4]arenes.

### Synthesis of 5,11,17,23-tetra-tert-butyl-25,26,27,28-tetrahydroxycalix[4]arene (7):<sup>82,83</sup>



A mixture of *p*-*t*-butylphenol **6** (127.4 g, 848 mmol), formaldehyde solution (37%, 1.06 mol, 80 mL) and NaOH (0.63 g, 15.8 mmol) dissolved in H<sub>2</sub>O (1.6 mL) were heated to 120°C in order to remove water using a Dean-Stark apparatus. Following this, the reaction was cooled to RT and diphenyl ether (1 L) and toluene (500 mL) were added. The resulting mixture was heated to 260°C for 1-2 hrs until the temperature reached 180 – 190°C, after which the reaction was heated at reflux for 4 hrs. Water and toluene were removed with the Dean-Stark apparatus during this time. The reaction was cooled to 60°C and EtOAc (770 mL) was added and the mixture cooled to RT. The reaction was left to stir for 1 h and the solid precipitate was collected, triturated with acetic acid (100 mL), washed with EtOAc (4 x 25 mL) and filtered to afford compound **7** as a white crystalline solid. (83.0 g, 128 mmol, 60%). <sup>1</sup>H NMR (200 MHz, 25°C, CDCl<sub>3</sub>): δ = 10.34 (s, 4H, OH), 7.05 (s, 8H, ArH), 4.26 (d, 4H, <sup>2</sup>J = 13.7, ArCH<sub>2</sub>Ar), 3.50 (d, 4H, <sup>2</sup>J = 13.7, ArCH<sub>2</sub>Ar), 1.21 (s, 36H, C(CH<sub>3</sub>)<sub>3</sub>) ppm.

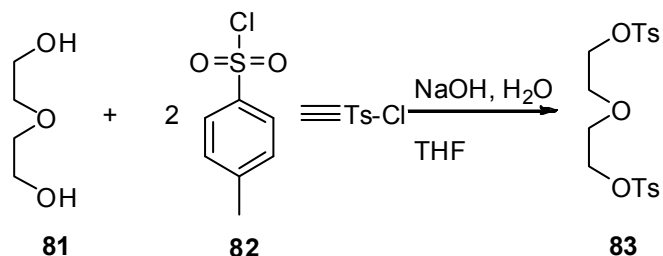
### Synthesis of 25,26,27,28-tetrahydroxycalix[4]arene (14):<sup>3,23,83</sup>



'Butyl-calix[4]arene **7** (40.0 g, 61.6 mmol), toluene (470 mL) and phenol (8.2 g, 87.1 mmol) were reacted with AlCl<sub>3</sub> (46.0 g, 345 mmol). HCl gas was removed from the reaction using a constant flow of nitrogen gas. After stirring constantly for 3 hrs, the reaction was poured onto ice (600 g) **caution HCl!!!** The reaction flask was washed with DCM (1.2 L) and H<sub>2</sub>O (300 mL). The organic layer was separated, washed with 1M HCl (2 x 500 mL) and water (2 x 500 mL), dried (MgSO<sub>4</sub>) and concentrated. Et<sub>2</sub>O (200 mL) was added to precipitate compound **14** as a pale yellow solid that was

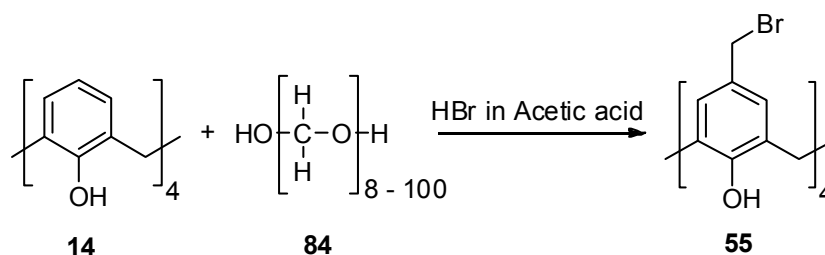
collected by filtration. (19.8 g, 46.7 mmol, 75.6%).  $^1\text{H}$  NMR (200 MHz,  $25^\circ\text{C}$ ,  $\text{CDCl}_3$ ):  $\delta$  = 10.19 (s, 4H, OH), 7.04 (d,  $^2J$  = 8, 8H, ArH), 6.71 (dd,  $^2J$  = 8, 7.2Hz, 4H, ArH), 4.22 (m, 4H, ArCH<sub>2</sub>Ar), 3.55 (m, 4H, ArCH<sub>2</sub>Ar) ppm.

#### Synthesis of diethyleneglycol di-*p*-toluenesulfonate (**83**):<sup>40</sup>



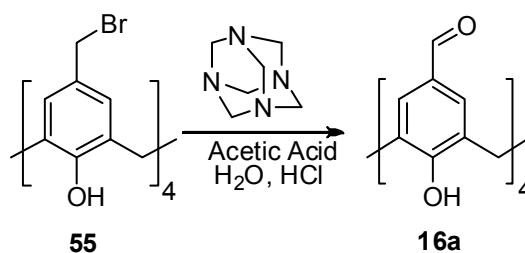
Diethyleneglycol **81** (75.1 g, 0.71 mol) was dissolved in an ice-cold solution of sodium hydroxide (80.6 g, 2.02 mol) in water (ca 300 mL). A solution of *p*-toluenesulphonyl chloride **82** (283.8 g, 1.5 mol) in THF (ca 400 mL) was added dropwise keeping the reaction vessel at  $0 - 5^\circ\text{C}$ . After addition was completed the reaction mixture was stirred for 3 hrs at  $0^\circ\text{C}$ , the reaction was poured on to ice water (500 mL), and the precipitate was collected by filtration. The product was purified by recrystallisation from hot methylated spirits (~700 mL). Diethyleneglycol di-*p*-toluenesulfonate **83** was filtered as a white crystalline solid. (241.9 g, 0.58 mol, 82%).  $^1\text{H}$  NMR (400 MHz,  $25^\circ\text{C}$ ,  $\text{CDCl}_3$ ):  $\delta$  = 7.87 (4H, ArH), 7.35 (4H, ArH), 4.08 (d, 4H, SOCH<sub>2</sub>CH<sub>2</sub>O), 3.60 (d, 4H, SOCH<sub>2</sub>CH<sub>2</sub>O), 2.42 (s, 6H, CH<sub>3</sub>Ar) ppm.

#### 5,11,17,23-tetrabromomethyl-25,26,27,28-tetrahydrocalix[4]arene (**55**):<sup>26,83</sup>



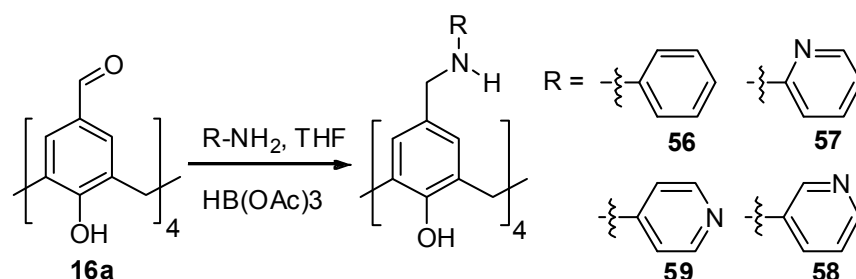
Calix[4]arene **14** (4.41 g, 10.4 mmol) and *p*-formaldehyde **84** (2.51 g, 83.6 mmol) were dispersed in HBr (45 mL, 33% v/v in acetic acid). The reaction was heated to  $50^\circ\text{C}$  overnight, and after cooling to RT, the suspension was poured onto iced water (150 mL) and was stirred for 30 min. The pink product **55** was filtered, washed with water (2 x 250 mL) and dried. (7.97 g, 10.1 mmol, 97%) NMR (200 MHz,  $25^\circ\text{C}$ ,  $\text{CDCl}_3$ ):  $\delta$  10.10 (s, 4H, OH), 7.06 (s, 8H, ArH), 4.32 (s, 8H, CH<sub>2</sub>Br), 4.11 (bs, 4H, ArCH<sub>2</sub>Ar), 3.59 (bs, 4H, ArCH<sub>2</sub>Ar) ppm.

### 5,11,17,23-tetraformyl-25,26,27,28-tetrahydroxycalix[4]arene (**16a**):<sup>26</sup>



Bromomethyl-calix[4]arene **55** (5.01 g, 6.29 mmol) and HMTA (7.06 g, 50.4 mmol) were suspended in glacial acetic acid (33 mL) and were stirred for 30 min at RT. Water (33 mL) was added, and stirred for 30 min at ambient temperature, then refluxed for 2 hrs. *Conc.* HCl (8 mL) was added and refluxed for a further 2 hrs. Then the mixture was cooled to RT, and the yellow precipitate was filtered, washed with water (400 mL) and then methylated spirit (60 mL) and dried to yield compound **16a** (3.04 g, 5.67 mmol, 90%). <sup>1</sup>H NMR (200 MHz, 25°C, CDCl<sub>3</sub>)  $\delta$  = 9.76 (s, 4H, COH), 7.65 (s, 8H, ArH), 4.23 (bs, 4H, ArCH<sub>2</sub>Ar), 3.71 (bs, 4H, ArCH<sub>2</sub>Ar) ppm.

### General synthesis for the reductive amination of formyl calix[4]arenes **16a**:<sup>84</sup>



Formyl-calix[4]arene **16a** was dispersed in dry THF (60 mL/mmol) with molecular sieves (4Å). Aniline or the appropriate amino-pyridine (5 mol eq.) was added to the solution, stirred for 30 min. (The dispersed cloudy solution turned clear after about 10 min). Sodium triacetoxyborohydride (5.5 mol eq.) was added and the mixture stirred overnight. Sat. ammonium chloride (10 mL) was added to quench the reaction and extracted with THF. The organic layer was washed with water, dried (MgSO<sub>4</sub>), and evaporated. The product was purified by crystallisation.

***5,11,17,23-tetra((phenylamino)methyl) -25,26,27,28-tetrahydroxycalix[4]arene (56)***

Crystallised from chloroform and hexane, to afford **56** as a white solid. (0.183 g, 0.22 mmol, 55%). MS (MALDI)  $m/z$  = 867.4  $[M+Na]^+$ ;  $^1H$ -NMR (200 MHz, 25°C,  $CDCl_3$ )  $\delta$  = 7.22 – 7.10 (m, 8H,  $NHArH$ ), 7.03 (s, 8H,  $ArH$ ), 6.72 (t, 4H,  $NHArH$ ), 6.59 (d, 8H,  $NHArH$ ), 4.25 (d,  $^2J$  = 14, 4H,  $ArCH_2Ar$ ), 4.10 (s, 8H,  $CH_2NHAr$ ), 3.50 (d,  $^2J$  = 14, 4H,  $ArCH_2Ar$ ) ppm. IR (KBr)  $cm^{-1}$  = 3422(N-H), 1602, 1506, 1478, 1224, 1149(C-N), 749, 692, 504.

***5,11,17,23-tetra((pyridine-2-ylamino)methyl) -25,26,27,28-tetrahydroxycalix[4]arene (57)***

Crystallised from THF/ $H_2O$  and hexane, to afford compound **57** as a white/yellow solid. (1.32 g). MS (MALDI)  $m/z$  = 849.3  $[M+H]^+$ , 871.2  $[M+Na]^+$ ; IR (KBr)  $cm^{-1}$  = 3400(N-H), 2926, 1654, 1603, 1484, 1285, 1150(C-N), 772.

***5,11,17,23-tetra(pyridine-3-ylamino)methyl) -25,26,27,28-tetrahydroxycalix[4]arene (58)***

Crystallised from THF/ $H_2O$  and hexane, to afford compound **58** as a yellow solid. (1.06 g). MS (MALDI)  $m/z$  = 849.4  $[M+H]^+$ , 871.3  $[M+Na]^+$ ; IR (KBr)  $cm^{-1}$  = 3378(N-H), 1591, 1484, 1438, 1304, 1148(C-N), 796, 707.

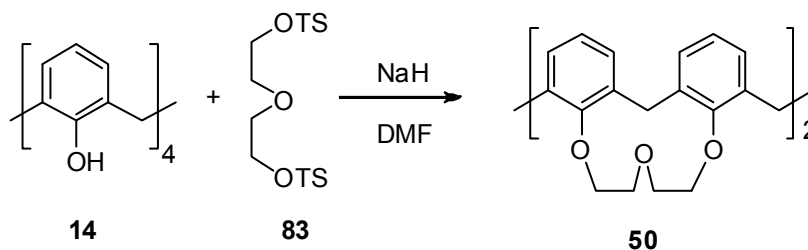
***5,11,17,23-tetra(pyridine-4-ylamino)methyl) -25,26,27,28-tetrahydroxycalix[4]arene (59)***

Crystallised from THF/ $H_2O$  and hexane, to afford compound **59** as a white solid. (1.24 g). IR (KBr)  $cm^{-1}$  = 3434(N-H), 2926, 1654, 1591, 1483, 1438, 1305, 1284, 1147(C-N), 912, 798.

For all of these compounds, the NMR spectra show the presence of starting material, indicated by a persistent aldehyde signal. Reaction conditions need to be improved for this particular synthetic procedure.

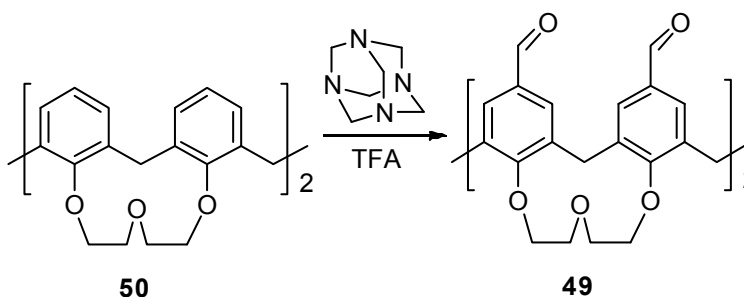


### Synthesis of 25,26,27,28-biscrown-3-calix[4]arene (**50**):<sup>20,21</sup>



Calix[4]arene **14** (3.2 g, 7.71 mmol) was dissolved in dimethylformamide (DMF) (610 mL). Sodium hydride (1.58 g, 39.5 mmol, 60% dispersion in mineral oil) was added after 30 min. diethyleneglycol di-*p*-toluenesulfonate **83** (7.21 g, 19.3 mmol) dissolved in DMF (50 mL) was added drop wise. The reaction was left to react for 48 hrs at 50°C. Methanol (10 mL) was added to quench the reaction. After evaporation to dryness, 1M HCl (100 mL) was added. The crude product was extracted with EtOAc (600 mL), washed with water (2 x 200 mL), dried (MgSO<sub>4</sub>) and evaporated. The product was purified by flash chromatography (EtOAc:Hexane (40:60)) to afford compound **50** as a white solid. (2.46 g, 3.7 mmol, 57.8%). <sup>1</sup>H NMR (200 MHz, 25°C, CDCl<sub>3</sub>) δ = 7.12 – 6.91 (m, 8H, ArH), 6.72 (t, 4H, ArH), 5.01 (d, <sup>2</sup>J = 12, 2H, ArCH<sub>2</sub>Ar), 4.47 (d, <sup>2</sup>J = 12, 2H, ArCH<sub>2</sub>Ar), 4.35 – 4.15 (m, 12H, OCH<sub>2</sub>CH<sub>2</sub>O), 3.97 – 3.73 (m, 4H), 3.22 (dd, <sup>2</sup>J = 12.0, <sup>3</sup>J = 9.8, 4H, OCH<sub>2</sub>CH<sub>2</sub>O) ppm.

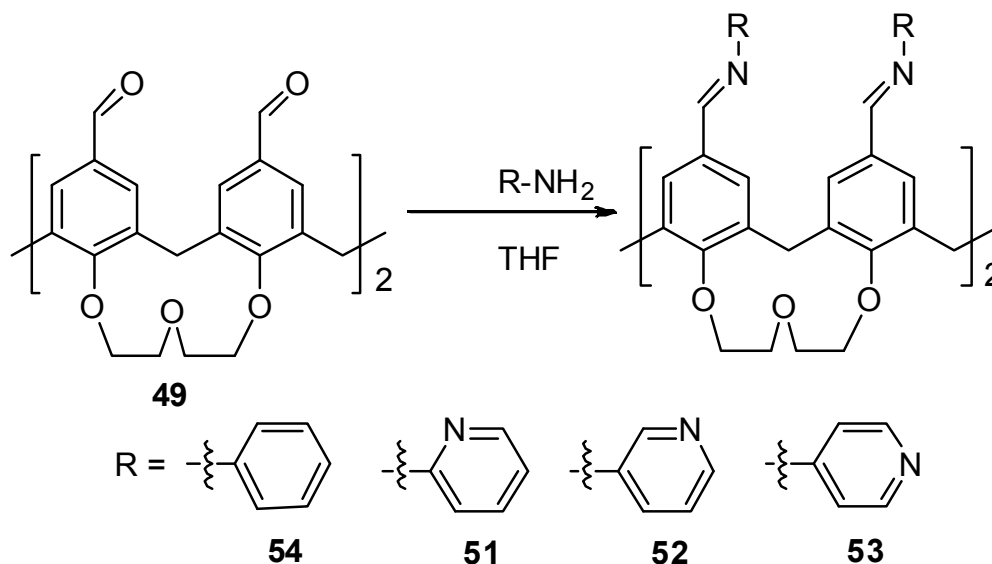
### Synthesis of 5,11,17,23-tetraformyl-25,26,27,28-biscrown-3-calix[4]arene (**49**):<sup>85</sup>



Biscrown-ether-calix[4]arene **50** (0.34 g, 0.6 mmol) and HMTA (1.55 g, 11 mmol) were dissolved in trifluoroacetic acid (6 mL) and was refluxing for 24 hrs. The hot reaction was poured onto ice water (35 mL) and the product was extracted with CHCl<sub>3</sub> (2 x 150 mL). The organic layer was washed with water (2 x 100 mL) dried (MgSO<sub>4</sub>) and evaporated. Addition of hexane (50 mL) precipitated compound **49** as a pale yellow solid. (0.299 g, 0.4 mmol, 74%). <sup>1</sup>H-NMR (200 MHz, 25°C, CDCl<sub>3</sub>): δ 9.74 (s, 4H, COH), 7.59 (d, 4H, ArH), 7.56 (d, 4H, ArH), 5.19 (d, <sup>2</sup>J = 12, 2H,

ArCH<sub>2</sub>Ar), 4.55 (d, <sup>2</sup>J = 12, 2H, ArCH<sub>2</sub>Ar), 4.43 – 4.13 (m, 12H, OCH<sub>2</sub>CH<sub>2</sub>O), 3.99 – 3.77 (m, 4H, OCH<sub>2</sub>CH<sub>2</sub>O), 3.39 (dd, <sup>2</sup>J = 23.8, <sup>3</sup>J = 11.5, 4H, ArCH<sub>2</sub>Ar) ppm.

**General synthesis for the Schiff-base reaction using formyl-biscrown-ether-calix[4]arene 49:<sup>24</sup>**



Tetra-formyl-biscrown-ether-calix[4]arene (**49**) and molecular sieves (4Å) were dispersed in dry THF (60 mL/mmol). Aniline or the appropriate amino – pyridine (5 molar eq.) was added, and the reaction was stirred overnight. The reaction was concentrated in *vacuo* and prior to reaching dryness, was dropped into hexane. The precipitate was filtered and dried.

**5,11,17,23-tetra((phenyl(imino)methyl)-25,26,27,28-biscrown-3-calix[4]arene (**54**)**

Compound **54** was isolated as a pale yellow solid. (0.128 g, 0.12 mmol, 46%); MS (MALDI) *m/z* = very noisy in the expected region; IR (KBr) cm<sup>-1</sup> = 2923, 1686, 1601(N=C), 1476, 1458.0, 1286, 1259, 1132, 1055, 918, 752.8, 694.

**5,11,17,23-tetra((pyridin-2-ylimino)methyl)-25,26,27,28-biscrown-3-calix[4]arene (**51**)**

Compound **51**, a pale yellow solid. (0.153g).

**5,11,17,23-tetra((pyridin-3-imino)methyl)-25,26,27,28-biscrown-3-calix[4]arene (52)**

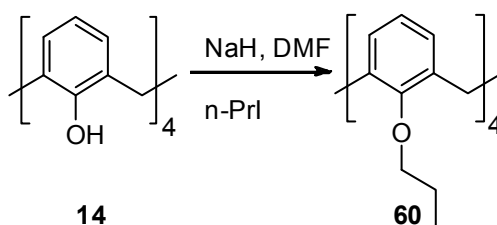
Compound **52**, a pale yellow solid. (0.182g).

**5,11,17,23-tetra((pyridin-4-imino)methyl)-25,26,27,28-biscrown-3-calix[4]arene (53)**

Compound **53**, a pale yellow solid. (0.034g).

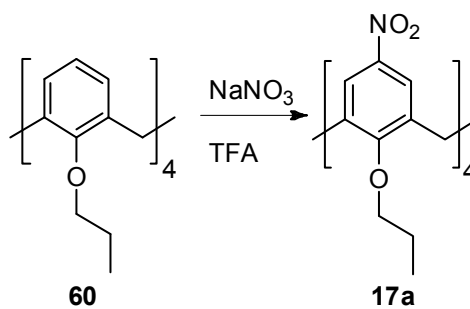
The IR spectra of compounds **51-54** show the presence of both N=C and C=O stretches, and the MS do not show the expected molecular ion peaks. The reaction is clearly not reaching completion and tuning of the experimental conditions is also required to improve this synthesis.

**Synthesis of 25,26,27,28-tetrapropoxycalix[4]arene (60):<sup>17,83</sup>**



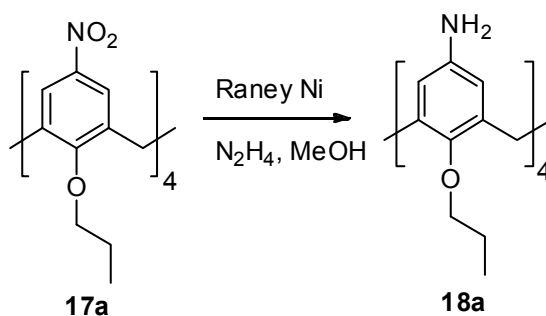
Calix[4]arene **14** (5.00 g, 11.8 mmol) was dissolved in DMF (150 mL), NaH (4.09 g, 102 mmol, 60% in mineral oil) was added. After 30 min, iodo propane (9.8 mL, 101 mmol) was added. The reaction was left to react for 1 h at 70°C. After cooling to RT, methanol (10 mL) was added and evaporated to dryness. Water (50 mL) was added and stirred for 10 min. The product was filtered off, washed with water and a small amount of methanol. Compound **60** was isolated *via* crystallisation from acetone over seven days. (4.75 g, 8.02 mmol, 68%). <sup>1</sup>H-NMR (200 MHz, 25°C, CDCl<sub>3</sub>): δ 6.55 (m, 12H, ArH), 4.40 (d, <sup>2</sup>J = 13, 4H, ArCH<sub>2</sub>Ar), 3.82 (t, 8H, OCH<sub>2</sub>CH<sub>2</sub>), 3.22 (d, <sup>2</sup>J = 13, 4H, ArCH<sub>2</sub>Ar), 1.92 (sextet, 8H, OCH<sub>2</sub>CH<sub>2</sub>) and 0.98 (t, 12H, OCH<sub>2</sub>CH<sub>2</sub>CH<sub>3</sub>) ppm.

### Synthesis of 5,11,17,23-tetranitro-25,26,27,28-tetrapropoxycalix[4]arene (**17a**):<sup>40</sup>



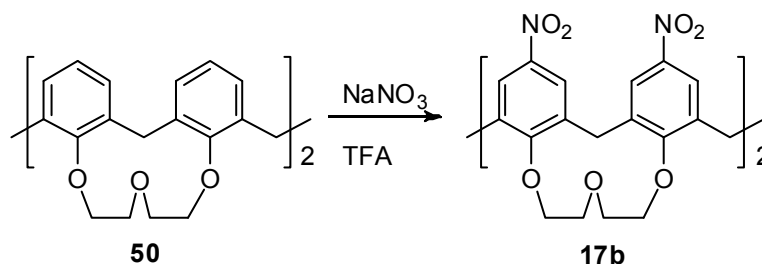
Propyl-calix[4]arene **60** (3.77 g, 6.35 mmol) was dissolved in TFA (20 mL). NaNO<sub>3</sub> (13.04 g, 153 mmol) was added and left stirring at RT over night (or upon the dark colour disappearing). The reaction then was poured onto ice/water (300 mL) and extracted with DCM (200 mL). The organic phase was washed with water up to neutrality and dried (MgSO<sub>4</sub>). The product **17a** (4.83 g, 6.25 mmol, 98%) was obtained as a orange-brown solid after evaporation. <sup>1</sup>H-NMR (200 MHz, 25°C, CDCl<sub>3</sub>): δ 7.52 (s, 8H, ArH), 4.45 (d, <sup>2</sup>J = 13, 4H, ArCH<sub>2</sub>Ar), 3.88 (t, 8H, OCH<sub>2</sub>CH<sub>2</sub>), 3.24 (d, <sup>2</sup>J = 13, 4H, ArCH<sub>2</sub>Ar), 1.86 (sextet, 8H, OCH<sub>2</sub>CH<sub>2</sub>) and 0.98 (t, 12H, OCH<sub>2</sub>CH<sub>2</sub>CH<sub>3</sub>) ppm.

### Synthesis of 5,11,17,23-tetraamino-25,26,27,28-tetrapropoxycalix[4]arene (**18a**):<sup>41</sup>



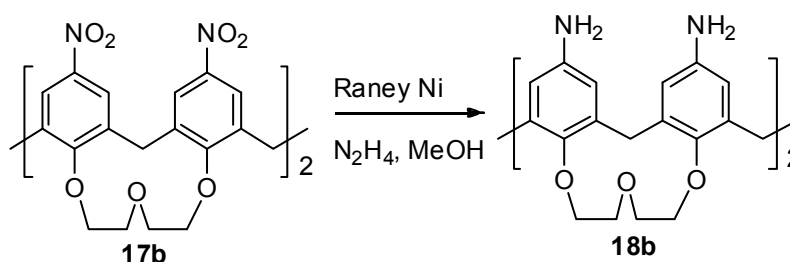
Nitro-calix[4]arene **17a** (0.535 g, 0.69 mmol) and Raney nickel (1 mL) were dispersed in methanol (30 mL). N<sub>2</sub>H<sub>4</sub>·H<sub>2</sub>O (3 mL) was added and the reaction was refluxed over night. Raney nickel was filtered off and washed with methanol (10 mL) and the filtrate was evaporated to yield **18a** (0.407 g, 0.62 mmol, 90%) as orange-brown solid. <sup>1</sup>H-NMR (200 MHz, 25°C, CDCl<sub>3</sub>): δ 6.09 (s, 8H, ArH), 4.32 (d, <sup>2</sup>J = 13, 4H, ArCH<sub>2</sub>Ar), 3.69 (t, 8H, OCH<sub>2</sub>CH<sub>2</sub>), 3.02 (d, <sup>2</sup>J = 13, 4H, ArCH<sub>2</sub>Ar), 2.60 (bs, 8H, NH<sub>2</sub>), 1.82 (six, 8H, OCH<sub>2</sub>CH<sub>2</sub>) and 0.92 (t, 12H, OCH<sub>2</sub>CH<sub>2</sub>CH<sub>3</sub>) ppm. MS (ESI) *m/z* = 652 [M]<sup>+</sup>.

### Synthesis of 5,11,17,23-tetranitro-25,26,27,28-biscrown-3-calix[4]arene (**17b**):<sup>40</sup>



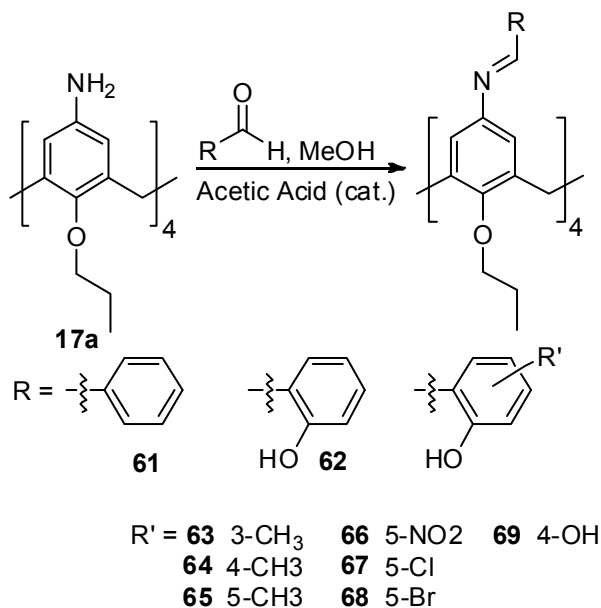
Biscrown-calix[4]arene **50** (2.91 g, 5.15 mmol) was dissolved in TFA (20 mL).  $\text{NaNO}_3$  (10.59 g, 125 mmol) was added and left stirring at RT over night (or upon the dark colour disappearing). The reaction then was poured onto ice/water (250 mL) and extracted with DCM (150 mL). The organic phase was washed with water up to neutrality and dried ( $\text{MgSO}_4$ ). The product **17b** (3.18 g, 4.27 mmol, 83%) was obtained as an orange-brown solid after evaporation.  $^1\text{H-NMR}$  (200 MHz,  $25^\circ\text{C}$ ,  $\text{CDCl}_3$ ): 7.92 (dd,  $^4J = 6, 3$ , 8H, ArH), 5.21 (d,  $^2J = 12$ , 2H,  $\text{ArCH}_2\text{Ar}$ ), 4.49 (d,  $^2J = 12$ , 2H,  $\text{ArCH}_2\text{Ar}$ ), 4.49 – 4.09 (m, 12H,  $\text{OCH}_2\text{CH}_2\text{O}$ ), 3.92 – 3.79 (m, 4H,  $\text{OCH}_2\text{CH}_2\text{O}$ ), 3.40 (t,  $^2J = 23.8$ , 11.5, 4H,  $\text{ArCH}_2\text{Ar}$ ) ppm.

### Synthesis of 5,11,17,23-tetramino-25,26,27,28-biscrown-3-calix[4]arene (**18b**):<sup>41</sup>



Nitro calix[4]arene **17b** (0.488 g, 0.66 mmol) and Raney nickel (1 mL) were dispersed in methanol (30 mL).  $\text{N}_2\text{H}_4 \cdot \text{H}_2\text{O}$  (3 mL) was added and the reaction was left to reflux over night. Raney nickel was filtered off and washed with methanol (10 mL) and the filtrate was evaporated to yield **18b** (0.302 g, 0.48 mmol, 74%) as a dark orange-brown solid.  $^1\text{H-NMR}$  (200 MHz,  $25^\circ\text{C}$ ,  $\text{CDCl}_3$ ): 6.32 (m, 8H, ArH), 4.82 (d,  $^2J = 12$ , 2H,  $\text{ArCH}_2\text{Ar}$ ), 4.31 (d,  $^2J = 12$ , 2H,  $\text{ArCH}_2\text{Ar}$ ), 4.24 – 4.09 (m, 12H,  $\text{OCH}_2\text{CH}_2\text{O}$ ), 3.82 – 3.65 (m, 4H,  $\text{OCH}_2\text{CH}_2\text{O}$ ), 3.19 – 2.72 (bs, 4H,  $\text{NH}_2$ ), 2.97 (t, 4H,  $\text{ArCH}_2\text{Ar}$ ) ppm; MS (ESI)  $m/z = 647.37$   $[\text{M}+\text{Na}]^+$ .

## General Synthesis for the Schiff-base reaction of amino-propyl-calix[4]arene **17a**:<sup>41</sup>



Amino calix[4]arene **17a** and the appropriate benzaldehyde (5.4 mol eq.) were dissolved in ethanol (40 mL/mmol of **17a**). Acetic acid (1-2 drops) were added and the reaction was left to reflux over night. The reaction was cooled to RT, filtered, washed with ethanol (15 mL) and dried (MgSO<sub>4</sub>) to obtain the product.

### 5,11,17,23-tetrakis(phenylmethimino)-25,26,27,28-tetrapropoxycalix[4]arene (**61**)

Compound **61** (0.070 g, 0.07 mmol, 62%) was isolated as colourless crystals (methanol/DCM). <sup>1</sup>H-NMR (200 MHz, 25°C, CDCl<sub>3</sub>): δ 8.05 (s, 4H, N=CH), 7.57 (m, 8H, N=CHArH), 7.19 (m, 12H, N=CHArH), 6.70 (s, 8H, ArHN=CH), 4.45 (d, <sup>2</sup>J = 13, 4H, ArCH<sub>2</sub>Ar), 3.87 (t, 8H, OCH<sub>2</sub>CH<sub>2</sub>), 3.19 (d, <sup>2</sup>J = 13, 4H, ArCH<sub>2</sub>Ar), 1.92 (sextet, 8H, OCH<sub>2</sub>CH<sub>2</sub>) and 0.99 (t, 12H, CH<sub>2</sub>CH<sub>3</sub>) ppm; IR (KBr) cm<sup>-1</sup> = 2927, 1627(N=C), 1460, 1211, 1001, 962, 756, and 692.

### 5,11,17,23-tetrakis((2-hydroxy-phenyl)methimino)-25,26,27,28-tetrapropoxycalix[4]arene (**62**)

Compound **62** (0.150 g, 0.14 mmol, 48%) was isolated as orange-brown solid. <sup>1</sup>H-NMR (400 MHz, 25°C, CDCl<sub>3</sub>): 13.22 (bs, 4H, OH), 8.25 (s, 4H, N=CH), 7.20 – 7.10 (m, 8H, ArH-N=C), 6.77 – 6.67 (m, 16H, ArH-N=C), 4.52 (d, <sup>2</sup>J = 13, 4H, ArCH<sub>2</sub>Ar), 3.92 (t, 8H, OCH<sub>2</sub>CH<sub>2</sub>), 3.26 (d, <sup>2</sup>J = 13, 4H, ArCH<sub>2</sub>Ar), 1.99 (sextet, 8H, OCH<sub>2</sub>CH<sub>2</sub>) and 1.02 (t, 12H, OCH<sub>2</sub>CH<sub>2</sub>CH<sub>3</sub>) ppm; <sup>13</sup>C-NMR (100 MHz, 25°C, CDCl<sub>3</sub>): 160.8 (N=CH), 160.7 (q, Ar-C), 155.8 (q, Ar-C), 142.7 (q, Ar-C), 135.7 (q, 2 x Ar-C), 132.2 (Ar-CH), 131.9 (Ar-CH), 120.9 (2 x Ar-CH), 119.2 (q, Ar-C), 118.9 (Ar-CH), 117.2 (Ar-CH), 77.1 (O-CH<sub>2</sub>CH<sub>2</sub>), 31.3 (O-CH<sub>2</sub>CH<sub>2</sub>), 23.2 (Ar-CH<sub>2</sub>-Ar), and 10.3

(CH<sub>3</sub>) ppm; MP = dec. >225°C; MS (ESI)  $m/z$  = 1069.53 [M]<sup>+</sup> 1091.40 [M+Na]<sup>+</sup>; IR (KBr) cm<sup>-1</sup> = 3448 (OH), 2962, 2933, 2875, 1618 (N=C), 1573, 1465, 1279, 1210, 1151, 1003, and 753.

***5,11,17,23-tetrakis((2-hydroxy-3-methyl-phenyl)methimino)-25,26,27,28-tetrapropoxycalix[4]arene (63)***

Compound **63** (0.171 g, 0.15 mmol, 50%) was isolated as an orange-brown solid. <sup>1</sup>H-NMR (400 MHz, 25°C, CDCl<sub>3</sub>): 13.54 (bs, 4H, OH), 8.29 (s, 4H, N=CH), 7.11 – 7.05 (m, 8H, N=C-ArH), 6.73 (s, 8H, ArH-N=C), 6.68 (t, 4H, N=C-ArH), 4.58 (d, <sup>2</sup>J = 13, 4H, ArCH<sub>2</sub>Ar), 3.99 (t, 8H, OCH<sub>2</sub>CH<sub>2</sub>), 3.31 (d, <sup>2</sup>J = 13, 4H, ArCH<sub>2</sub>Ar), 2.19 (s, 12H, Ar-CH<sub>3</sub>), 2.03 (sextet, 8H, OCH<sub>2</sub>CH<sub>2</sub>) and 1.10 (t, 12H, CH<sub>2</sub>CH<sub>3</sub>) ppm; <sup>13</sup>C-NMR (100 MHz, 25°C, CDCl<sub>3</sub>): 160.9 (N=CH), 159.1 (q, Ar-C), 155.8 (q, Ar-C), 142.7 (q, Ar-C), 135.7 (q, 2 x Ar-C), 133.4 (Ar-CH), 129.6 (Ar-CH), 125.6 (q, Ar-C), 120.8 (2 x Ar-CH), 118.4 (q, Ar-C), 118.0 (Ar-CH), 77.1 (O-CH<sub>2</sub>CH<sub>2</sub>), 31.3 (O-CH<sub>2</sub>CH<sub>2</sub>), 23.2 (Ar-CH<sub>2</sub>-Ar), 15.4 (Ar-CH<sub>3</sub>), and 10.3 (CH<sub>3</sub>) ppm; MP = dec. >270°C; MS (ESI)  $m/z$  = 1125.53 [M]<sup>+</sup> and 1147.47 [M+Na-H]<sup>+</sup>; IR (KBr) cm<sup>-1</sup> = 3447 (OH), 2962, 2933, 2876, 1615 (N=C), 1580, 1460, 1383, 1269, 1214, 1084, 1036, 1003, 963, 848, 745.

***5,11,17,23-tetrakis((2-hydroxy-4-methyl-phenyl)methimino)-25,26,27,28-tetrapropoxycalix[4]arene (64)***

Compound **64** (0.148 g, 0.13 mmol, 42%) was isolated as an orange-brown solid. <sup>1</sup>H-NMR (400 MHz, 25°C, CDCl<sub>3</sub>): 12.99 (bs, 4H, OH), 8.17 (s, 4H, N=CH), 6.97 – 6.90 (m, 8H, ArH-N=C), 6.70 – 6.60 (m, 12H, N=C-ArH), 4.52 (d, <sup>2</sup>J = 13, 4H, ArCH<sub>2</sub>Ar), 3.95 (t, 8H, OCH<sub>2</sub>CH<sub>2</sub>), 3.28 (d, <sup>2</sup>J = 13, 4H, ArCH<sub>2</sub>Ar), 2.17 (s, 12H, Ar-CH<sub>3</sub>), 1.99 (sextet, 8H, OCH<sub>2</sub>CH<sub>2</sub>) and 1.03 (t, 12H, CH<sub>2</sub>CH<sub>3</sub>) ppm; <sup>13</sup>C-NMR (100 MHz, 25°C, CDCl<sub>3</sub>): 160.9 (N=CH), 158.7 (q, Ar-C), 155.7 (q, Ar-C), 142.9 (q, Ar-C), 135.7 (q, 2 x Ar-C), 133.3 (Ar-CH), 131.8 (Ar-CH), 127.6 (q, Ar-C), 120.9 (2 x Ar-CH), 118.8 (q, Ar-C), 116.6 (Ar-CH), 77.2 (O-CH<sub>2</sub>CH<sub>2</sub>), 31.3 (O-CH<sub>2</sub>CH<sub>2</sub>), 23.5 (Ar-CH<sub>2</sub>-Ar), 20.3 (Ar-CH<sub>3</sub>), and 10.1 (CH<sub>3</sub>) ppm; MP = dec. >260°C; MS (ESI)  $m/z$  = 1125.50 [M]<sup>+</sup>; IR (KBr) cm<sup>-1</sup> = 3436 (OH), 2926, 1617 (N=C), 1577, 1464, 1380, 1354, 1303, 1243, 1216, 1127, 1006, 964, 805, and 589.

***5,11,17,23-tetrakis((2-hydroxy-5-methyl-phenyl)methimino)-25,26,27,28-tetrapropoxycalix[4]arene (65)***

Compound **65** (0.180 g, 0.16 mmol, 52%) was isolated as an orange-brown solid.  $^1\text{H-NMR}$  (400 MHz, 25°C,  $\text{CDCl}_3$ ): 12.99 (bs, 4H, OH), 8.17 (s, 4H,  $\text{N=CH}$ ), 6.98 – 6.90 (m, 8H,  $\text{ArH-N=C}$ ), 6.70 – 6.62 (m, 12H,  $\text{N=C-ArH}$ ), 4.52 (d,  $^2J = 13$ , 4H,  $\text{ArCH}_2\text{Ar}$ ), 3.92 (t, 8H,  $\text{OCH}_2\text{CH}_2$ ), 3.25 (d,  $^2J = 13$ , 4H,  $\text{ArCH}_2\text{Ar}$ ), 2.20 (s, 12H,  $\text{Ar-CH}_3$ ), 1.97 (sextet, 8H,  $\text{OCH}_2\text{CH}_2$ ) and 1.01 (t, 12H,  $\text{CH}_2\text{CH}_3$ ) ppm;  $^{13}\text{C-NMR}$  (100 MHz, 25°C,  $\text{CDCl}_3$ ): 160.9 ( $\text{N=CH}$ ), 158.6 (q,  $\text{Ar-C}$ ), 155.7 (q,  $\text{Ar-C}$ ), 142.9 (q,  $\text{Ar-C}$ ), 135.7 (q, 2 x  $\text{Ar-C}$ ), 133.3 ( $\text{Ar-CH}$ ), 131.8 ( $\text{Ar-CH}$ ), 127.6 (q,  $\text{Ar-C}$ ), 120.9 (2 x  $\text{Ar-CH}$ ), 118.8 (q,  $\text{Ar-C}$ ), 116.4 ( $\text{Ar-CH}$ ), 77.1 ( $\text{O-CH}_2\text{CH}_2$ ), 31.3 ( $\text{O-CH}_2\text{CH}_2$ ), 23.2 ( $\text{Ar-CH}_2\text{-Ar}$ ), 20.2 ( $\text{Ar-CH}_3$ ), and 10.3 ( $\text{CH}_3$ ) ppm; MP = dec.  $>250^\circ\text{C}$ ; MS (ESI)  $m/z = 1125.49 [\text{M}]^+$ ; IR (KBr)  $\text{cm}^{-1} = 3448$  (OH), 1626 ( $\text{N=C}$ ), 1490, 1281, 1215, 1159, and 1007.

***5,11,17,23-tetrakis((2-hydroxy-5-nitro-phenyl)methimino)-25,26,27,28-tetrapropoxycalix[4]arene (66)***

Compound **66** (0.175 g, 0.14 mmol, 45%) was isolated as an orange-brown solid. MP = dec.  $>160^\circ\text{C}$ ; MS (ESI)  $m/z = 1249.47 [\text{M}]^+$ ; IR (KBr)  $\text{cm}^{-1} = 3448$  (OH), 2932, 1617 ( $\text{N=C}$ ), 1586, 1520, 1479, 1384, 1339, 1284, 1219, 1098, 1003, 962, 830, and 751.

***5,11,17,23-tetrakis((2-hydroxy-5-chloro-phenyl)methimino)-25,26,27,28-tetrapropoxycalix[4]arene (67)***

Compound **67** (0.221 g, 0.18 mmol, 58%) was isolated as an orange-brown solid.  $^1\text{H-NMR}$  (400 MHz, 25°C,  $\text{CDCl}_3$ ): 13.27 (bs, 4H, OH), 8.20 (s, 4H,  $\text{N=CH}$ ), 7.18 (d,  $^2J = 3$ , 4H,  $\text{N=C-ArH}$ ), 7.08 (dd,  $^2J = 9$ , 3, 4H,  $\text{N=C-ArH}$ ), 6.70 (d,  $^2J = 9$ , 4H,  $\text{N=C-ArH}$ ), 6.67 (s, 8H,  $\text{ArH-N=C}$ ), 4.50 (d,  $^2J = 13$ , 4H,  $\text{ArCH}_2\text{Ar}$ ), 3.88 (t, 8H,  $\text{OCH}_2\text{CH}_2$ ), 3.21 (d,  $^2J = 13$ , 4H,  $\text{ArCH}_2\text{Ar}$ ), 1.90 (sextet, 8H,  $\text{OCH}_2\text{CH}_2$ ) and 1.00 (t, 12H,  $\text{CH}_2\text{CH}_3$ ) ppm;  $^{13}\text{C-NMR}$  (100 MHz, 25°C,  $\text{CDCl}_3$ ): 159.3 (q,  $\text{Ar-C}$ ), 159.1 ( $\text{N=CH}$ ), 156.3 (q,  $\text{Ar-C}$ ), 142.0 (q,  $\text{Ar-C}$ ), 135.8 (q, 2 x  $\text{Ar-C}$ ), 132.2 ( $\text{Ar-CH}$ ), 130.5 ( $\text{Ar-CH}$ ), 123.2 (q,  $\text{Ar-C}$ ), 121 (2 x  $\text{Ar-CH}$ ), 119.9 (q,  $\text{Ar-C}$ ), 118.2 ( $\text{Ar-CH}$ ), 77.2 ( $\text{O-CH}_2\text{CH}_2$ ), 31.3 ( $\text{O-CH}_2\text{CH}_2$ ), 23.2 ( $\text{Ar-CH}_2\text{-Ar}$ ), and 10.3 ( $\text{CH}_3$ ) ppm; MP = dec.  $>274^\circ\text{C}$ ; MS (ESI)  $m/z = 1207.20 [\text{M}]^+$  and 1229.07  $[\text{M}+\text{Na-H}]^+$ ; IR (KBr)  $\text{cm}^{-1} = 3436$  (OH), 2963, 1619 ( $\text{N=C}$ ), 1569, 1478, 1385, 1278, 1217, 1198, 1004, 962, 882, 819, and 652.



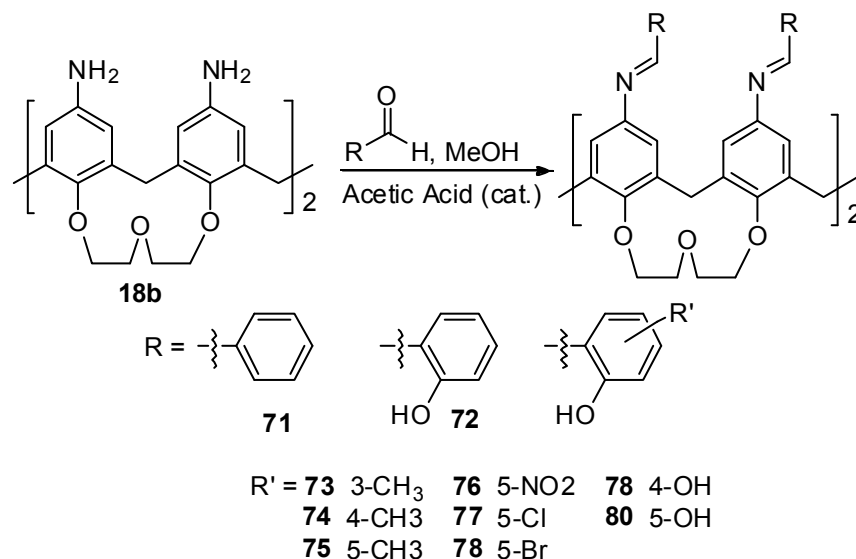
**5,11,17,23-tetrakis((2-hydroxy-5-bromo-phenyl)methimino)-25,26,27,28-tetrapropoxycalix[4]arene (68)**

Compound **68** (0.265 g, 0.19 mmol, 61%) was isolated as an orange-brown solid. MP = dec. >220°C; MS (ESI)  $m/z$  = 1385.01  $[M]^+$ ; IR (KBr)  $\text{cm}^{-1}$  = 3436 (OH), 2924, 1615 (N=C), 1586, 1518, 1479, 1339, 1285, 1227, 1132, 1087, 916, 831, and 751.

**5,11,17,23-tetrakis((2,4-dihydroxy-phenyl)methimino)-25,26,27,28-tetrapropoxycalix[4]arene (69)**

Compound **69** (0.194 g, 0.17 mmol, 55%) was isolated as a red solid. MP = dec. >280°C; MS (ESI)  $m/z$  = 1133.27  $[M]^+$  and 1155.47  $[M+\text{Na}-\text{H}]^+$ ; IR (KBr)  $\text{cm}^{-1}$  = 3414 (OH), 2962, 1620 (N=C), 1466, 1214, 999, and 846.

**General Synthesis for the Schiff-base reaction of amino-crown-ether-calix[4]arene:<sup>41</sup>**



Amino calix[4]arene **18b** and the appropriate benzaldehyde (5.4 mol eq.) were dissolved in ethanol (40 mL/mmol of **18b**). Acetic acid (1-2 drops) was added and the reaction was left to reflux over night. The reaction was cooled to RT, filtered, washed with ethanol (10 mL) and dried ( $\text{MgSO}_4$ ).

**5,11,17,23-tetrakis(phenylmethimino)-25,26,27,28-biscrown-3-calix[4]arene (71)**

Compound **71** (0.054 g, 0.06 mmol, 33%) was isolated as an orange-brown solid.  $^1\text{H-NMR}$  (400 MHz, 25°C,  $\text{CDCl}_3$ ): 8.32 (4H,  $\text{N}=\text{CH}$ ), 7.98 – 7.68 (m, 8H,  $\text{N}=\text{C-ArH}$ ), 7.49 – 7.25 (m, 12H,  $\text{N}=\text{C-ArH}$ ), 7.00 – 6.89 (m, 8H,  $\text{ArH-N}=\text{C}$ ), 5.11 (d,  $^2J = 12$ , 2H,  $\text{ArCH}_2\text{Ar}$ ), 4.59 (d,  $^2J = 12$ , 2H,  $\text{ArCH}_2\text{Ar}$ ), 4.42 – 4.01 (m, 12H,  $\text{OCH}_2\text{CH}_2\text{O}$ ), 3.99 –

3.79 (m, 4H, OCH<sub>2</sub>CH<sub>2</sub>O), 3.41 – 3.22 (m, 4H, ArCH<sub>2</sub>Ar) ppm; <sup>13</sup>C-NMR (100 MHz, 25°C, CDCl<sub>3</sub>): 159.1 (N=CH), 153.9 (q, ArC), 147.3 (q, ArC), 136.4 (q, ArC), 135.9 (q, ArC), 135.7 (q, ArC), 134.5 (ArCH), 129.7 (ArCH), 129.0 (ArCH), 128.6 (2 x ArCH), 121.7 (ArCH), 120.8 (ArCH), 76.5 (OCH<sub>2</sub>CH<sub>2</sub>O), 74.7 (OCH<sub>2</sub>CH<sub>2</sub>O), 31.0 (0.5 x ArCH<sub>2</sub>Ar) and 30.1 (0.5 x ArCH<sub>2</sub>Ar) ppm; MS (ESI) *m/z* = 977.4 [M]<sup>+</sup> and 999.47 [M+Na]<sup>+</sup>; IR (KBr) cm<sup>-1</sup> = 2920, 1625 (N=C), 1576, 1455, 1369, 1286, 1214, 1134, 1059, 917, 757, and 693.

**5,11,17,23-tetrakis((2-hydroxy-phenyl)methimino)-25,26,27,28-biscrown-3-calix[4]arene (72)**

Compound **72** (0.217 g, 0.21 mmol, 67%) was isolated as an orange-brown solid. <sup>1</sup>H-NMR (400 MHz, 25°C, CDCl<sub>3</sub>): 13.09 (bs, 4H, OH), 8.36 (4H, N=CH), 7.29 – 7.22 (m, 4H, N=C-ArH), 7.20 – 7.12 (m, 4H, N=C-ArH), 7.01 – 6.98 (m, 8H, ArH-N=C), 6.89 – 6.70 (m, 8H, N=C-ArH), 5.15 (d, <sup>2</sup>J = 12, 2H, ArCH<sub>2</sub>Ar), 4.58 (d, <sup>2</sup>J = 12, 2H, ArCH<sub>2</sub>Ar), 4.40 – 4.18 (m, 12H, OCH<sub>2</sub>CH<sub>2</sub>O), 3.99 – 3.78 (m, 4H, OCH<sub>2</sub>CH<sub>2</sub>O), 3.40 – 3.25 (m, 4H, ArCH<sub>2</sub>Ar) ppm; <sup>13</sup>C-NMR (100 MHz, 25°C, CDCl<sub>3</sub>): 161.7 (N=CH), 160.9 (q, ArC), 154.4 (q, ArC), 144.2 (q, ArC), 136.2 (q, ArC), 136.1 (q, ArC), 132.7 (ArCH), 132.2 (ArCH), 121.7 (ArCH), 121.0 (ArCH), 119.1 (q, ArC), 118.8 (ArCH), 117.0 (ArCH), 77.0 (OCH<sub>2</sub>CH<sub>2</sub>O), 74.7 (OCH<sub>2</sub>CH<sub>2</sub>O), 30.9 (0.5 x ArCH<sub>2</sub>Ar) and 30.1 (0.5 x ArCH<sub>2</sub>Ar) ppm; MP = dec. >265°C; MS (ESI) *m/z* = 1041.40 [M]<sup>+</sup> and 1064.40 [M+Na]<sup>+</sup>; IR (KBr) cm<sup>-1</sup> = 3448 (OH), 2921, 2862, 1619 (N=C), 1573, 1455, 1277, 1226, 1138, 1057, 1007, 906, 883, and 755.

**5,11,17,23-tetrakis((2-hydroxy-3-methyl-phenyl)methimino)-25,26,27,28-biscrown-3-calix[4]arene (73)**

Compound **73** (0.191 g, 0.17 mmol, 52%) was isolated as an orange-brown solid. <sup>1</sup>H-NMR (400 MHz, 25°C, CDCl<sub>3</sub>): 13.48 (bs, 4H, OH), 8.42 (4H, N=CH), 7.17 (dd, <sup>2</sup>J = 18, 8, 8H, N=C-ArH), 7.00 (d, 8H, ArH-N=C), 6.73 (t, 4H, N=C-ArH), 5.10 (d, <sup>2</sup>J = 12, 2H, ArCH<sub>2</sub>Ar), 4.58 (d, <sup>2</sup>J = 12, 2H, ArCH<sub>2</sub>Ar), 4.36 – 4.21 (m, 12H, OCH<sub>2</sub>CH<sub>2</sub>O), 3.98 – 3.78 (m, 4H, OCH<sub>2</sub>CH<sub>2</sub>O), 3.35 (dd, <sup>2</sup>J = 21, 12, 4H, ArCH<sub>2</sub>Ar) and 2.26 (s, 12H, CH<sub>3</sub>) ppm; <sup>13</sup>C-NMR (100 MHz, 25°C, CDCl<sub>3</sub>): 161.9 (N=CH), 159.3 (q, ArC), 154.4 (q, ArC), 144.2 (q, ArC), 136.2 (q, ArC), 136.0 (q, ArC), 133.7 (ArCH), 130.0 (ArCH), 126.0 (q, ArC), 121.7 (ArCH), 120.9 (q, ArC), 118.4 (ArCH), 118.3 (ArCH), 77.0 (OCH<sub>2</sub>CH<sub>2</sub>O), 74.7 (OCH<sub>2</sub>CH<sub>2</sub>O), 30.9 (0.5 x ArCH<sub>2</sub>Ar), 30.1 (0.5 x ArCH<sub>2</sub>Ar) and 15.5 (CH<sub>3</sub>) ppm; MP = dec. >250°C; MS (ESI) *m/z* = 1097.53 [M]<sup>+</sup> and 1119.47

$[M+Na-H]^+$ ; IR (KBr)  $\text{cm}^{-1}$  = 3448 (OH), 2918, 2860, 1615 (N=C), 1455, 1268, 1248, 1220, 1137, 1084, 1137, 1084, 1057, 876, 775, and 746.

***5,11,17,23-tetrakis((2-hydroxy-4-methyl-phenyl)methimino)-25,26,27,28-biscrown-3-calix[4]arene (74)***

Compound **74** (0.239 g, 0.22 mmol, 66%) was isolated as an orange-brown solid.  $^1\text{H-NMR}$  (400 MHz,  $25^\circ\text{C}$ ,  $\text{CDCl}_3$ ): 13.08 (bs, 4H, OH), 8.39 (4H, N=CH), 7.20 (d, 4H, N=C-ArH), 6.99 (dd, 8H, ArH-N=C), 6.74 (s, 4H, N=C-ArH), 6.69 (d, 4H, N=C-ArH), 5.10 (d,  $J = 12$ , 2H,  $\text{ArCH}_2\text{Ar}$ ), 4.55 (d,  $J = 12$ , 2H,  $\text{ArCH}_2\text{Ar}$ ), 4.38 – 4.20 (m, 12H,  $\text{OCH}_2\text{CH}_2\text{O}$ ), 3.91 – 3.80 (m, 4H,  $\text{OCH}_2\text{CH}_2\text{O}$ ), 3.30 (dd,  $^2J = 20$ , 12, 4H,  $\text{ArCH}_2\text{Ar}$ ) and 2.30 (s, 12H,  $\text{CH}_3$ ) ppm;  $^{13}\text{C-NMR}$  (100 MHz,  $25^\circ\text{C}$ ,  $\text{CDCl}_3$ ): 161.4 (N=CH), 161.1 (q, ArC), 154.3 (q, ArC), 144.3 (q, ArC), 144.1 (q, ArC), 136.2 (q, ArC), 136.0 (q, ArC), 132.1 (ArCH), 121.7 (ArCH), 120.9 (ArCH), 120.1 (ArCH), 117.4 (ArCH), 117.1 (q, ArC), 77.2 ( $\text{OCH}_2\text{CH}_2\text{O}$ ), 74.7 ( $\text{OCH}_2\text{CH}_2\text{O}$ ), 30.9 (0.5 x  $\text{ArCH}_2\text{Ar}$ ), 30.1 (0.5 x  $\text{ArCH}_2\text{Ar}$ ) and 21.8 ( $\text{CH}_3$ ) ppm; MP = dec.  $>243^\circ\text{C}$ ; MS (ESI)  $m/z = 1097.47 [M]^+$  and 1119.33  $[M+Na-H]^+$ ; IR (KBr)  $\text{cm}^{-1}$  = 3446 (OH), 2918, 1615 (C=N), 1564, 1455, 1357, 1283, 1212, 1131, 1057, 1008, 875, and 800.

***5,11,17,23-tetrakis((2-hydroxy-5-methyl-phenyl)methimino)-25,26,27,28-biscrown-3-calix[4]arene (75)***

Compound **75** (0.189 g, 0.17 mmol, 53%) was isolated as an orange-brown solid.  $^1\text{H-NMR}$  (400 MHz,  $25^\circ\text{C}$ ,  $\text{CDCl}_3$ ): 12.91 (bs, 4H, OH), 8.36 (4H, N=CH), 7.10 – 7.01 (m, 8H, N=C-ArH), 6.98 (dd, 8H, ArH-N=C), 6.79 (d, 4H, N=C-ArH), 5.12 (d,  $^2J = 12$ , 2H,  $\text{ArCH}_2\text{Ar}$ ), 4.57 (d,  $^2J = 12$ , 2H,  $\text{ArCH}_2\text{Ar}$ ), 4.36 – 4.19 (m, 12H,  $\text{OCH}_2\text{CH}_2\text{O}$ ), 3.98 – 3.76 (m, 4H,  $\text{OCH}_2\text{CH}_2\text{O}$ ), 3.35 (dd,  $^2J = 22$ , 12, 4H,  $\text{ArCH}_2\text{Ar}$ ) and 2.21 (s, 12H,  $\text{CH}_3$ ) ppm;  $^{13}\text{C-NMR}$  (100 MHz,  $25^\circ\text{C}$ ,  $\text{CDCl}_3$ ): 161.7 (N=CH), 158.8 (q, ArC), 154.4 (q, ArC), 144.3 (q, ArC), 136.4 (q, ArC), 136.2 (q, ArC), 133.8 (ArCH), 132.2 (ArCH), 127.9 (q, ArC), 121.7 (ArCH), 121.0 (ArCH), 118.8 (q, ArC), 116.3 (ArCH), 77.2 ( $\text{OCH}_2\text{CH}_2\text{O}$ ), 74.7 ( $\text{OCH}_2\text{CH}_2\text{O}$ ), 30.9 (0.5 x  $\text{ArCH}_2\text{Ar}$ ), 30.1 (0.5 x  $\text{ArCH}_2\text{Ar}$ ) and 20.2 ( $\text{CH}_3$ ) ppm; MP = dec.  $>258^\circ\text{C}$ ; MS (ESI)  $m/z = 1097.47 [M]^+$  and 1120.33  $[M+Na]^+$ ; IR (KBr)  $\text{cm}^{-1}$  = 3435 (OH), 2920, 2862, 1624 (N=C), 1580, 1490, 1474, 1456, 1280, 1222, 1137, 1058, 1015, 917, 879, 819, and 782.

***5,11,17,23-tetrakis((2-hydroxy-5-nitro-phenyl)methimino)-25,26,27,28-biscrown-3-calix[4]arene (76)***

Compound **76** (0.293 g, 0.24 mmol, 73%) was isolated as an orange-brown solid. <sup>1</sup>H-NMR (400 MHz, 25°C, D6-Aceton): 13.52 (bs, 4H, OH), 8.92 (4H, N=CH), 7.81 – 7.77 (m, 8H, N=C-ArH), 7.40 – 7.21 (m, 8H, ArH-N=C), 6.98 – 6.82 (m, 4H, N=C-ArH), 4.61 – 4.38 (m, 4H, ArCH<sub>2</sub>Ar), 4.20 – 3.40 (m, 16H, OCH<sub>2</sub>CH<sub>2</sub>O), 3.08 – 2.71 (m, 4H, ArCH<sub>2</sub>Ar) ppm; <sup>13</sup>C-NMR (100 MHz, 25°C, D6-Aceton): 156.6 (q, ArC), 137.2 (N=CH), 134.6 (ArCH), 131.5 (2 x ArCH), 130.3 (q, ArC), 128.9 (ArCH), 126.3 (q, ArC), 124.8 (q, ArC), 123.6 (q, ArC), 119.7 (q, ArC), 118.9 (ArCH), 112.2 (q, ArC), 77.8 (OCH<sub>2</sub>CH<sub>2</sub>O), 31.6 (0.5 x ArCH<sub>2</sub>Ar), and 24.2 (0.5 x ArCH<sub>2</sub>Ar) ppm; MP = dec. >180°C; MS (ESI) *m/z* = 1222.87 [M+H]<sup>+</sup>; IR (KBr) cm<sup>-1</sup> = 3435 (OH), 2961, 2932, 2874, 1617 (N=C), 1475, 1384, 1277, 1216, 1123, 1004, 963, 881, 817.

***5,11,17,23-tetrakis((2-hydroxy-5-chloro-phenyl)methimino)-25,26,27,28-biscrown-3-calix[4]arene (77)***

Compound **77** (0.199 g, 0.17 mmol, 54%) was isolated as an orange-brown solid. <sup>1</sup>H-NMR (400 MHz, 25°C, D6-DMSO): 13.17 (bs, 4H, OH), 8.70 (4H, N=CH), 7.50 (s, 4H, N=C-ArH), 7.45 – 7.30 (m, 8H, N=C-ArH), 6.90 (d, 8H, ArH-N=C), 5.02 (d, <sup>2</sup>*J* = 12, 2H, ArCH<sub>2</sub>Ar), 4.50 (d, <sup>2</sup>*J* = 12, 2H, ArCH<sub>2</sub>Ar), 4.32 – 4.12 (m, 12H, OCH<sub>2</sub>CH<sub>2</sub>O), 3.81 – 3.62 (m, 4H, OCH<sub>2</sub>CH<sub>2</sub>O) and 3.43 (m, 4H, ArCH<sub>2</sub>Ar) ppm; <sup>13</sup>C-NMR (100 MHz, 25°C, D6-DMSO): 161.6 (N=CH), 158.9 (q, ArC), 154.5 (q, ArC), 143.4 (q, ArC), 136.4 (q, ArC), 132.3 (ArCH), 130.9 (ArCH), 127.4 (q, ArC), 122.4 (q, ArC), 122.1 (ArCH), 121.2 (ArCH), 120.4 (q, ArC), 118.5 (ArCH), 76.7 (OCH<sub>2</sub>CH<sub>2</sub>O), 74.3 (OCH<sub>2</sub>CH<sub>2</sub>O), 29.6 (0.5 x ArCH<sub>2</sub>Ar), and 29.1 (0.5 x ArCH<sub>2</sub>Ar) ppm; MP = dec. >275°C; MS (ESI) *m/z* = 1179.07 [M]<sup>+</sup> and 1201.27 [M+Na-H]<sup>+</sup>; IR (KBr) cm<sup>-1</sup> = 3448 (OH), 2925, 1620 (N=C), 1522, 1475, 1347, 1276, 1226, 1137, 1085, 1055, 876, and 821.

***5,11,17,23-tetrakis((2-hydroxy-5-bromo-phenyl)methimino)-25,26,27,28-biscrown-3-calix[4]arene (78)***

Compound **78** (0.257 g, 0.19 mmol, 60%) was isolated as an orange-brown solid. <sup>1</sup>H-NMR (400 MHz, 25°C, D6-Aceton): 13.30 (bs, 4H, OH), 8.60 (4H, N=CH), 7.49 – 7.22 (m, 8H, N=C-ArH), 7.21 – 7.10 (m, 4H, ArH-N=C), 6.93 – 6.78 (m, 4H, ArH-N=C), 6.55 – 6.43 (m, 4H, N=C-ArH), 5.21 (d, <sup>2</sup>*J* = 12, 2H, ArCH<sub>2</sub>Ar), 4.69 (d, <sup>2</sup>*J* = 12, 2H, ArCH<sub>2</sub>Ar), 4.43 – 4.10 (m, 12H, OCH<sub>2</sub>CH<sub>2</sub>O), 3.90 – 3.60 (m, 4H, OCH<sub>2</sub>CH<sub>2</sub>O),

and 3.50 – 3.35 (m, 4H, ArCH<sub>2</sub>Ar) ppm; <sup>13</sup>C-NMR (100 MHz, 25°C, D6-Aceton): 161.7 (N=CH), 160.4 (q, ArC), 155.8 (q, ArC), 144.4 (q, ArC), 137.4 (q, ArC), 137.2 (ArCH), 135.0 (ArCH), 131.8 (ArCH), 128.7 (ArCH), 124.6 (q, ArC), 119.5 (ArCH), 119.5 (q, ArC), 110.6 (q, ArC), 77.6 (OCH<sub>2</sub>CH<sub>2</sub>O), 75.3 (OCH<sub>2</sub>CH<sub>2</sub>O), 31.2 (0.5 x ArCH<sub>2</sub>Ar), and 27.6 (0.5 x ArCH<sub>2</sub>Ar) ppm; MP = dec. >230°C; MS (ESI) *m/z* = 1357.00 [M]<sup>+</sup>; IR (KBr) cm<sup>-1</sup> = 3435 (OH), 2920, 1618 (N=C), 1475, 1354, 1275, 1225, 1129, 1084, 1057, 1008, 915, 875, 818, and 628.

***5,11,17,23-tetrakis((2,4-dihydroxy-phenyl)methimino)-25,26,27,28-biscrown-3-calix[4]arene (79)***

Compound **79** (0.202 g, 0.18 58%) was isolated as an orange-brown solid. MP = dec. >300°C; MS (ESI) *m/z* = 1104.47 [M]<sup>+</sup> and 1129.00 [M+Na+2H]<sup>+</sup>; IR (KBr) cm<sup>-1</sup> = 3428 (OH), 2927, 1624 (N=C), 1517, 1456, 1345, 1222, 1128, 1083, 1052, 918, and 799.

***5,11,17,23-tetrakis((2,5-dihydroxy-phenyl)methimino)-25,26,27,28-biscrown-3-calix[4]arene (80)***

Compound **80** (0.119 g, 0.11 mmol, 34%) was isolated as a black solid. <sup>1</sup>H-NMR (400 MHz, 25°C, D6-DMSO): 12.31 (s, 8H, OH), 8.64 (4H, N=CH), 7.45 – 7.20 (m, 8H, ArH), 7.00 – 6.60 (m, 12H, ArH), 5.09 (d, <sup>2</sup>*J* = 12, 2H, ArCH<sub>2</sub>Ar), 4.49 (d, <sup>2</sup>*J* = 12, 2H, ArCH<sub>2</sub>Ar), 4.34 – 4.07 (m, 12H, OCH<sub>2</sub>CH<sub>2</sub>O), 3.82 – 3.52 (m, 4H, OCH<sub>2</sub>CH<sub>2</sub>O), 3.40 – 3.20 (m, 4H, ArCH<sub>2</sub>Ar) ppm; MP = dec. >300°C; MS (ESI) *m/z* = 1105.47 [M]<sup>+</sup> and 1127.80 [M+Na-H]<sup>+</sup>; IR (KBr) cm<sup>-1</sup> = 3428 (OH), 2927, 1618 (N=C), 1578, 1521, 1454, 1345, 1221, 1134, 1052, 918, 875, and 823.

*Conclusion*  
*And*  
*Future Work*

## ***Conclusion***

In conclusion the synthesis of the amino-pyridine Schiff-base and reduction products was successful, but these synthetic routes require improvement. Characterisation of these products is difficult due to noisy NMR spectra that may be due to the formation of isomers. The crystallisation of these products was not successful and the ultimate goal of forming supramolecular molecular assemblies and coordination polymers was not realised due to time constraints and ligand availability.

The Schiff-bases to be formed from *p*-aminocalix[4]arenes and different 2-hydroxybenzaldehydes were successfully synthesised and characterised. The ligands derived from upper-rim aminocalix[4]arenes are more stable than those isolated from formyl derivatives as might be expected due to intramolecular hydrogen bonding interactions. Time constraints associated with this project prevented the investigation of supramolecular assemblies or metal complexes based on these new building blocks.

The single crystal X-ray structure of compound **49** was obtained during the course of this study. Structural analysis confirmed the rigid structure of the constrained molecule and showed an ethyl acetate molecule interacting with the cavity of the host. The extended structure shows the molecule to pack in an anti-parallel fashion. Structural analyses of upper-rim Schiff-bases will provide insight into the potential assembly of these new building blocks.

## Future Work

The ligands synthesised during this project can potentially be used to assemble new supramolecular architectures. Given the precedent of metal binding with related Schiff-bases, this may be especially true the calix[4]arenes substituted at the upper rim with 2-hydroxybenzaldehydes. The resulting potential supramolecular complexes, formed with the ligands synthesised, can be investigated with respect to structural stability, stability towards guest exchange, and analysing differences between the flexible propoxy and more rigid crown-ether calix[4]arene derivatives. The steric effects of the methyl group (compounds **63-65** and **73-75**) in the different upper-rim groups should also play a role in determining self-assembly. In addition to this, increasing steric bulk at these positions can be examined in detail by changing the methyl group to ethyl, propyl, iso-propyl and *t*-butyl.

Future work may also include increasing the size of the ligand library by using different substituted benzaldehydes. One such substitution could be the use of 5-iodo-2-hydroxy benzaldehyde. This can potentially be used to influence assembly based on halogen-halogen interactions and nitro-halogen interactions. Furthermore, the tetra-nitrocalix[4]arenes (**66** and **76**) could be combined with Schiff-base products of 5-iodo-2-hydroxy benzaldehyde and the relevant *p*-amino-calix[4]arenes to form hetero-dimeric capsules. This is based on the literature precedent that iodine<sup>86</sup> and bromine<sup>87</sup> can interact with an oxygen atom of the nitro group. When iodine is used, two main interactions of iodine and oxygen have been discovered. One is where both the oxygens of a nitro group interact with the same iodo group, while the other is where both oxygens interact with two different iodo groups as illustrated in Figure 46. The synthesis of hetero-capsules with nitro- and iodo- substituted calixarenes should be interesting from a supramolecular point of view as such species are rare.<sup>88</sup>

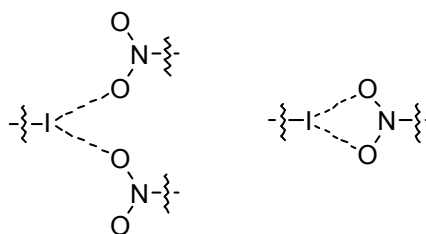


**Figure 46.** Intermolecular interaction of an iodo-group with the oxygen atoms of a nitro-group.



The pyridine based ligands (compounds **51-53** and **57-59**) can potentially be used to synthesise small capsules and coordination polymers with different assembly-directing metals as hinges or nodes. Reduction of the C=N bond should affect the shape and rigidity of these ligands, and in turn affect the self-assembly process by means of introducing flexibility and rotation around the resulting C-N bond.

## ***References***

- (1) Steed, J. W.; Atwood, J. L. *Supramolecular Chemistry 2<sup>nd</sup> Edition* John Wiley and Sons Ltd: Chichester, **2009**, p 1-5, 27-37.
- (2) Palmer, L. C.; Rebek, J. *Org. Biomol. Chem.* **2004**, 2, 3051-3059.
- (3) Hof, F.; Craig, S. L.; Nuckolls, C.; Rebek, J. *Angew. Chem. Int. Ed.* **2002**, 41, 1488-1508.
- (4) Nakabayashi, K.; Kawano, M.; Yoshizawa, M.; Ohkoshi, S.; Fujita, M. *J. Am. Chem. Soc.* **2004**, 126, 16694-16695.
- (5) Yamaguchi, T.; Fujita, M. *Angew. Chem. Int. Ed.* **2008**, 47, 2067-2069.
- (6) Fujita, M.; Tominaga, M.; Hori, A.; Therrien, B. *Acc. Chem. Res.* **2005**, 38, 371-380.
- (7) Christofi, A. M.; Garratt, P. J.; Hogarth, G.; Ibbett, A.J.; Ng, Y.-F.; Steed, J. W. *Tetrahedron*, **2002**, 58, 4543-4549.
- (8) Hunter, C. A.; Lawson, K. R.; Perkins, J.; Urch, C. J. *J. Chem. Soc., Perkin Trans. 2*, **2001**, 651-669.
- (9) Ma, J. C.; Dougherty, D. *Chem. Rev.*, **1997**, 97, 1303-1324.
- (10) Berryman, O. B.; Bryantsev, V. S.; Stay, D. P.; Johnson, D. W.; Hay, B. P. *J. Am. Chem. Soc.*, **2007**, 129, 48-58.
- (11) Kitaigorodskii, A. I. *Organic Chemical Crystallography* Consultants Bureau: New York, 1961.
- (12) Pyykkö, P. *Chem. Rev.*, **1997**, 97, 597-636.
- (13) Dodziuk, H. *Introduction to Supramolecular Chemistry* Kluwer Academic Publishers: Dordrecht, **2002**, p 1-2, 183-191.
- (14) Asfari, Z.; Böhmer, V.; Harrowfield, J.; Vicens, J. *Calixarenes 2001*; Kluwer Academic Publishers: London, **2001**, p 1-20.
- (15) Solov'eva, S. E.; Omran, A. O.; Gruener, M.; Habicher, W. D.; Antipin, I. S.; Konovalov, A. *J. Struct. Chem.* **2005**, 46, S16-S21.
- (16) Botana, E.; Nattinen, K.; Prados, P.; Rissanen, K.; de Mendoza, J. *Org. Lett.* **2004**, 6, 1091-1094.
- (17) Ajami, D.; Rebek, J. *Angew. Chem. Int. Ed.* **2007**, 46, 9283-9286.
- (18) Pinalli, R.; Cristini, V.; Sottili, V.; Geremia, S.; Campagnolo, M.; Caneschi, A.; Dalcanale, E. *J. Am. Chem. Soc.* **2004**, 126, 6516-6517.
- (19) Atwood, J. L.; Szumna, A. *J. Am. Chem. Soc.* **2002**, 124, 10646-10647.
- (20) Gerkenmeier, T.; Iwanek, W.; Agena, C.; Frohlich, R.; Kotila, S.; Nather, C.; Mattay, J. *Eur. J. Org. Chem.* **1999**, 2257-2262.

- (21) Park, S. J.; Shin, D. M.; Sakamoto, S.; Yamaguchi, K.; Chung, Y. K.; Lah, M. S.; Hong, J. I. *Chem. Eur. J.* **2004**, *11*, 235-241.
- (22) Schätz, R.; Weber, C.; Schilling, G.; Öser, T.; Huber-Patz, U.; Irngartinger, H.; Von der Lieth, C.-W.; Pipkorn, R. *Liebigs Ann.*, **1995**, 1401-1408.
- (23) Shu, C. M.; Chung, W. S.; Wu, S. H.; Ho, Z. C.; Lin, L. G. *J. Org. Chem.* **1999**, *64*, 2673-2679.
- (24) Wahler, J. *Synthesis of upper-rim Schiff base calix[4]arenes as potential supramolecular building blocks*, March - August 2008.
- (25) Dijkstra, P. J.; Brunink, J. A. J.; Bugge, K. E.; Reinhoudt, D. N.; Harkema, S.; Ungaro, R.; Ugozzoli, F.; Ghidini, E. *J. Am. Chem. Soc.* **1989**, *111*, 7567-7575.
- (26) Van Loon, J. D.; Arduini, A.; Coppi, L.; Verboom, W.; Pochini, A.; Ungaro, R.; Harkema, S.; Reinhoudt, D. N. *J. Org. Chem.* **1990**, *55*, 5639-5646.
- (27) Groenen, L. C.; van Loon, J.-D.; Verboom, W.; Harkema, S.; Casnati, A.; Ungaro, R.; Pochini, A.; Ugozzoli, F.; Reinhoudt, D. N. *J. Am. Chem. Soc.*, **1991**, *113*, 2385-2392.
- (28) Arduini, A.; McGregor, W. M.; Paganuzzi, D.; Pochini, A.; Secchi, A.; Ugozzoli, F.; Ungaro, R. *J. Chem. Soc., Perkin Trans. 2* **1996**, 839-846.
- (29) Arduini, A.; Fabbi, M.; Mantovani, M.; Mirone, L.; Pochini, A.; Secchi, A.; Ungaro, R. *J. Org. Chem.* **1995**, *60*, 1454-1457.
- (30) Klimentová, J.; Vojtišek, P.; Sklenářova, M. *J. Mol. Struc.* **2007**, *871*, 33-41
- (31) Gutsche, C. D.; Levine, J. A.; Sujeeth, P. K. *J. Org. Chem.* **1985**, *50*, 5802-5806.
- (32) Atwood, J. L.; Barbour, L. J.; Dalgarno, S. J.; Hardie, M. J.; Raston, C. L.; Webb, H. R. *J. Am. Chem. Soc.* **2004**, *126*, 13170-13171.
- (33) Conn, M. M.; Rebek, J. *Chem. Rev.* **1997**, *97*, 1647-1668.
- (34) Cotton, F. A.; Lei, P.; Lin, C.; Murillo, C. A.; Wang, X. P.; Yu, S. Y.; Zhang, Z. X. *J. Am. Chem. Soc.* **2004**, *126*, 1518-1525.
- (35) Vatsouro, I.; Rudzevich, V.; Bohmer, V. *Org. Lett.* **2007**, *9*, 1375-1377.
- (36) Pellet-Rostaing, S.; Chitry, F.; Nicod, L.; Lemaire, M. *J. Chem. Soc., Perkin Trans. 2* **2001**, 1426-1432.
- (37) Ihm, H.; Paek, K. *Bull. Korean Chem. Soc.* **1995**, *16*, 71-73.
- (38) Komori, T.; Shinkai, S. *Chem. Lett.* **1992**, 901-904.
- (39) Guo, T. D.; Zheng, Q. Y.; Yang, L. M.; Huang, Z. T. *J. Inclusion Phenom. Macrocyclic Chem.* **2000**, *36*, 327-333.
- (40) Arora, V.; Chawla, H. M.; Santra, A. *Tetrahedron* **2002**, *58*, 5591-5597.

- (41) Arduini, A.; Fanni, S.; Manfredi, G.; Pochini, A.; Ungaro, R.; Sicuri, A. R.; Ugozzoli, F. *J. Org. Chem.* **1995**, *60*, 1448-1453.
- (42) Arduini, A.; Manfredi, G.; Pochini, A.; Sicuri, A. R.; Ungaro, R. *J. Chem. Soc., Chem. Commun.* **1991**, 936-937.
- (43) Arduini, A.; Mirone, L.; Paganuzzi, D.; Pinalli, A.; Pochini, A.; Secchi, A.; Ungaro, R. *Tetrahedron* **1996**, *52*, 6011-6018.
- (44) Klimentová, J.; Vojtišek, P. *J. Mol. Struc.*, **2007**, *826*, 48-63.
- (45) Arduini, A.; Domiano, L.; Ogliosi, L.; Pochini, A.; Secchi, A.; Ungaro, R. *J. Org. Chem.* **1997**, *62*, 7866-7868.
- (46) Durmaz, M.; Alpaydin, S.; Sirit, A.; Yilmaz, M. *Tetrahedron-Asymmetry* **2007**, *18*, 900-905.
- (47) Dalgarno, S. J.; Cave, G. W. V.; Atwood, J. L. *Angew. Chem. Int. Ed.* **2006**, *45*, 570-574.
- (48) Orr, G. W.; Barbour, L. J.; Atwood, J. L. *Science* **1999**, *285*, 1049-1052.
- (49) Dalgarno, S. J.; Atwood, J. L.; Raston, C. L. *Chem. Commun.* **2006**, 4567-4574.
- (50) Dalgarno, S. J.; Warren, J. E.; Antesberger, J.; Glass, T. E.; Atwood, J. L. *New J. Chem.* **2007**, *31*, 1891-1894.
- (51) Lazar, A. N.; Dupont, N.; Navaza, A.; Coleman, A. W. *Chem. Commun.* **2006**, 1076-1078.
- (52) Zadmard, R.; Schrader, T.; Grawe, T.; Kraft, A. *Org. Lett.* **2002**, *4*, 1687-1690.
- (53) MacGillivray, L. R.; Atwood, J. L. *Nature* **1997**, *389*, 469-472.
- (54) Dalgarno, S. J.; Bassil, D. B.; Tucker, S. A.; Atwood, J. L. *Angew. Chem. Int. Ed.* **2006**, *45*, 7019-7022.
- (55) Dalgarno, S. J.; Tucker, S. A.; Bassil, D. B.; Atwood, J. L. *Science* **2005**, *309*, 2037-2039.
- (56) Atwood, J. L.; Barbour, L. J.; Jerga, A. *Proc. Natl. Acad. Sci. U. S. A.* **2002**, *99*, 4837-4841.
- (57) Barrett, E. S.; Dale, T. J.; Rebek, J. *J. Am. Chem. Soc.* **2008**, *130*, 2344-2350.
- (58) Barrett, E. S.; Dale, T. J.; Rebek, J. *J. Am. Chem. Soc.* **2007**, *129*, 3818-3819.
- (59) Avram, L.; Cohen, Y. *Org. Lett.* **2003**, *5*, 3329-3332.
- (60) Dalgarno, S. J.; Power, N. P.; Atwood, J. L. *Coord. Chem. Rev.* **2008**, *252*, 825-841.
- (61) McKinlay, R. M.; Cave, G. W. V.; Atwood, J. L. *Proc. Natl. Acad. Sci. U. S. A.* **2005**, *102*, 5944-5948.

- (62) Antesberger, J.; Cave, G. W. V.; Ferrarelli, M. C.; Heaven, M. W.; Raston, C. L.; Atwood, J. L. *Chem. Commun.* **2005**, 892-894.
- (63) Jaunky, W.; Hosseini M. W.; Planeix, A.; De Cian, A.; Kyritsakas, N.; Fischer, J. *Chem. Commun.* **1999**, 2313-2314.
- (64) Pascu, G. I.; Hotze, A. C. G.; Sanchez-Cano, C.; Kariuki, B. M.; Hannon, M. J. *Angew. Chem. Int. Ed.* **2007**, 46, 4374-4378.
- (65) Stang, P. J.; Olenyuk, B. *Acc. Chem. Res.* **1997**, 30, 502-518.
- (66) Ugono, O.; Moran, J. P.; Holman, K. T. *Chem. Commun.* **2008**, 1404-1406.
- (67) Baldini, L.; Ballester, P.; Casnati, A.; Gomila, R. M.; Hunter, C. A.; Sansone, F.; Ungaro, R. *J. Am. Chem. Soc.* **2003**, 125, 14181-14189.
- (68) Hardie, M. J.; Raston, C. L.; Wells, B. *Chem. Eur. J.* **2000**, 6, 3293-3298.
- (69) Hwang, G. T.; Kim, B. H. *Tetrahedron Lett.* **2000**, 41, 5917-5921.
- (70) Zhong, Z. L.; Ikeda, A.; Ayabe, M.; Shinkai, S.; Sakamoto, S.; Yamaguchi, K. *J. Org. Chem.* **2001**, 66, 1002-1008.
- (71) Vollhardt, K. P. C.; Schore, N. E. *Organic Chemistry 3<sup>rd</sup> Edition* W. H. Freeman and Company: New York, **1998**, p 749.
- (72) Chakraborti, A. K.; Bhagat, S.; Rudrawar, S. *Tetrahedron Lett.*, **2004**, 45, 7641-7644.
- (73) Albrecht, M.; Janser, I.; Meyer, S.; Weis, P.; Froehlich, R. *Chem. Commun.* **2003**, 2854-2855.
- (74) Albrecht, M.; Janser, I.; Burk, S.; Weis, P. *Dalton Trans.*, **2006**, 2875-2880.
- (75) Lacroix, P. G.; Averseng, F.; Malfant I.; Nakatani, K. *Inorg. Chim Acta*, **2004**, 357, 3825-3835.
- (76) Kleij, A. W.; Kuil, M.; Tooke, D. M.; Spek, A. L.; Reek, J. N. H. *Inorg. Chem.*, **2007**, 46, 5829-5831.
- (77) Kleij, A. W.; Kuil, M.; Tooke, D. M.; Lutz, M.; Spek, A. L.; Reek, J. N. H. *Chem. Eur. J.*, **2005**, 11, 4743-4750.
- (78) Alemi, A. A.; Shaabani, B. *Acta Chim. Slov.*, **2000**, 47, 363-369.
- (79) Rosu, T.; Gulea, A.; Pahontu, E.; Cotovaia, A. *Rev. Chim.*, **2007**, 58, 475-480.
- (80) Niu, Y.; Zhang, N.; Hou, H.; Zhu, Y.; Tang, M.; Ng, S. W. *J. Mol. Struct.*, **2007**, 827, 195-200.
- (81) Cui, X.; Khlobystov, A. N.; Chen, X.; Marsh, D. H.; Blake, A. J.; Lewis, W.; Champness, N. R.; Roberts, C. J.; Schröder, M. *Chem. Eur. J.*, **2009**, 15, 8861-8873.

- (82) Abdel-Magid, A. F.; Carson, K. G.; Harris, B. D.; Maryanoff, C. A.; Shah, R. D. *J. Org. Chem.*, **1996**, *61*, 3849-3862.
- (83) Gutsche, C. D.; Dhawan, B.; Levine, J. A.; No, K. H.; Bauer, L. J. *Tetrahedron*, **1983**, *39*, 409-426.
- (84) Gomez, S.; Peters, J. A.; Maschmeyer, T. *Adv. Synth. Catal.* **2002**, *344*, 1037-1057.
- (85) Abdel-Magid, A. F.; Mehrman, S. J. *Org. Process Res. Dev.* **2006**, *10*, 971-1031.
- (86) Thaimattam, R.; Sharma, C. V. K.; Clearfield, A.; Desiraju, G. R. ; *Cryst. Growth. Des.*, **2001**, *1*, 103-106.
- (87) Thallapally, P. K.; Desiraju, G. R.; Bagieu-Beucher, M.; Masse, R.; Bourgogne, C.; Nicoud, J.-F. *Chem. Commun.*, **2002**, 1052-1053.
- (88) Saha, B. K.; Nangia, A.; Jeskólski, M. *Cryst. Eng. Comm.*, **2005**, *7*, 355-358.

## ***Appendix***



Crystal data and structure refinement for compound **49**.

Identification code	X82763
Formula	C <sub>44</sub> H <sub>44</sub> O <sub>12</sub>
Formula weight	764.66
Size	0.4 x 0.3 x 0.05 mm
Crystal morphology	Colourless block
Temperature	100(2) K
Wavelength	0.71073 Å
Crystal system	Monoclinic
Space group	<i>P</i> 2 <sub>1</sub> / <i>c</i>
Unit cell dimensions	<i>a</i> = 11.1097(15) Å $\alpha = 90^\circ$ <i>b</i> = 16.586(2) Å $\beta = 98.008(5)^\circ$ <i>c</i> = 20.986(3) Å $\gamma = 90^\circ$
Volume	3829.3(9) Å <sup>3</sup>
<i>Z</i>	4
Density (calculated)	1.326 mg/m <sup>3</sup>
Absorption coefficient	0.096 mm <sup>-1</sup>
<i>F</i> (000)	1616
Data collection range	$1.96 \leq \theta \leq 25.72^\circ$
Index ranges	$-13 \leq h \leq 13, -20 \leq k \leq 20, -25 \leq l \leq 25$
Reflections collected	62178
Independent reflections	7276 [ <i>R</i> (int) = 0.1016]
Observed reflections	4193 [ <i>I</i> > 2σ( <i>I</i> )]
Absorption correction	multi-scan
Max. and min. transmission	0.9952 and 0.9624
Refinement method	Full
Data / restraints / parameters	7276 / 70 / 513
Goodness of fit	1.04
Final <i>R</i> indices [ <i>I</i> > 2σ( <i>I</i> )]	<i>R</i> <sub>1</sub> = 0.0876, <i>wR</i> <sub>2</sub> = 0.2323
<i>R</i> indices (all data)	<i>R</i> <sub>1</sub> = 0.155, <i>wR</i> <sub>2</sub> = 0.2833
Largest diff. peak and hole	1.461 and -1.068 e.Å <sup>-3</sup>

**Table 1.** Atomic co-ordinates ( $\times 10^4$ ) and equivalent isotropic displacement parameters ( $\text{\AA}^2 \times 10^4$ ) with standard uncertainties (s.u.s) in parentheses.  $U_{\text{eq}}$  is defined as  $1/3$  of the trace of the orthogonalized  $U_{ij}$  tensor.

	x	y	z	$U_{\text{eq}}$
O(1)	963.1(3)	183.82(19)	64.64(14)	20.9(7)
O(2)	955.6(3)	372.85(19)	86.97(14)	20.8(7)
O(3)	959.3(3)	91.3(2)	359.82(16)	28.0(8)
O(4)	701.1(3)	211.04(19)	13.24(15)	22.5(7)
O(5)	675.9(3)	388.31(19)	15.67(15)	21.7(7)
O(6)	1153.0(3)	289.42(19)	29.51(15)	22.4(7)
O(7)	1008.6(4)	400.7(2)	393.92(16)	34.7(9)
O(8)	666.3(3)	315.3(2)	-104.57(16)	29.9(8)
C(9)	1021.3(4)	337.3(3)	197.4(2)	18.2(10)
C(10)	948.4(4)	154.9(3)	124.9(2)	19.0(10)
C(11)	851.3(4)	63.8(3)	190.9(2)	20.5(10)
C(12)	1000.5(4)	158.9(3)	239.9(2)	19.5(10)
C(13)	610.1(4)	393.8(3)	66.4(2)	19.7(10)
C(14)	943.7(4)	413.3(3)	281.3(2)	21.6(10)
C(15)	619.9(4)	163.4(3)	39.8(2)	21.4(10)
C(16)	947.0(4)	384.8(3)	151.5(2)	17.7(10)
C(17)	865.1(4)	454.7(3)	235.1(2)	20.8(10)
C(18)	944.4(5)	433.7(3)	349.4(2)	26.7(11)
C(19)	1019.2(4)	353.9(3)	261.7(2)	19.7(10)
C(20)	775.4(4)	485.9(3)	120.7(2)	21.5(10)
C(21)	919.2(4)	95.6(3)	245.3(2)	19.9(10)
C(22)	906.7(4)	64.3(3)	309.4(2)	23.3(11)
C(23)	578.7(4)	456.9(3)	165.2(2)	23.0(11)
C(25)	785.8(4)	58.6(3)	70.6(2)	23.7(11)
C(26)	1108.2(4)	218.0(3)	-4.5(2)	23.9(11)
O(27) <sup>pu</sup>	297.8(4)	403.8(3)	219.3(2)	30.2(11)
C(28)	504.5(4)	197.1(3)	43.5(2)	23.8(11)
C(29)	865.7(4)	441.6(3)	169.5(2)	19.9(10)
C(30)	1096.6(5)	364.5(3)	9.3(2)	25.6(11)
C(31)	505.3(4)	346.0(3)	66.4(2)	21.5(10)
C(32)	1062.7(4)	409.4(3)	66.6(2)	22.7(11)
C(33)	1092.6(4)	265.6(3)	177.2(2)	19.3(10)
C(34)	470.2(4)	414.2(3)	164.0(2)	25.4(11)
C(35)	435.5(4)	357.7(3)	115.7(2)	24.1(11)
C(36)	1073.3(4)	156.4(3)	41.8(2)	23.5(11)
C(37)	457.1(5)	77.2(3)	101.8(3)	36.3(14)
C(38)	1014.8(4)	190.1(3)	180.3(2)	19.8(10)

**Table 1.** (continued)

C(39)	863.9(4)	93.2(3)	129.2(2)	19.0(10)
C(40)	424.0(5)	152.7(3)	75.7(3)	32.0(13)
C(41)	571.1(5)	45.6(3)	96.2(2)	31.3(12)
C(42)	685.2(5)	400.0(3)	-95.4(2)	32.2(12)
C(43)	469.9(4)	279.9(3)	16.1(2)	23.5(11)
C(44)	725.0(5)	190.9(3)	-50.4(2)	30.3(12)
C(45)	651.6(4)	446.6(3)	116.8(2)	20.3(10)
C(46)	655.1(4)	88.3(3)	66.8(2)	24.1(11)
C(47)	622.3(5)	429.3(3)	-41.5(2)	27.2(11)
C(48) <sup>pu</sup>	393(2)	432.4(12)	217.0(9)	27(3)
C(49)	768.4(5)	265.9(3)	-80.2(3)	32.2(12)
C(50) <sup>pu</sup>	380(2)	36.3(19)	141.6(13)	48(4)
O(52) <sup>pu</sup>	285.5(5)	64.8(5)	158.4(3)	56(2)
O(103) <sup>d</sup>	496.9(4)	246.8(3)	279.21(18)	52.7(12)
C(100) <sup>d</sup>	665.4(7)	246.7(4)	223.5(3)	61.5(19)
O(109) <sup>d</sup>	554.9(10)	127.9(7)	252.0(5)	177(4)
C(108) <sup>d</sup>	575.0(8)	203.0(6)	250.4(3)	92(3)
C(106) <sup>d</sup>	336.2(10)	268.1(7)	335.8(4)	121(4)
C(105) <sup>d</sup>	401.5(9)	208.1(7)	309.4(4)	111(4)
O(52a) <sup>pu</sup>	377.6(12)	-34.9(9)	155.0(7)	60(4)
O(28) <sup>pu</sup>	400.3(13)	463.1(9)	255.5(8)	39(3)
C(50a) <sup>pu</sup>	359(5)	28(4)	131(3)	50(5)
C(48a) <sup>pu</sup>	402(6)	418(4)	208(3)	31(5)

Key to superscripts on atoms with refinement constraints/restraints:

*d* - distance or angle restraint on site

*u* -  $U_{iso}$  or  $U_{ij}$  restraint (rigid bond)

*p* - partial occupancy constraint

**Table 2.** Anisotropic displacement parameters ( $\text{\AA}^2 \times 10^3$ ). The anisotropic displacement factor exponent takes the form:

$$-2\pi^2[h^2 a^{*2} U_{11} + \dots + 2 h k a^* b^* U_{12}]$$

	$U_{11}$	$U_{22}$	$U_{33}$	$U_{23}$	$U_{13}$	$U_{12}$
O(1)	17.2(16)	25.3(18)	20.3(17)	1.4(13)	2.7(13)	3.9(13)
O(2)	19.5(17)	25.8(18)	16.7(16)	-1.3(13)	0.8(13)	-1.2(14)
O(3)	36(2)	26.9(19)	22.0(18)	-0.4(15)	5.3(16)	3.4(16)
O(4)	19.4(17)	23.9(18)	24.2(17)	1.5(14)	3.4(14)	-2.8(14)
O(5)	19.5(17)	27.0(18)	18.7(17)	3.4(13)	3.4(13)	3.3(14)
O(6)	22.8(17)	23.1(18)	20.3(17)	-0.8(13)	-0.6(13)	1.2(14)
O(7)	54(2)	31(2)	17.6(18)	1.5(15)	-0.2(17)	0.1(18)
O(8)	36(2)	28(2)	23.1(18)	1.6(15)	-1.6(15)	5.9(16)
C(9)	15(2)	17(2)	22(2)	-1.8(18)	0.7(19)	-4.2(18)
C(10)	18(2)	21(2)	17(2)	1.9(19)	-0.4(19)	3.7(19)
C(11)	19(2)	17(2)	25(3)	1.1(19)	0.1(19)	0.8(19)
C(12)	19(2)	18(2)	21(2)	1.3(19)	1.5(19)	5.7(19)
C(13)	15(2)	25(3)	19(2)	5.0(19)	3.4(18)	6.2(19)
C(14)	23(2)	20(2)	22(2)	1.8(19)	4(2)	-7(2)
C(15)	22(2)	21(2)	20(2)	2.4(19)	-2.2(19)	-3(2)
C(16)	17(2)	19(2)	17(2)	1.6(18)	-0.5(18)	-3.6(18)
C(17)	18(2)	21(2)	23(2)	-1(2)	5.2(19)	-4.4(19)
C(18)	33(3)	24(3)	23(3)	-3(2)	5(2)	-5(2)
C(19)	21(2)	19(2)	18(2)	2.3(19)	0.1(19)	-4.7(19)
C(20)	23(3)	20(2)	20(2)	3.9(19)	1(2)	1(2)
C(21)	23(2)	13(2)	24(2)	1.8(19)	7(2)	5.0(19)
C(22)	24(3)	19(2)	29(3)	4(2)	9(2)	5(2)
C(23)	23(3)	29(3)	17(2)	3(2)	1.1(19)	8(2)
C(25)	25(3)	19(2)	25(3)	0(2)	-3(2)	0(2)
C(26)	25(3)	27(3)	19(2)	-3(2)	3(2)	1(2)
O(27)	20(3)	37(3)	35(3)	3(2)	9(2)	2(2)
C(28)	21(2)	25(3)	24(3)	3(2)	-2(2)	-3(2)
C(29)	19(2)	16(2)	25(2)	0.5(19)	1.4(19)	-5.1(19)
C(30)	31(3)	22(3)	26(3)	5(2)	8(2)	-3(2)
C(31)	18(2)	23(3)	22(2)	7(2)	-0.3(19)	3(2)
C(32)	26(3)	20(2)	22(2)	3.9(19)	6(2)	-2(2)
C(33)	19(2)	18(2)	20(2)	2.1(18)	0.4(19)	-1.7(18)
C(34)	20(3)	33(3)	23(3)	9(2)	5(2)	5(2)
C(35)	15(2)	32(3)	26(3)	12(2)	2(2)	0(2)
C(36)	25(3)	22(3)	24(3)	-2(2)	4(2)	4(2)

**Table 2.** (continued)

C(37)	22(3)	40(3)	44(3)	20(3)	-5(2)	-6(2)
C(38)	17(2)	16(2)	26(3)	1.3(19)	3.1(19)	5.4(19)
C(39)	17(2)	18(2)	22(2)	0.4(19)	1.9(19)	5.4(19)
C(40)	17(2)	41(3)	37(3)	15(2)	0(2)	-1(2)
C(41)	25(3)	28(3)	38(3)	13(2)	-7(2)	-5(2)
C(42)	42(3)	28(3)	29(3)	8(2)	10(2)	5(2)
C(43)	16(2)	28(3)	25(3)	6(2)	-2.2(19)	-1(2)
C(44)	41(3)	27(3)	24(3)	0(2)	10(2)	4(2)
C(45)	19(2)	18(2)	23(2)	5.8(19)	1.3(19)	5.9(19)
C(46)	24(3)	25(3)	21(2)	-1(2)	-6(2)	-3(2)
C(47)	33(3)	21(3)	28(3)	9(2)	4(2)	4(2)
C(48)	25(5)	39(8)	20(6)	1(5)	8(4)	16(5)
C(49)	33(3)	34(3)	32(3)	7(2)	14(2)	9(2)
C(50)	19(8)	52(7)	68(9)	36(6)	-8(6)	-13(6)
O(52)	17(3)	80(5)	71(5)	49(4)	7(3)	-2(3)
O(103)	43(7)	54(8)	81(9)	23(7)	-3(7)	-2(6)
C(100)	34(7)	48(8)	36(7)	-9(6)	9(6)	6(6)
O(109)	26(10)	50(9)	72(11)	42(8)	-1(9)	-15(9)
C(108)	29(8)	39(11)	26(10)	-1(8)	1(8)	11(8)

**Table 3.** Hydrogen atom co-ordinates ( $\times 10^3$ ) and isotropic displacement parameters ( $\text{\AA}^2 \times 10^2$ ) with s.u.s in parentheses.

	x	y	z	$U_{\text{eq}}$
H(11)	7953.	215.	1952.	25.
H(12)	10463.	1807.	2775.	23.
H(17)	8098.	4927.	2485.	25.
H(18)	8913.	4752.	3595.	32.
H(19)	10705.	3242.	2933.	24.
H(20a)	7700.	5431.	1337.	26.
H(20b)	8033.	4845.	779.	26.
H(22)	8538.	197.	3118.	28.
H(23)	6033.	4934.	1994.	28.
H(25a)	7873.	-10.	729.	28.
H(25b)	8193.	750.	312.	28.
H(26a)	11718.	1957.	-281.	29.
H(26b)	10366.	2317.	-362.	29.
H(30a)	10228.	3544.	-219.	31.
H(30b)	11533.	3975.	-122.	31.
H(32a)	11310.	4076.	1023.	27.
H(32b)	10459.	4666.	551.	27.
H(33a)	11701.	2599.	2065.	23.
H(33b)	11114.	2736.	1329.	23.
H(35)	3637.	3269.	1166.	29.
H(36a)	10593.	1035.	201.	28.
H(36b)	11392.	1501.	784.	28.
H(40)	3463.	1742.	799.	38.
H(41)	5918.	-66.	1129.	38.
H(42a)	6534.	4290.	-1355.	39.
H(42b)	7734.	4112.	-856.	39.
H(43a)	3812.	2819.	18.	28.
H(43b)	5117.	2898.	-219.	28.
H(44a)	6500.	1706.	-766.	36.
H(44b)	7878.	1483.	-483.	36.
H(47a)	6327.	4883.	-363.	33.
H(47b)	5342.	4172.	-504.	33.
H(48)	4242.	4690.	2500.	33.
H(49a)	8234.	2963.	-475.	39.
H(49b)	8144.	2512.	-1156.	39.
H(50)	4029.	-164.	1561.	57.
H(10a)	7420.	2448.	2529.	92.

**Table 3.** (continued)

---

H(10b)	6395.	3029.	2167.	92.
H(10c)	6772.	2225.	1822.	92.
H(10d)	3913.	2993.	3671.	182.
H(10e)	2727.	2434.	3574.	182.
H(10f)	2988.	3040.	3015.	182.
H(10g)	3471.	1769.	2770.	134.
H(10h)	4378.	1705.	3434.	134.
H(50a)	2793.	507.	1286.	60.
H(48a)	3400.	3787.	2036.	38.

---

**Table 4.** Interatomic distances (Å) with s.u.s in parentheses.

---

O(1)-C(10)	1.384(5)	O(1)-C(36)	1.449(5)
O(2)-C(16)	1.384(5)	O(2)-C(32)	1.451(5)
O(3)-C(22)	1.221(6)	O(4)-C(15)	1.374(5)
O(4)-C(44)	1.437(6)	O(5)-C(13)	1.375(5)
O(5)-C(47)	1.435(5)	O(6)-C(30)	1.432(6)
O(6)-C(26)	1.435(6)	O(7)-C(18)	1.223(6)
O(8)-C(42)	1.429(6)	O(8)-C(49)	1.434(6)
C(9)-C(19)	1.381(6)	C(9)-C(16)	1.418(6)
C(9)-C(33)	1.521(6)	C(10)-C(39)	1.400(6)
C(10)-C(38)	1.413(6)	C(11)-C(21)	1.382(6)
C(11)-C(39)	1.409(6)	C(12)-C(38)	1.383(6)
C(12)-C(21)	1.400(7)	C(13)-C(45)	1.402(7)
C(13)-C(31)	1.408(7)	C(14)-C(17)	1.392(6)
C(14)-C(19)	1.392(7)	C(14)-C(18)	1.467(7)
C(15)-C(46)	1.402(7)	C(15)-C(28)	1.410(7)
C(16)-C(29)	1.393(6)	C(17)-C(29)	1.395(6)
C(20)-C(45)	1.514(6)	C(20)-C(29)	1.520(6)
C(21)-C(22)	1.466(6)	C(23)-C(45)	1.395(6)
C(23)-C(34)	1.396(7)	C(25)-C(39)	1.517(6)
C(25)-C(46)	1.526(7)	C(26)-C(36)	1.499(7)
O(27)-C(48)	1.17(2)	C(28)-C(40)	1.402(7)
C(28)-C(43)	1.519(7)	C(30)-C(32)	1.505(7)
C(31)-C(35)	1.390(7)	C(31)-C(43)	1.535(7)
C(33)-C(38)	1.529(6)	C(34)-C(48a)	1.27(6)
C(34)-C(35)	1.395(7)	C(34)-C(48)	1.526(17)
C(37)-C(41)	1.391(7)	C(37)-C(40)	1.394(8)
C(37)-C(50)	1.45(3)	C(37)-C(50a)	1.55(6)
C(41)-C(46)	1.382(7)	C(42)-C(47)	1.491(7)
C(44)-C(49)	1.502(7)	C(50)-O(52)	1.24(3)
O(103)-C(108)	1.339(11)	O(103)-C(105)	1.457(12)
C(100)-C(108)	1.419(12)	O(109)-C(108)	1.266(11)
C(106)-C(105)	1.392(14)	O(52a)-C(50a)	1.17(6)
O(28)-C(48a)	1.25(5)		

---



**Table 5.** Angles between interatomic vectors (°) with s.u.s in parentheses.

C(10)-O(1)-C(36)	114.0(3)	C(16)-O(2)-C(32)	113.6(3)
C(15)-O(4)-C(44)	117.4(4)	C(13)-O(5)-C(47)	114.3(3)
C(30)-O(6)-C(26)	117.6(3)	C(42)-O(8)-C(49)	114.7(4)
C(19)-C(9)-C(16)	117.8(4)	C(19)-C(9)-C(33)	120.6(4)
C(16)-C(9)-C(33)	121.4(4)	O(1)-C(10)-C(39)	118.6(4)
O(1)-C(10)-C(38)	119.6(4)	C(39)-C(10)-C(38)	121.8(4)
C(21)-C(11)-C(39)	120.9(4)	C(38)-C(12)-C(21)	120.8(4)
O(5)-C(13)-C(45)	118.1(4)	O(5)-C(13)-C(31)	119.5(4)
C(45)-C(13)-C(31)	122.4(4)	C(17)-C(14)-C(19)	119.2(4)
C(17)-C(14)-C(18)	118.9(4)	C(19)-C(14)-C(18)	121.9(4)
O(4)-C(15)-C(46)	120.8(4)	O(4)-C(15)-C(28)	116.7(4)
C(46)-C(15)-C(28)	122.3(4)	O(2)-C(16)-C(29)	119.9(4)
O(2)-C(16)-C(9)	118.2(4)	C(29)-C(16)-C(9)	121.9(4)
C(14)-C(17)-C(29)	121.5(4)	O(7)-C(18)-C(14)	124.4(5)
C(9)-C(19)-C(14)	121.6(4)	C(45)-C(20)-C(29)	109.7(4)
C(11)-C(21)-C(12)	120.2(4)	C(11)-C(21)-C(22)	120.8(4)
C(12)-C(21)-C(22)	119.0(4)	O(3)-C(22)-C(21)	124.7(5)
C(45)-C(23)-C(34)	120.8(5)	C(39)-C(25)-C(46)	110.6(4)
O(6)-C(26)-C(36)	110.1(4)	C(40)-C(28)-C(15)	117.7(4)
C(40)-C(28)-C(43)	120.9(4)	C(15)-C(28)-C(43)	121.4(4)
C(16)-C(29)-C(17)	117.8(4)	C(16)-C(29)-C(20)	122.5(4)
C(17)-C(29)-C(20)	119.7(4)	O(6)-C(30)-C(32)	110.0(4)
C(35)-C(31)-C(13)	118.0(4)	C(35)-C(31)-C(43)	119.7(4)
C(13)-C(31)-C(43)	122.2(4)	O(2)-C(32)-C(30)	109.6(4)
C(9)-C(33)-C(38)	108.0(4)	C(48a)-C(34)-C(35)	116.(3)
C(48a)-C(34)-C(23)	124.(3)	C(35)-C(34)-C(23)	120.4(4)
C(48a)-C(34)-C(48)	8.(4)	C(35)-C(34)-C(48)	122.4(10)
C(23)-C(34)-C(48)	117.3(9)	C(31)-C(35)-C(34)	120.5(4)
O(1)-C(36)-C(26)	107.9(4)	C(41)-C(37)-C(40)	119.9(5)
C(41)-C(37)-C(50)	119.5(13)	C(40)-C(37)-C(50)	120.1(13)
C(41)-C(37)-C(50a)	122.(3)	C(40)-C(37)-C(50a)	117.(2)
C(50)-C(37)-C(50a)	12.(3)	C(12)-C(38)-C(10)	118.5(4)
C(12)-C(38)-C(33)	118.8(4)	C(10)-C(38)-C(33)	122.5(4)
C(10)-C(39)-C(11)	117.8(4)	C(10)-C(39)-C(25)	122.5(4)
C(11)-C(39)-C(25)	119.7(4)	C(37)-C(40)-C(28)	120.6(5)
C(46)-C(41)-C(37)	121.5(5)	O(8)-C(42)-C(47)	110.3(4)
C(28)-C(43)-C(31)	111.0(4)	O(4)-C(44)-C(49)	107.8(4)
C(23)-C(45)-C(13)	117.6(4)	C(23)-C(45)-C(20)	121.5(4)
C(13)-C(45)-C(20)	120.7(4)	C(41)-C(46)-C(15)	117.9(5)
C(41)-C(46)-C(25)	120.5(4)	C(15)-C(46)-C(25)	121.2(4)
O(5)-C(47)-C(42)	107.2(4)	O(27)-C(48)-C(34)	123.7(14)
O(8)-C(49)-C(44)	109.7(4)	O(52)-C(50)-C(37)	125.(2)
C(108)-O(103)-C(105)	120.8(7)	O(109)-C(108)-O(103)	113.3(10)

**Table 5.** (continued)

---

O(109)-C(108)-C(100)	130.5(11)	O(103)-C(108)-C(100)	116.2(9)
C(106)-C(105)-O(103)	107.9(10)	O(52a)-C(50a)-C(37)	123.(5)
O(28)-C(48a)-C(34)	134.(6)		

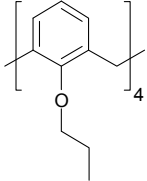
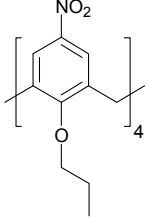
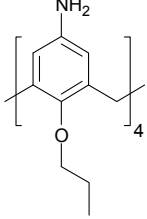
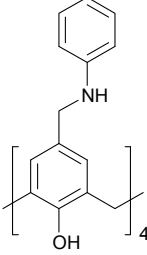
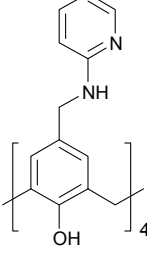
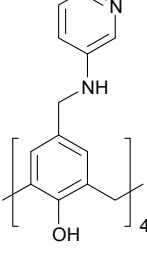
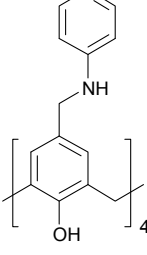
---

***Index of Compounds  
Synthesised***

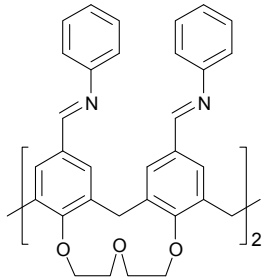
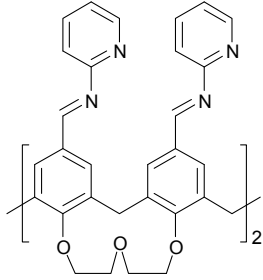
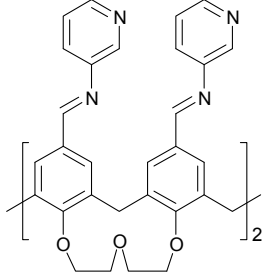
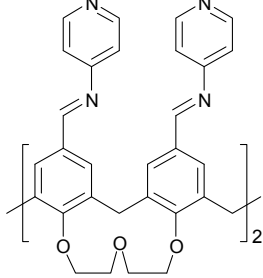
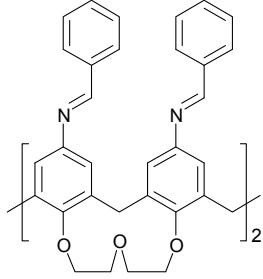
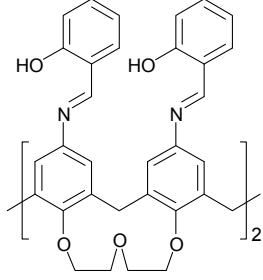
**Table 6.** Synthesised compounds

Compound Name	Structure	Number
<i>5,11,17,23-tetra-tert-butyl-25,26,27,28-tetrahydroxycalix[4]arene</i>		7
<i>25,26,27,28-tetrahydroxycalix[4]arene</i>		14
<i>5,11,17,23-tetrabromomethyl-25,26,27,28-tetrahydroxycalix[4]arene</i>		55
<i>5,11,17,23-tetraformyl-25,26,27,28-tetrahydroxycalix[4]arene</i>		16a
<i>diethyleneglycol di-p-toluenesulfonate</i>		83
<i>25,26,27,28-biscrown-3-calix[4]arene</i>		50
<i>5,11,17,23-tetraformyl-25,26,27,28-biscrown-3-calix[4]arene</i>		49
<i>5,11,17,23-tetranitro-25,26,27,28-biscrown-3-calix[4]arene</i>		17b
<i>5,11,17,23-tetramino-25,26,27,28-biscrown-3-calix[4]arene</i>		18b

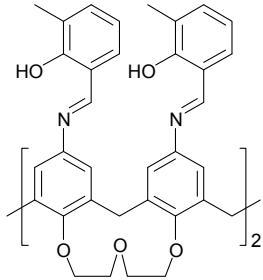
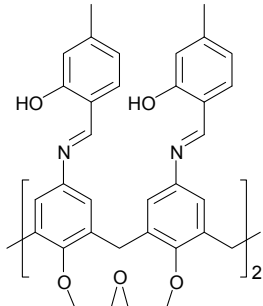
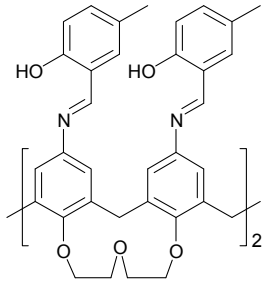
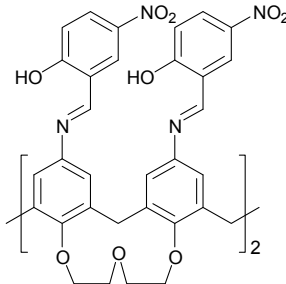
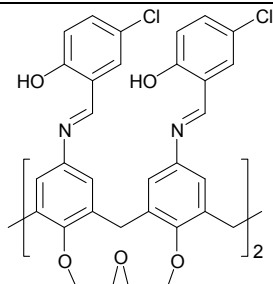
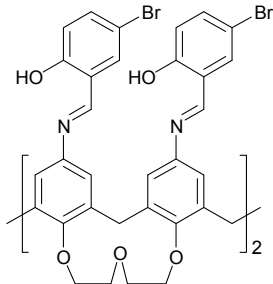
**Table 6.** (Continued)

25,26,27,28-tetrapropoxycalix[4]arene		60
5,11,17,23-tetranitro-25,26,27,28-tetrapropoxycalix[4]arene		17a
5,11,17,23-tetraamino-25,26,27,28-tetrapropoxycalix[4]arene		18a
5,11,17,23-tetra((phenylamino)methyl) - 25,26,27,28-tetrahydroxycalix[4]arene		56
5,11,17,23-tetra((pyridine-2-ylamino)methyl) - 25,26,27,28-tetrahydroxycalix[4]arene		57
5,11,17,23-tetra(pyridine-3-ylamino)methyl) - 25,26,27,28-tetrahydroxycalix[4]arene		58
5,11,17,23-tetra(pyridine-4-ylamino)methyl) - 25,26,27,28-tetrahydroxycalix[4]arene		59

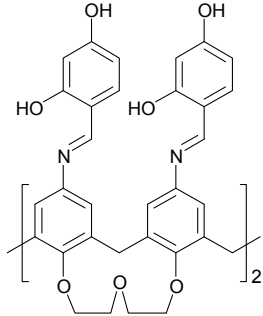
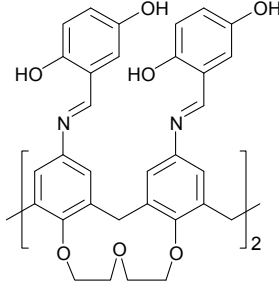
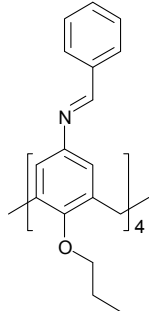
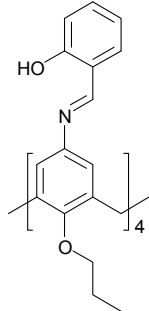
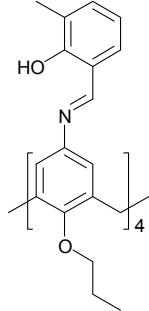
**Table 6.** (Continued)

<p><i>5,11,17,23-tetra((phenyl(imino)methyl)-25,26,27,28-biscrown-3-calix[4]arene</i></p>		<p>54</p>
<p><i>5,11,17,23-tetra((pyridin-2-ylimino)methyl)-25,26,27,28-biscrown-3-calix[4]arene</i></p>		<p>51</p>
<p><i>5,11,17,23-tetra((pyridin-3-ylimino)methyl)-25,26,27,28-biscrown-3-calix[4]arene</i></p>		<p>52</p>
<p><i>5,11,17,23-tetra((pyridin-4-ylimino)methyl)-25,26,27,28-biscrown-3-calix[4]arene</i></p>		<p>53</p>
<p><i>5,11,17,23-tetrakis(phenylmethimino)-25,26,27,28-biscrown-3-calix[4]arene</i></p>		<p>71</p>
<p><i>5,11,17,23-tetrakis((2-hydroxy-phenyl)methimino)-25,26,27,28-biscrown-3-calix[4]arene</i></p>		<p>72</p>

**Table 6.** (Continued)

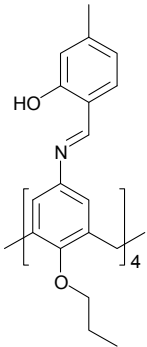
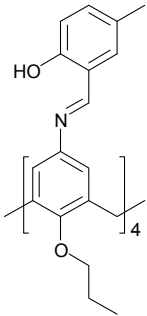
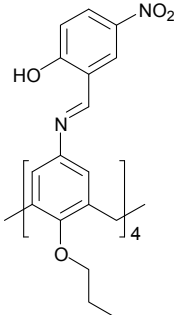
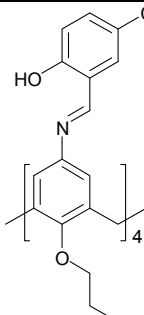
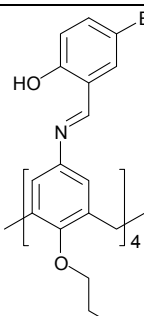
<p><i>5,11,17,23-tetrakis((2-hydroxy-3-methyl-phenyl)methimino)-25,26,27,28-biscrown-3-calix[4]arene</i></p>		<p>73</p>
<p><i>5,11,17,23-tetrakis((2-hydroxy-4-methyl-phenyl)methimino)-25,26,27,28-biscrown-3-calix[4]arene</i></p>		<p>74</p>
<p><i>5,11,17,23-tetrakis((2-hydroxy-5-methyl-phenyl)methimino)-25,26,27,28-biscrown-3-calix[4]arene</i></p>		<p>75</p>
<p><i>5,11,17,23-tetrakis((2-hydroxy-5-nitro-phenyl)methimino)-25,26,27,28-biscrown-3-calix[4]arene</i></p>		<p>76</p>
<p><i>5,11,17,23-tetrakis((2-hydroxy-5-chloro-phenyl)methimino)-25,26,27,28-biscrown-3-calix[4]arene</i></p>		<p>77</p>
<p><i>5,11,17,23-tetrakis((2-hydroxy-5-bromo-phenyl)methimino)-25,26,27,28-biscrown-3-calix[4]arene</i></p>		<p>78</p>

**Table 6.** (Continued)

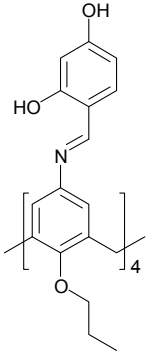
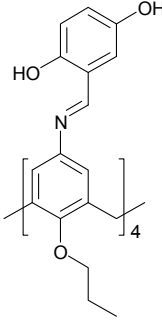
<p><i>5,11,17,23-tetrakis((2,4-dihydroxy-phenyl)methimino)-25,26,27,28-biscrown-3-calix[4]arene</i></p>		<p>79</p>
<p><i>5,11,17,23-tetrakis((2,5-dihydroxy-phenyl)methimino)-25,26,27,28-biscrown-3-calix[4]arene</i></p>		<p>80</p>
<p><i>5,11,17,23-tetrakis(phenylmethimino)-25,26,27,28-tetrapropoxycalix[4]arene</i></p>		<p>61</p>
<p><i>5,11,17,23-tetrakis((2-hydroxy-phenyl)methimino)-25,26,27,28-tetrapropoxycalix[4]arene</i></p>		<p>62</p>
<p><i>5,11,17,23-tetrakis((2-hydroxy-3-methyl-phenyl)methimino)-25,26,27,28-tetrapropoxycalix[4]arene</i></p>		<p>63</p>



**Table 6.** (Continued)

<p><i>5,11,17,23-tetrakis((2-hydroxy-4-methyl-phenyl)methimino)-25,26,27,28-tetrapropoxycalix[4]arene</i></p>		<p>64</p>
<p><i>5,11,17,23-tetrakis((2-hydroxy-5-methyl-phenyl)methimino)-25,26,27,28-tetrapropoxycalix[4]arene</i></p>		<p>65</p>
<p><i>5,11,17,23-tetrakis((2-hydroxy-5-nitro-phenyl)methimino)-25,26,27,28-tetrapropoxycalix[4]arene</i></p>		<p>66</p>
<p><i>5,11,17,23-tetrakis((2-hydroxy-5-chloro-phenyl)methimino)-25,26,27,28-tetrapropoxycalix[4]arene</i></p>		<p>67</p>
<p><i>5,11,17,23-tetrakis((2-hydroxy-5-bromo-phenyl)methimino)-25,26,27,28-tetrapropoxycalix[4]arene</i></p>		<p>68</p>

**Table 6.** (Continued)

<p><i>5,11,17,23-tetrakis((2,4-dihydroxy-phenyl)methimino)-25,26,27,28-tetrapropoxycalix[4]arene</i></p>		<p>69</p>
<p><i>5,11,17,23-tetrakis((2,5-dihydroxy-phenyl)methimino)-25,26,27,28-tetrapropoxycalix[4]arene</i></p>		<p>70</p>